

Transportation of Heavy Crude Oil Through Pipeline

A Dissertation submitted

In partial fulfillment of the requirements for the degree of

Master of Engineering
In
Thermal Engineering

By

Praveen Kumar
Registration No.: 801583019

Under the Supervision of
Dr. Satish Kumar




MECHANICAL ENGINEERING DEPARTMENT
THAPAR UNIVERSITY, PATIALA

July, 2017

CERTIFICATE

I hereby declare that the thesis entitled “**Transportation of Heavy Crude Oil Through Pipeline**” is an authentic record of my work carried out as requirements for the award of the degree of **Master of Engineering in Thermal Engineering** at **Thapar University, Patiala** under the supervision of **Dr. Satish Kumar**, Assistant Professor, Mechanical Department, Thapar University, Patiala during July, 2015 to July, 2017. No part of the matter embodied in this report has been submitted to any other university or institute for the award of any degree.

Date: 14/06/2017


Praveen Kumar

It is certified that the above statement made by the student is correct to the best of my knowledge and belief.


Dr. Satish Kumar
Assistant Professor
Mechanical Engineering Department
Thapar University, Patiala - 147004

*Dedicated
To
My parents*

Acknowledgements

First, I would like to express my great appreciation and my sincere gratitude to my supervisor, Dr. Satish Kumar for his excellent supervision, continuous encouragement and having high patience to listen to all my queries and suggest accordingly .the faith of Dr. Satish Kumar in me always compelled me to work hard, apart from thesis his attitude toward life, work and valuable words taught me many things.

I appreciate the facilities provided by Thapar University to carry out my studies and gain practical knowledge. I gratefully acknowledge SAI labs, Thapar University for providing the result in time.

A special debt of gratitude is owed to the authors whose I have consulted and quoted in this work.

Finally am sincerely grateful to my parents who deserve big thanks for their great support and constant encouragement.



Praveen Kumar

M.E.-Thermal Engineering

801583019

Abstract

In present work, flow characteristics of high sulphur crude oil (HSCO) with addition of low sulphur crude oil and natural surfactant. Madhuca longifolia and low sulphur crude oil (LSCO) are used as additives in high sulphur crude oil. Both of additives were mixed in high sulphur crude oil in concentration 10 to 15% by volume. The rheological characteristics of the heavy crude oil suspension were determined using ISO certified Rheometer for the range of shear rate varying from 0 to 500 s⁻¹. During the experimentation, temperature range varies from 25–45°C. The rheological characteristics of the HSCO include steady state flow behavior, yield stress and thixotropic characteristic etc. Optical microscopy and Dynamic light scattering was used to analyze the size of wax crystals and crystal size distribution respectively. Fourier transform infrared spectroscopy was used to analyze the flowability mechanism of HSCO and its emulsions. HSCO shows the non-Newtonian flow characteristics at low temperature and decreases with increase in temperature. Rheological results of HSCO show that there is a reduction in viscosity with addition of Madhuca longifolia and LSCO. However, viscosity of HSCO was reduced more with LSCO as compare to Madhuca longifolia. C=C, C=H and C=O bonds dissipate in presence of Madhuca longifolia surfactant functional group.

The detailed analysis on transportation and flow behavior of crude oil through pipeline is simulated by using commercial Computational fluid dynamics (CFD) code FLUENT. Standard and RNG k-ε turbulence scheme was used to predict the flow behaviour of crude oil in the pipeline. The influence of design parameters namely radius-to-diameter (r/D) ratio, pipe diameter (D) on flow behaviour of crude oil in pipeline was investigated. The radius-to-diameter (r/D) ratio varied from 1.5 to 3.0. The velocity of flow was varied in between range of 0.5-2.0 m/s for surfactant concentration having range of 10 to 25 % (by volume). The optimum value of r/D ratio was found to exist in between range 1.5 to 2.0.

Keywords: Crude oil; Madhuca longifolia; Dynamic Light Scattering (DLS); Fourier transform infrared spectroscopy (FTIR); Optical Microscopy (OM); Computational fluid dynamics (CFD)

Contents

List of figures.....	vii
List of tables.....	xi
Nomenclature.....	xii
1 Introduction.....	1
1.1 Crude oil.....	1
1.2 Transportation of crude oil.....	2
1.3 Method of transportation.....	2
1.3.1 Heating.....	3
1.3.2 Oil -Water Emulsion.....	4
1.3.3 Core Annular Flow.....	6
1.3.4 Partial Field Upgrading.....	6
1.4 Rheology.....	7
1.4.1 Newtonian vs. non-Newtonian Liquid.....	8
1.4.2 Rheometer.....	8
1.4.3 Types of rheometer.....	8
1.4.4 Applications of rheology.....	9
1.4.5 Rheological Models.....	10
1.5 Rheological Tests.....	10
1.5.1 Shear-Rate Dependent Non-Newtonian Behaviour.....	11
1.4.4Time Dependent Non-Newtonian Behavior.....	12
1.6 Morphology.....	13
1.6.1 Dynamic light scattering (DLS).....	13
1.6.2 Fourier transform infrared spectroscopy (FTIR).....	14
1.7 Organization of thesis.....	14
2 Literature Review.....	16
2.1 Review.....	16
3 Experimentations & Results.....	23
3.1 Material.....	23

3.2 Preparation of Emulsion.....	23
3.3 Experiment setup.....	25
3.4 Results and Discussion.....	26
3.4.1 Rheological properties measurement.....	26
3.4.2 Steady Flow Behavior.....	26
3.4.3 Yield stress Flow behavior.....	30
3.4.4 Thixotropic Flow behavior.....	33
3.5 Optical Microscopy.....	36
3.6 Fourier Transform Infrared Spectroscopy.....	39
3.7 Dynamic Light Scattering.....	41
4 Pressure drop characteristics of crude oil in pipeline bend.....	44
4.1 Introduction.....	44
4.2 Piping materials and attributes.....	45
4.3 Flow Domain.....	45
4.4 Discretization of the Domain.....	47
4.5 Boundary Conditions.....	47
4.6 Results and discussion.....	49
4.6.1 Pressure field analysis.....	50
4.6.2 Influence of radius-to-diameter ratio.....	53
4.6.3 Influence of pipe diameter.....	55
4.6.4 Influence of velocity.....	56
4.6.5 Influence of natural additive concentration.....	58
5 Conclusions.....	60
6.1 Scope for future work.....	60
References.....	61
Web references.....	65
Publications.....	65

List of Figures

Figure 1.1	Production of crude oil from earth surface	1
Figure 1.2	Flow sequence in petroleum product	2
Figure 1.3	Transportation method of crude oil	3
Figure 1.4	Flow chart of Pipeline System for Crude Oil Transportation	4
Figure 1.5	Preparation of water-in-oil emulsion	5
Figure 1.6	Scheme of a pipeline design allowing core flow of heavy oils after a standstill	5
Figure 1.7	Process flow diagram of the Heavy oil Upgrading process	6
Figure 1.8	Deformation of liquid under an applied shear force F	7
Figure 1.9	Different type of rheometer	9
Figure 1.10	Non-Newtonian models: Independent fluids	11
Figure 1.11	Time dependent fluids	12
Figure 1.12	Dynamic light scattering	13
Figure 1.13	Fourier transform infrared spectrometer	14
Figure 1.14	Flow chart of thesis organization	15
Figure 3.1	(a) 90% HSCO-10% LSCO (b) 85% HSCO-15% LSCO (c) 90% HSCO -10% Madhuca longifolia (d) 85% HSCO-15% Madhuca longifolia	23
Figure 3.2	Flow diagram of surfactant extraction from Madhuca longifolia	24
Figure 3.3	Rheometer (Anton Paar, Germany)	26
Figure 3.4	Viscosity behavior of 90% high sulphur crude oil -10% Madhuca longifolia	27
Figure 3.5	Viscosity behavior of 85% high sulphur crude oil -15% Madhuca longifolia	28
Figure 3.6	Viscosity behavior of 90% % high sulphur crude oil -10% light sulphur crude oil	28
Figure 3.7	Viscosity behavior of 85% high sulphur crude oil -15% light sulphur crude oil	29
Figure 3.8	Viscosity behavior of 100% % high sulphur crude oil at different	29

	temperature.	
Figure 3.9	Yield stress behavior of 90% high sulphur crude oil -10% Madhuca longifolia	30
Figure3.10	Yield stress behavior of 85% high sulphur crude oil -15% Madhucalongifolia	31
Figure 3.11	Yield stress behavior of 90% % high sulphur crude oil -10% light sulphur crude oil	31
Figure 3.12	Yield stress behavior of 85% high sulphur crude oil -15% light sulphur crude oil	32
Figure 3.13	Yield stress behavior of 100% % high sulphur crude oil at different temperature.	32
Figure 3.14	Thixotropic behavior of 90% high sulphur crude oil -10% Madhuca longifolia	33
Figure 3.15	Thixotropic behavior of 85% high sulphur crude oil -15% Madhuca longifolia	34
Figure 3.16	Thixotropic behavior of 90% % high sulphur crude oil -10% light sulphur crude oil	34
Figure 3.17	Thixotropic behavior of 85% high sulphur crude oil -15% light sulphur crude oil	35
Figure 3.18	Thixotropic behavior of 100% HSCO at different temperature	35
Figure 3.19	Optical Microscope	36
Figure 3.20	Optical microscopic images of 100% high sulphur crude oil	37
Figure 3.21	Optical microscopic images of 85% high sulphur crude oil -15% light crude oil	37
Figure 3.22	Optical microscopic images of 85% high sulphur crude oil -15% Madhuca longifolia at 25 °C	38
Figure 3.23	Photograph of Fourier Transform Infrared Spectrometer	38
Figure 3.24	FTIR spectra of HSCO without additives	40
Figure 3.25	FTIR spectra of HSCO with 85% HSCO + 15% LSCO	40
Figure 3.26	FTIR spectra of HSCO with 85% HSCO + 15% Madhuca longifolia at 25 °C	41
Figure 3.27	Photograph of Dynamic Light Scattering instrument	41
Figure 3.28	Average particle size of Average particle size of 100% HSCO	42

	paraffin crystals ranges from 700–1200 nm	
Figure 3.29	Average particle size of 85% HCSO-15% Madhuca longifolia wax crystal ranging from 210–350 nm	43
Figure 3.30	Average particle size of 85% HCSO-15% LSCO wax crystal ranging from 600–1100 nm.	43
Figure 4.1	Geometry of pipe bend	44
Figure 4.2	Geometry of Pipe bend at different curvature-ratio diameter (a) $R_c/D = 1.5$, (b) $R_c/D = 2.0$ (c) $R_c/D = 2.5$ (d) $R_c/D = 3.0$	46
Figure 4.3	Geometry of Pipe bend at different diameter (a) $D = 100$ mm, (b) $D = 150$ mm, (c) $D = 200$ m, (d) $D = 250$ m	46
Figure 4.4	Discretization of the domain	47
Figure 4.5	Pressure drop charterstics of crude oil in 100 mm pipeline of different radius-to-diameter at different velocities	49
Figure 4.6	Pressure drop charterstics of crude oil in pipeline ($r/D = 1.5$) of different diameter at different velocities	50
Figure 4.7	Pressure drop contours at different R/D ratio	50
Figure 4.8	Pressure drop contours at different velocity	51
Figure 4.9	Velocity contours at outlet of pipe bend with concentration 20% NS,80% HCO with velocity 1m/s at different curvature-ratio diameter (a) $R_c/D = 1.5$, (b) $R_c/D = 2.0$ (c) $R_c/D = 2.5$ (d) $R_c/D = 3.0$	52
Figure 4.10	Turbulence intensity contours at outlet of pipe bend with concentration 20% NS,80% HCO with velocity 1m/s at different curvature-ratio diameter (a) $R_c/D = 1.5$, (b) $R_c/D = 2.0$ (c) $R_c/D = 2.5$ (d) $R_c/D = 3.0$	52
Figure 4.11	Turbulence intensity contours at outlet of pipe bend with concentration 20% NS,80% HCO with velocity 1m/s at different curvature-ratio diameter (a) $R_c/D = 1.5$, (b) $R_c/D = 2.0$ (c) $R_c/D = 2.5$ (d) $R_c/D = 3.0$	53
Figure 4.12	Velocity contours at outlet of pipe bend with concentration 20% NS,80% HCO with velocity 1m/s at different diameter (a) $D = 100$ mm, (b) $D = 150$ mm (c) $D = 200$ mm (d) $D = 250$ mm	54
Figure 4.13	Turbulence intensity contours at outlet of pipe bend with concentration 20% NS,80% HCO with velocity 1m/s at different (a)	54

	D =100 mm, (b) D = 150 mm (c) D = 200 mm (d) D = 250 mm	
Figure 4.14	Contours of HCO and NS phase with concentration 20% NS,80% HCO with velocity 1m/s different at different (a) D =100 mm, (b) D = 150 mm (c) D = 200 mm (d) D = 250 mm	55
Figure 4.15	Velocity contours at outlet of pipe bend with concentration 20% NS,80% HCO and diameter 100 mm with different velocity (a) v =0.5 m/s(b) v =1.0 m/s (c) v =1.5 m/s (d) v =2 m/s	56
Figure 4.16	Turbulence intensity contours at outlet of pipe bend with concentration 20% NS,80% HCO and diameter 100 mm with with different velocity (a) v =0.5 m/s (b) v =1.0 m/s (c) v =1.5 m/s (d) v=2 m/s	57
Figure 4.17	Contours of HCO and NS phase with concentration 20% NS,80% HCO with and diameter 100 mm different velocity velocity (a) v =0.5 m/s (b) v =1.0 m/s (c) v =1.5 m/s (d) v =2 m/s	57
Figure 4.18	Velocity contours at outlet of of HCO and NS phase with concentration by volume (a) 10% (b) 15% (c) 20% (d) 25% for diameter100 mm and velocity 1 m/s	58
Figure 4.19	Turbulence intensity contours at outlet of HCO and NS phase with concentration by volume (a) 10% (b) 15% (c) 20% (d) 25% for diameter100 mm and velocity 1 m/s	59
Figure 4.20	Contours of HCO and NS phase with concentration by volume (a) 10% (b) 15% (c) 20% (d) 25% for diameter100 mm and velocity 1 m/s	59

List of Tables

Table 3.1	Physical properties and test method	25
Table 3.2	Properties of crude oil at shear rate of 500s^{-1}	27
Table 3.3	Hysteresis area at different temperatures	36
Table 3.4	Wave numbers (cm^{-1}) of HSCO and its emulsions	39
Table 4.1	Description of Pipeline Geometry	45
Table 4.2	Properties of crude oil and additive	47

Nomenclature

Symbol	Description
S1	Pure Crude oil
S2	90% Crude oil+10% Madhuca longifolia
S3	85% Crude oil+15% Madhuca longifolia
S4	90% Crude oil+10% light crude oil
S5	85% Crude oil+15% light crude oil
wt. %	Weight percentage
Rc/D	Curvature-Diameter ratio

Greek Symbols

ν	Viscosity (mPa.s)
-------	-------------------

Acronyms

Abbreviation	Description
CR	Controlled rate mode
CS	Controlled stress mode
OSC	Oscillation test mode
HSCO	High sulphur crude oil
LSCO	Low sulphur crude oil
NS	Natural surfactant
OM	Optical Microscopy
FTIR	Fourier Transform Infrared Spectroscopy
DLS	Dynamic Light Scattering
CFD	Computational Fluid Dynamics
WAT	Wax appearance temperature
ASTM	American society of testing material

Chapter 1

Introduction

1.1 Crude oil

From the beginning of 21st century, the demand of energy is increased due to the continuous growth of industry. The demand of crude oil in petroleum sector has also increased worldwide. Heavy crude oil is the base product for extraction of petrochemical products. Pipeline transportation is very popular due to its economy, reliability, low maintenance cost, round the year availability at the user's end. It is also extremely safe and leads to minimum environmental pollution. The flow characteristics of crude oil in pipeline shows variations from one crude well to the other [Meriem et al., 2012]. It also depends on age and depth of crude oil well. Production of crude oil from earth is shown in Fig 1.1.

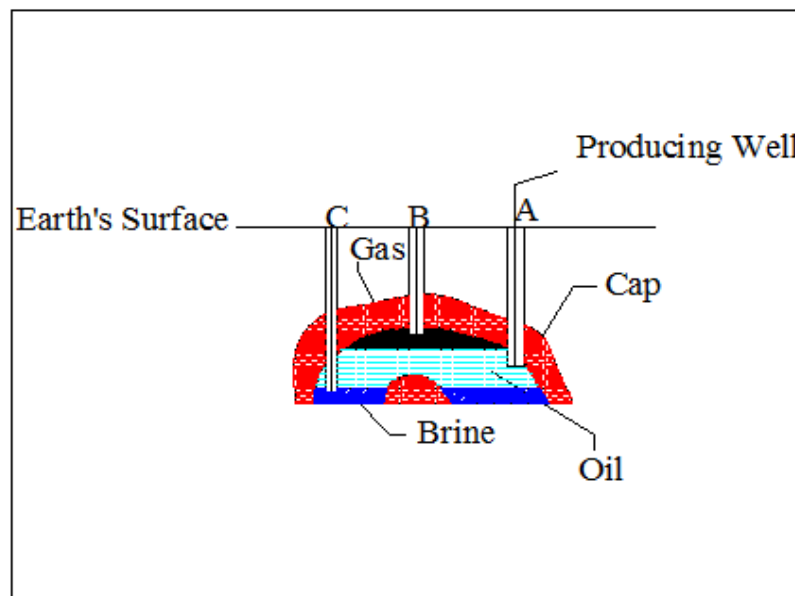


Figure 1.1: production of crude oil from earth surface

The crude oil shows the Non-Newtonian flow characteristics due to very difficult to transport very long distance [Chen et al., 2010]. During the transportation from sea to refinery, wax substance deposits on the pipeline wall causes the reduction in flow diameter of pipeline. This leads to blockage of transportation pipeline and failure of valve. The most important data required for design a transportation system is the rheological characteristics of the suspension at various operating conditions. Rheological characteristics of the crude oil

depend on several parameters such as flash point, pour point, specific gravity, operating temperature, yield stress and thixotropic structure etc. [Randoph and Larson, 1998; Banerjee et al., 2015]. The high viscosity of crude oil creates numerous problems during pumping through pipeline and requires more power for transportation and extraction. Pipeline flow of crude oil is made suitable by pretreating them with pour point depressants (PPDs) [Randoph and Larson 1998; Chen et al., 2010]. Sulphur, asphaltene and acids were found to be present in crude oil that produces harmful impact on transportation system [Randoph et al., 1998; Banerjee et al., 2015]. Small proportion of the some drag reducing agents able to reduces the viscosity of the crude oil suspension which helps in the improvement of pipeline flow characteristics. Zahrani and Fariss [1998] investigated the viscosity of crude oil with water. They found that viscosity of crude oil reduced with emulsification with water. Investigators studied the rheological characteristics of crude oil with addition of different types of additives [Khan, 1996; Farah et al., 1998; Tao and Tang 2014] . The flow sequences of petroleum product are shown in Fig 1.2.



Figure 1.2: Flow sequence in petroleum product [Source: Know more about piping]

1.2 Transportation of crude oil

Crude oil has high viscosity due to composition complexity which makes crude oil production, refining, and transportation is very expensive. In the petrochemical chain, the high production of oil is required so new method is developed in chain of production. In the pipeline, crude oil adheres to pipeline due to low mobility, high viscosity, wax and asphaltenes deposited on pipe wall and due to this transportation are affected. Pumping of crude oil in pipeline require more power. There are various methods for achieving well flowability of crude oil. The way of transportation and flow chart of pipeline system is shown in Fig 1.3 and Fig 1.4.

1.3 Method of transportation

- a) Heating
- b) Oil water emulsions
- c) Core annular flow
- d) Partial field upgrading

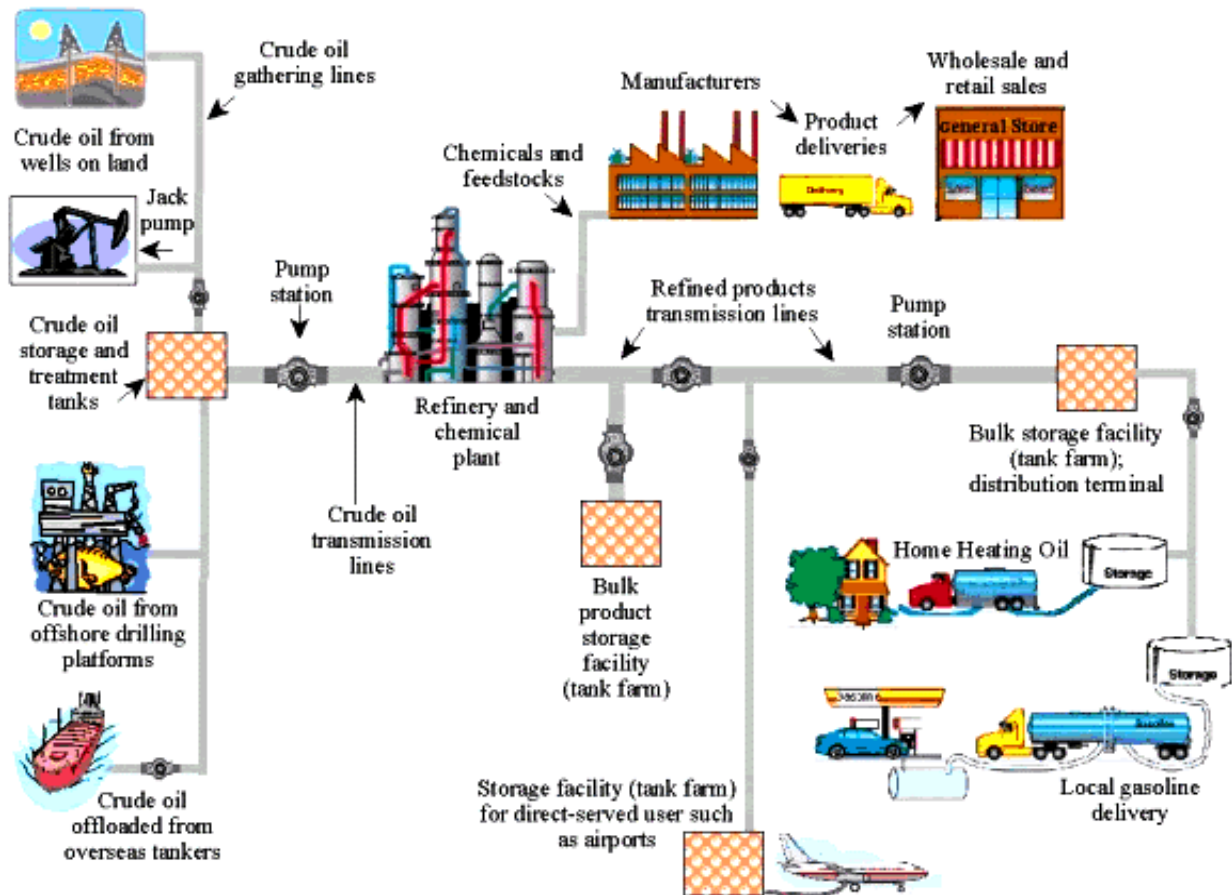


Figure 1.3: Transportation Method of crude oil [Source: Transmission lines]

1.3.1 Heating

Well transportation of crude oil heating is best method [Hasan et al., 2010]. The mechanism behind this process is that while the temperature increases viscosity also gets reduced. The designing of crude oil pipeline requires the value of oil viscosity to be less than 500 centistokes. Generally, crude oil pipeline operates at low vapour pressure constraints and natural gas and fuel oil fired heater is used directly on pipeline to serve heating. Variation of temperature in crude oil pipeline occurs in longitudinal direction which also results in

longitudinal expansion of pipe [Guevara et al., 2010]. So, expansion loop is provided to remove expansion the material used in thicker steel.

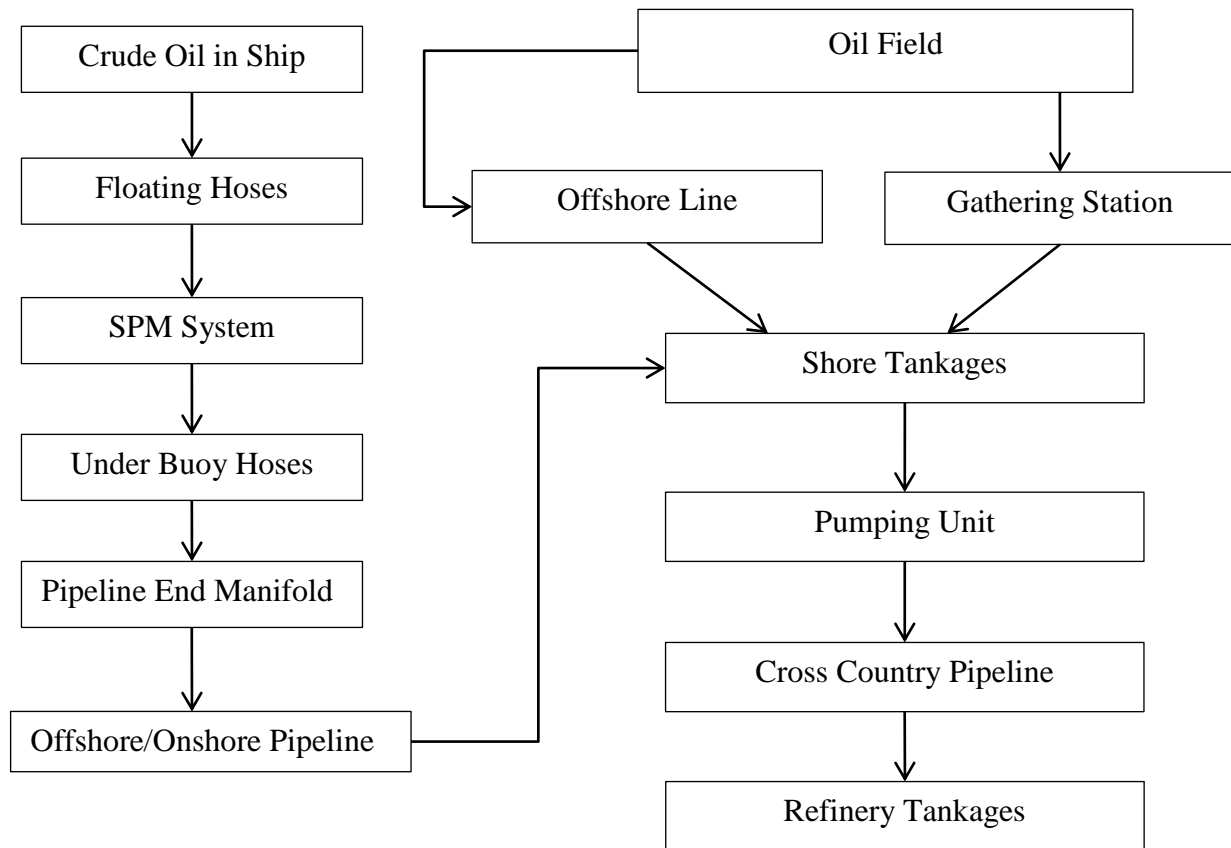


Figure 1.4: Flow chart of Pipeline System for Crude Oil Transportation

1.3.2 Oil -Water Emulsion

This is an effective method which decreases the viscosity of heavy crude oil by preparation of oil-water emulsion. Emulsion is a mixing of two fluids in which water is continuous and oil is dispersed. The mixing phenomena are carried by help of shaker and stirrer which is shown in Fig 1.5. Non-ionic surfactant is cheaper and not affected by water salinity whereas organic residues affect the oil nature. The viscosity of crude oil decreases exponentially with water and the curve obtain is very important for optimum selection of water to be present in the emulsion. From economy point-of-view, the main aim of oil in water emulsion preparation is

transportation of oil in larger quantity with little quantity of water. The necessary viscosity value for transport in pipelines 400 CP with 25-30% w/w water.

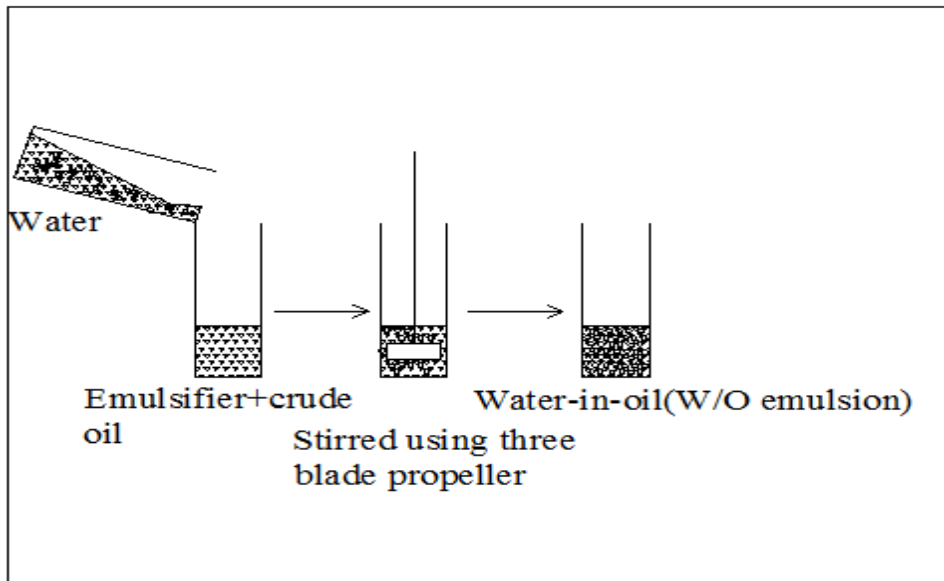


Figure 1.5: Preparation of water-in-oil emulsion

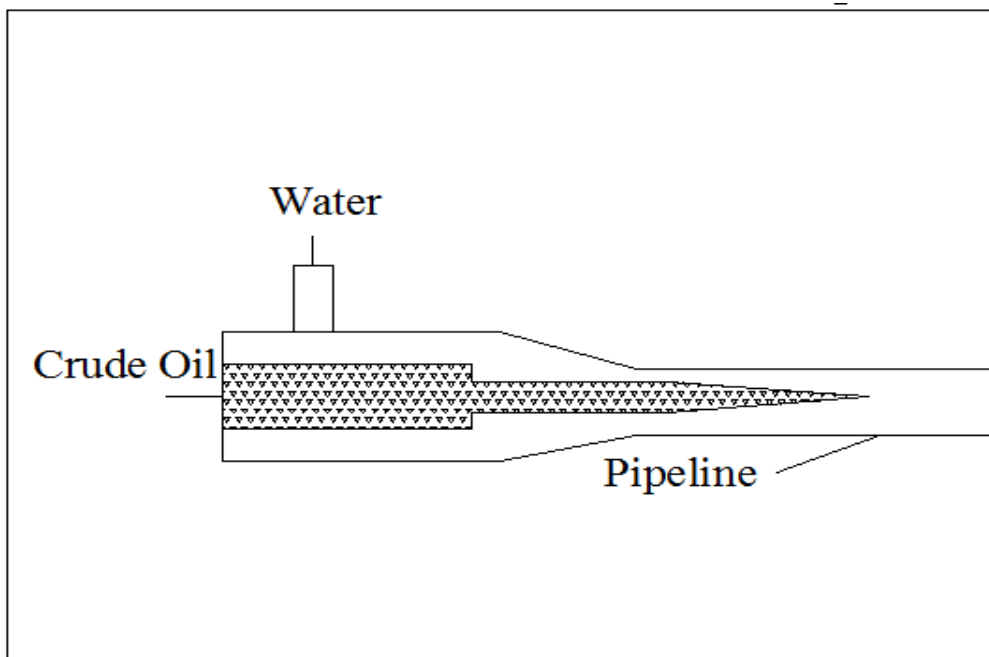


Figure 1.6: Scheme of a pipeline design allowing core flow of heavy oils after a standstill

1.3.3 Core Annular Flow

In a stopped system, for restarting the system again may require a large pressure. The pressure rating of all components is more complex. In this complexity, cleaning of flow system is also compulsory to remove the adhere oil which causes more expanses and down-time for well function of flow system. Various coating materials are used in the inner side of pipeline which reduces adhesion of crude oil in the inner surfaces. The core annular flow of crude oil is shown in Fig 1.6.

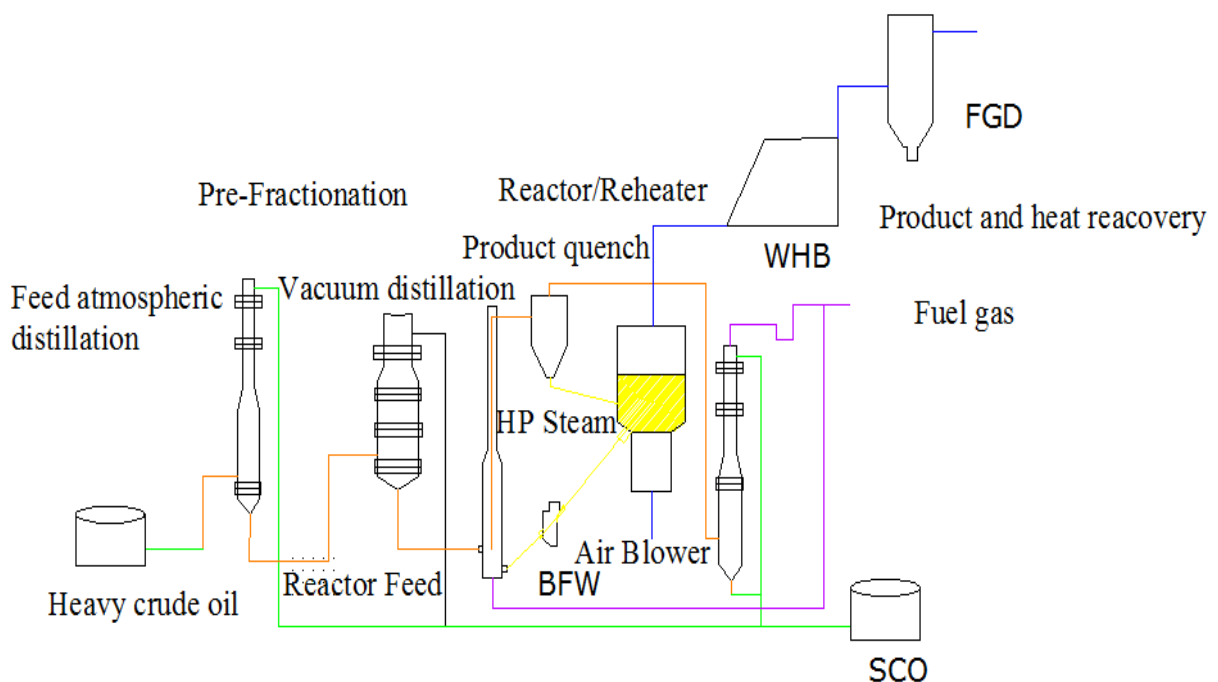


Figure 1.7: Process flow diagram of the Heavy oil Upgrading process

1.3.4 Partial Field Upgrading

Partial field upgrading is a method of modifying the composition of heavy oil by viscosity reduction without changes the refining characteristics. Upgrading technique has a key advantage of transporting the heavy crude oil without any change to the flow system [Urquhart, 1986]. Generally, upgrader is placed at gathering junction. Silverman and Cabrere [2012] introduce a method to upgrade the crude oil in cost efficient way which is shown in Fig 1.7. In this method, by application of circulating bed of hot sand it transform the valuable and lighter product. The presence of asphaltenes in the crude oil residue or completely dispersed and deposited on the sand in a thin layer. For this process two seconds are required.

The heaviest particles of crude oil are converted into coke which is deposited on sand particle. A minor product changed into non-condensable gas. Thin layer of coke on sand bed is burn in reheater. The energy provide by coke burning support to upgrading the reaction. The obtain product gas is used as in steam boiler and furnaces.

1.4 Rheology

The study of deformation and flow of fluid under the influences of an applied stress is known as rheology. In the rheology, force can be applied as a tension, compression, shearing process or combine of three. Simple type of deformation is shown in Fig 1.8.



Figure 1.8: Deformation of liquid under an applied shear force.

In this lower plate of parallel plate kept fixed and upper plate pulled with a velocity w.r.t. bottom plate. Force F is applied shearing forces in direction over surface A [Holmberg et al., 2004].

$$\tau = \frac{dF}{dA} \quad (1.1)$$

Shear strain is the displacement of any plane relative to a second plane, divided by the perpendicular distance between planes.it is the force causing such deformation [Aske et al., 2001].

$$\nu = \frac{dx}{dy} \quad (1.2)$$

Shear rate is the speed of deformation which can be determined from equation given below [Aske et al., 2001].

$$\gamma = \frac{dx}{dy} \quad (1.3)$$

1.4.1 Newtonian vs. Non-Newtonian Liquids

Newtonian behaviour of liquid occurs at constant viscosity which is independent on shear rate and flow type. Newtonian liquid reveals the uniform resistance to flow and independent of flow condition. The non-Newtonian fluid exhibits different resistance to behavior of flow at different shear. On-Newtonian liquids are generally [Chang et al., 2001]:

- Shear thinning or thixotropic: In this fluid viscosity decreases (thin) with increasing shear rate.
- Shear thickening or rheopectic: while fluid viscosity increases (thickness) with increasing shear rate.
- Viscoplastic or Bingham plastics: In which flow only if shear stress is more than characterstics stress, the yield stress.

Elasticity and time dependent stress:

In these fluids, stress changes and relaxation exponentially vary to inversely proportional to their relaxation time. Newtonian fluids and stress and relaxation in same phase with zero relaxation or shear rate.

1.4.2 Rheometer

It is a device used to predict the rheology of liquids and solid-liquid suspension. It deals to calculate appropriate way deformation under with applied stress and without applied stress in order to formulate constitutive equation .there are several rheometer available to measure viscosity, normal stress, relaxation time and elongation viscosity. The cone and plate, concentric cylinder and parallel plate rheometer are widely used to determine rheological characteristics [Zahrani, 1998].

1.4.3 Types of rheometer

Concentric cylinder

In the concentric cylinder rheometer, there are two concentric cylinders is used. One cylinder is fixed and other is driven at constant torque. The viscosity of fluid between two concentric cylinders governs the rotation. The faster spin of rotation at given torque the lower the

viscosity is measured. The elastic modulus is calculated as function of shear stress. Concentric rheometer is used to measure the elasticity, viscoelasticity and viscosity of non-Newtonian liquid.

Parallel plate

Parallel plate rheometer is used for those samples which is independent on shear rate. Parallel plate is not used for non-Newtonian fluid. In the parallel plate rheometer bottom plate is stationary and top plate is rotary. A constant torque is applied on upper plate and the angular deflection or rate of strain is measured.

Cone and plate

It is quite similar as parallel plate rheometer but upper plate is replaced as cone. Cone has slight angle and constant shear strain throughout the sample. So it is used for non-Newtonian fluid. Three type of rheometer is shown in Fig 1.9.

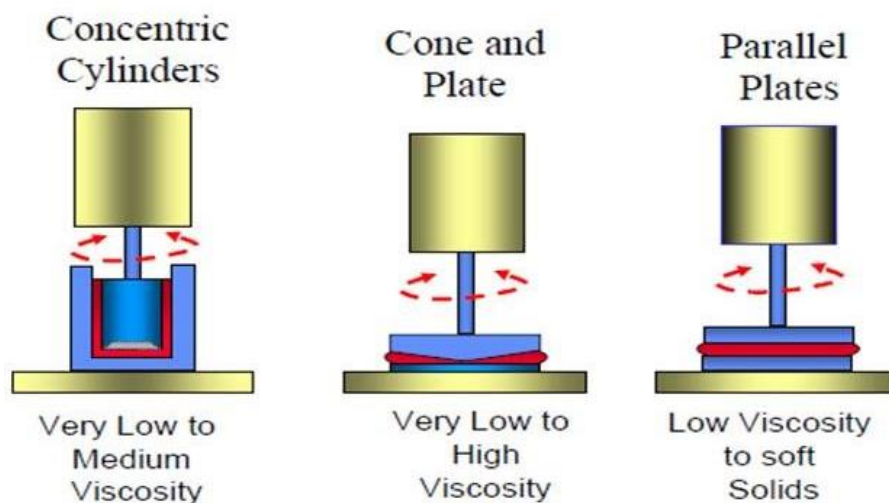


Figure 1.9: Different type of rheometer

1.4.4 Applications of rheology

There is a wide range of applications in industry, medical, biotechnology etc. Rheology is used in field of hemorheology for blood study, in geological field for study of solid-earth material, polymeric material and in paint industry for preparation of emulsion and rheology modifiers.

1.4.5 Rheological Models

Different rheological models are described as follows--

Power Law

Power law model is also referred as the Oswald-de wale power law .This mathematical relationship is very useful because of its simplicity, but approximately describes the behaviour of a real non-Newtonian fluid .Power Law equation is used for dilatant fluids or pseudoplastic fluid.

$$\tau = K\gamma^n \tag{1.4}$$

Where n is power index and k is consistency coefficient.

Bingham Model

A two-parameter rheological model widely used in the petroleum drilling fluid to describe flow behaviour of many type of muds .it may be describe mathematically by equation 1.5.This model is used for describe the plastic behavior of fluid where τ_B is yield stress η_P is viscosity yield stress is an important property the fluid restart to flow. It is the point that range of reversible elastic deformation and viscoelastic deformation flow [Goodwin and Hughes, 2008].

$$\tau = \tau_B + \eta_P\gamma \tag{1.5}$$

Casson model:

Casson model commonly used for visco-plastic fluids , which has its origins in modeling the flow of blood, but it has been found a good approximation for many other substances. It can be describe mathematically by equation 1.6.

$$(\tau)^{0.5} = (\tau_0)^{0.5} + K(\gamma)^{0.5} \tag{1.6}$$

1.5 Rheological Tests

Investigators have analytical way to measure their properties. In the rheological experiment force is apply to fluid and measuring the shape change or nature of flow behaviour of fluid.

1.5.1 Shear-Rate Dependent Non-Newtonian Behaviour

The viscosity is not depending on shear rate in a Newtonian liquid. The viscosity of many fluids changes with shear rate which is independent on length of time of the fluid subject to shear. Fluid viscosity is also referred to as apparent viscosity due to its inconstant Newtonian behaviour longer time. Two most non-Newtonian liquid are as follow which is shown in Fig 1.10.

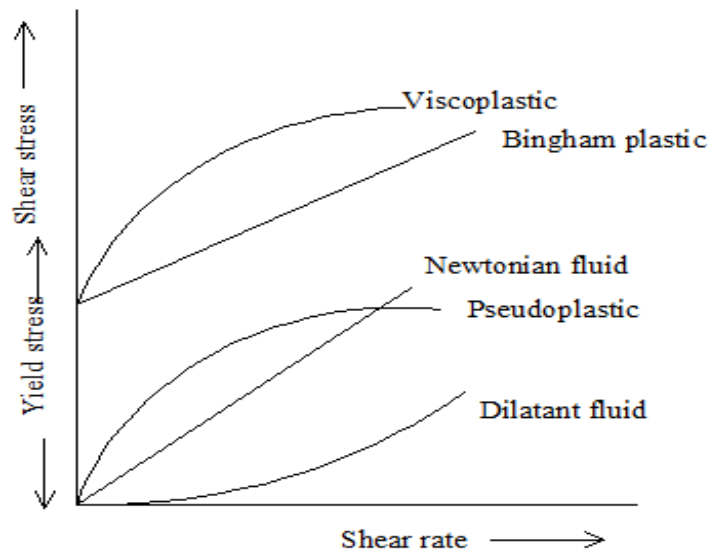


Figure 1.10: Non-Newtonian models: Independent fluids

Pseudo plastic fluids

They behave as a non-Newtonian fluid while shear rate increase with decrease in apparent viscosity. In the Pseudo plasticity may occur at different reason i.e. polymer in the flow may align themselves solvent molecule bond is removed and aggregated particles can break down.

Dilatant fluid

Dilatant fluid behavior is not common to pseudo plastic behaviour. In this apparent viscosity increases when the shear rate is increased so it is sometimes called as shear thickening.

Plastics

Bingham plastic it is sometimes called as viscoelastic flow when shear stress is more than yields stress, characteristics stress beyond this fluid behave as Newtonian shear thinning fluid and below this stress fluid behave as elastic solid [Reinhardt, 1997; Roberto et al., 2006].

$$\tau = E\gamma \quad (\text{for } \tau < \tau_0) \quad (1.7)$$

$$\tau - \tau_0 = \eta \frac{d\gamma}{dt} \quad (\text{for } \tau \geq \tau_0) \quad (1.8)$$

Where E is shear modulus, η is the viscosity and τ_0 is the yield stress Fluids that exhibit plastic behavior.

1.5.2 Time Dependent Non-Newtonian Behavior

The rheological characteristics of various type of fluid depend upon duration of applied shear stress. In particular cases this change is reversible and if fluid is stand for long duration of time the fluid will again recover its original apparent viscosity. In other cases the change brought about by shearing the sample is irreversible. Time dependent non-Newtonian fluid characteristics are classified in two different ways which is shown in Fig 1.11 [Krieger and Dougherty, 1959; Kane et al., 2004].

Thixotropic fluids

They are also known as shear thinning on increasing the shear rate the viscosity of fluid decreases (thins).

Rheopectie fluids

They are sometimes referred as shear thickening with increase of shear rate the viscosity of fluid increases (thickness)

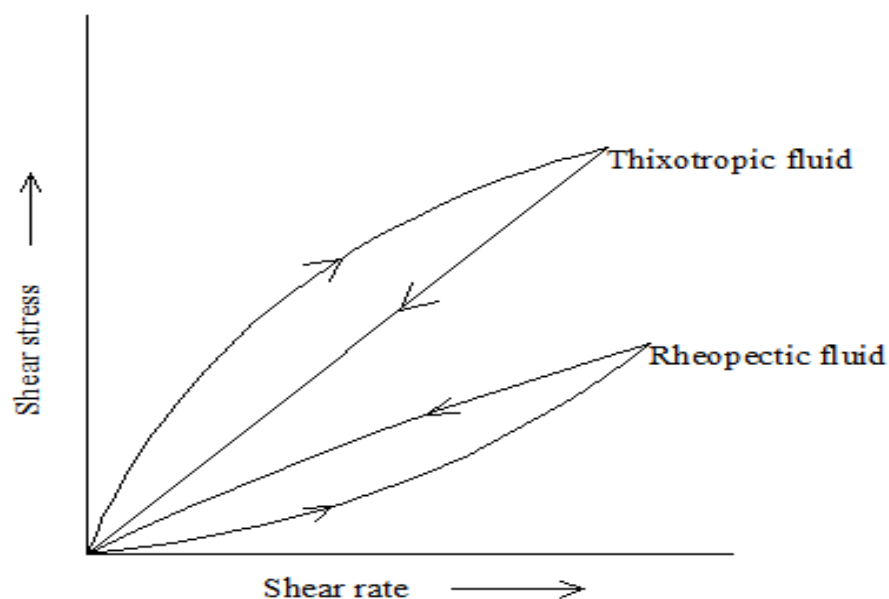


Figure 1.11: Time dependent fluids

1.6 Morphology

1.6.1 Dynamic light scattering (DLS)

DLS is also called as Quasi-Elastic Light Scattering (QELS). It is used to measure the size distribution of particles and molecules in this process the particle or molecule's Brownian motion scatter a laser light at different intensity. The Dynamic light scattering is shown in Fig 1.12. Different fluctuations of intensity yield the velocity of particles due to this particle size measure using the relation Stokes-Einstein. The random motion of particle is modeled by Stokes-Einstein relation:

$$d = \frac{kT}{3\pi\eta(T)D} \quad (1.9)$$

Where k is Boltzmann constant, T is temperature, D is diffusion coefficient, η is the viscosity and d is particle diameter.

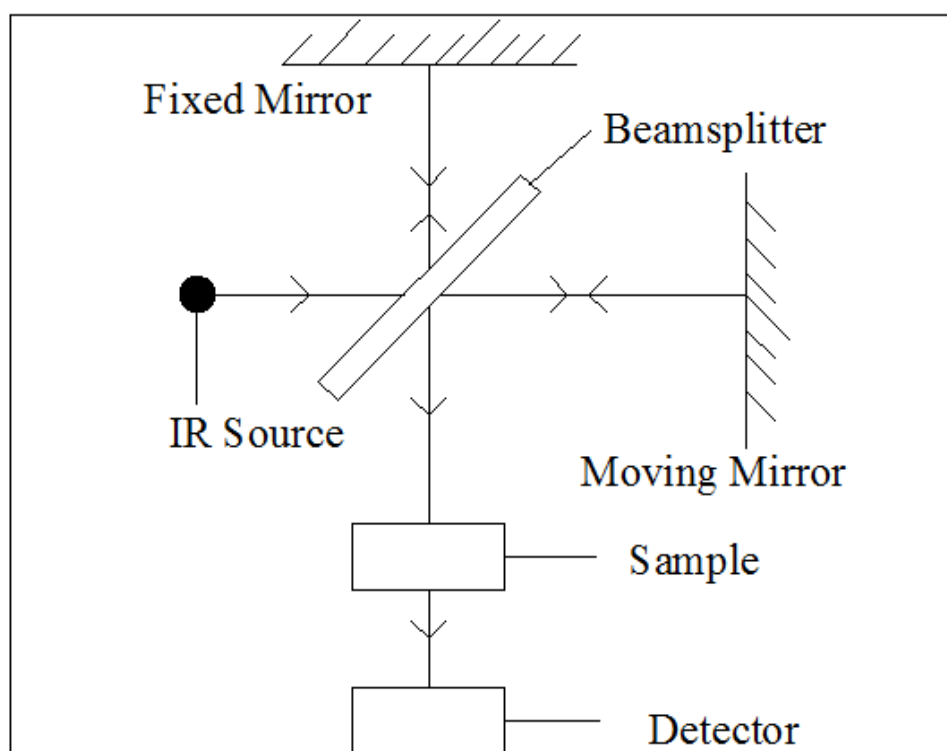


Figure 1.12: Dynamic light scattering

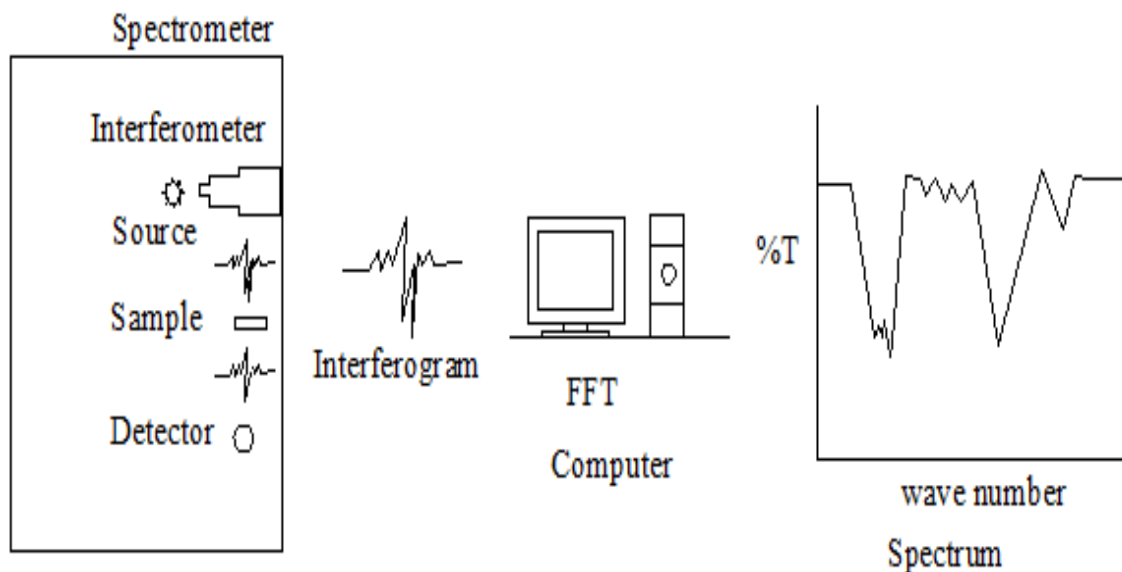


Figure 1.13: Fourier transform infrared spectrometer

1.6.2 Fourier transform infrared spectroscopy (FTIR)

Fourier transform infrared spectroscopy (FTIR) method is used to analyze the infrared spectrum of absorption of fluid. In this technique, the spectrometer collect high spectral infrared range of resolution data is shown in Fig 1.13. The FTIR spectrometer has significant advantage to dispersive spectrometer which counts the narrow range of wavelength. In the arrangement of spectrometer fixed mirror and moving mirror aligned at right angle to each other. Beam splitter is fixed in center and equidistance from both mirrors. The major work of beam splitter is bi-furcating of incident beam and recombines it. Due to reflection of moving mirror, it creates the path difference and get interference pattern. When two wave at 180° the minima is obtained and out of phase and maxima when there is no path between.

1.7 Organization of thesis

In this Chapter, introduction about the crude oil transportation has been discussed. Chapter 2 discusses the literature review. Chapter 3 discusses the experimental setup and the results of the work. Chapter 4 discusses the simulation in pipeline. Chapter 5 summarizes the conclusions drawn from this project.

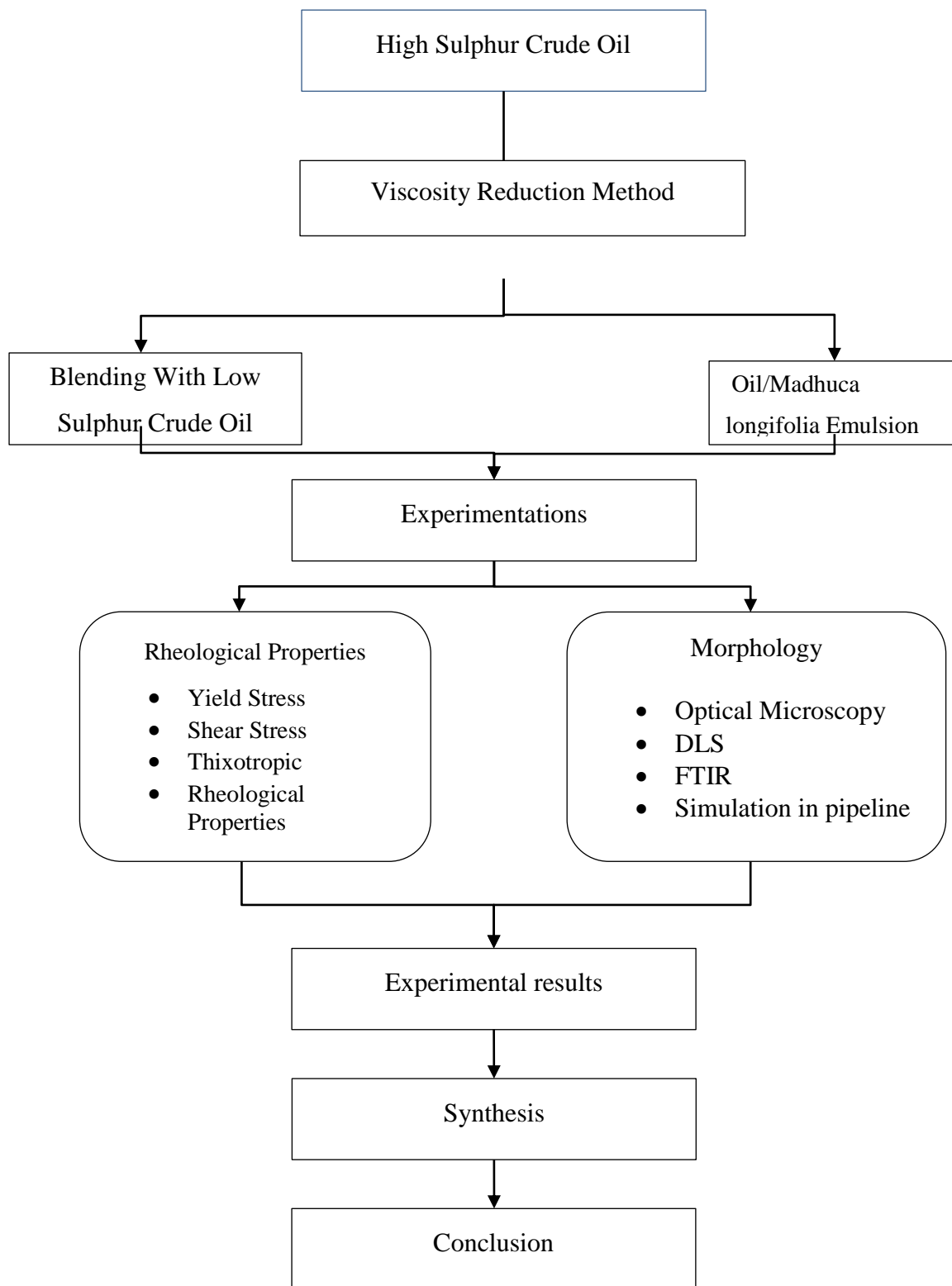


Figure 1.14: Flow chart of thesis organization

Chapter 2

Literature Review

2.1 Review

A lot of research work has been done in the past to investigate rheological characteristics of crude oil from different perspectives. Various factors that affect the transportation of crude oil have been investigated by researchers. Some of the literature scenario has been given below:

Hashim et al. [2003] investigated the influences of temperature on viscosity of crude oil. They developed a correlation for viscosity in wide range of API gravities at 20-50°C. They proposed the correlation on the basis of viscosity data of viscosity and API gravity data obtained at temperature of 130-220 °F. They established the correlation by verifying it with the help of data available of different density of crude oil. The proposed correlation showed best correlation with average absolute deviation (AAD) of 2.8%.

Ghannam and Esmail [2006] performed an experimentation to improve flowability of crude oil by using different methods. They used different methods for mixing of water and crude oil to prepare the oil-water emulsion. RheoStress RS100 was used to investigate the viscosity of crude oil. Rheometer consists of a cone–plate sensor having cone angle of 4°, 0.137-mm gap, cone diameter of 35 mm. Results show that mixing of kerosene in crude oil enhances the reduction of viscosity and smooth flowability.

Tao and Xu [2006] studied the application of magnetic field pulse in viscosity reduction of crude oil for a time interval. During this experimentation, the temperature of crude oil remains constant. They found that magnetic field the viscosity of crude oil decreased from 880 to 496 Centi Poise on applying a magnetic field of 0.15 T for 5 min. They also found that the viscosity was reduced significantly on applying the magnetic field for few seconds. This study was found beneficial in terms of energy consumption and viscosity reduction in off-shore and on-shore crude transportation.

Ahmed et al. [2007] studied the stability and rheological behaviour of Egyptian crude oil and

its water emulsions. They added nonionic (NPE) and anionic (TOS) surfactant mixture to stabilize the crude oil stabilized mechanism. They found that crude oil emulsified with water decrease the viscosity of crude oil significantly. The stability of crude oil-in-water emulsions enhances speed of rotation and surfactant concentration increases. Synthetic formation and fresh water have been mixing for study of viscosity and aqueous phase salinity of emulsion. The resultant surfactant mixture was obtained to enhance the production and low viscosity to crude oil helpful for transportation of crude oil in pipeline.

Bacon et al. [2011] studied the effect of weather on rheology of waxy crude oil. Experiments were conducted for crude oil sample collected from six different well. They observed that weathering condition were responsible for the viscosity of crude oil to more than twice in only 4 days after sample taken from well head. Also, thermal history of area was also significantly affects viscosity. A 5°C temperature variation caused 22% change in viscosity of crude oil. Results also show that pour point and viscosity was found that greatly vary with weathering.

Hasan et al. [2011] investigated the flow characteristic of heavy crude oil with the addition of light crude oil. They used 90% concentration of crude oil to perform the experiments. Results show that 90% oil-10% water emulsion decreases the viscosity of crude oil from 9.97 to 8.09 Pa.s. They found that blending of 90% crude oil with 10% alcohol reduces the viscosity from 10.0 to 2.0 Pa.s. Also, blending of 90% crude oil with 10% light crude oil reduces the viscosity from 9.97 to 6.49 at 25°C. The emulsion of 80% crude oil with 20% alcohol reduces its viscosity from 10 to 0.95 Pa.s at 25 °C whereas blending with 20% light crude oil reduces the viscosity of crude oil from 10 to 0.375 Pa.s at 25°C. They found that light crude oil is more suitable than ethyl alcohol and water.

Li and Gong [2011] studied the flowability of multiphase crude oil through pipeline. The flowability of crude oil in multiphase pipeline was achieved by booster pump due to mechanical action. The feature of the emulsion was varying from that of the crude oil and its flow pattern was not the identical as the Newtonian fluid flow in the crude oil transportation pipeline. They found that viscosity was varying with temperature whereas pressure and shear rate not function of temperature. Also, as the crude oil temperature decreases its nature changes from Newtonian to non-Newtonian.

Adeyanju and Oyekunle [2012] investigated the influence of temperature on flow behaviour of crude oil. The effect of thixotropic/yield pseudo plastic behaviour of two different sample were investigated. They performed the experiments at temperature range 35-80°C and shear rate range 2-200 s⁻¹ was covered. Temperature of Oil 1 was varied as range 25–60°C. They found that viscosity of crude oil was reduced in large extent at temperature 38°C and 40°C at different value of shear rates. They found that oil 1 behaves as non-Newtonian fluid behaviour below at 60°C while oil 2 behaves non-Newtonian nature at temperature below 45°C. It was observed crude oil wax content regain its lattice bonding and cohesive enhances after some days.

Benziane et al. [2012] investigated the flow behaviour of crude oil and their emulsion in pipeline. The experiments were carried out by using the RS600 Rheo Stress rheometer at 20°C. The emulsion was prepared with water by the help of magnetic stirrer. The stability of emulsion was identified by rheological characteristics including elastic modulus, complex viscosity, phase angle, non-Newtonian viscosity. The quasi-Newtonian behaviour demonstrated by pure light crude oil. Results show that preparation of emulsion with water at different concentration was found better by Ostwald de Waele and Herschel–Bulkley models.

Ghannam et al. [2012] investigated the rheological behaviour such as yield stress, steady flow behavior, transient flow characteristics, thixotropic nature and viscoelastic nature of fluid. They had used RheoStress (RS 100) rheometer to perform the experimentation. They had mixed 10 and 20% concentration of light crude oil to reduce the viscosity of heavy oil. Results show that the viscosity of crude oil temperature 25°C was reduced from 10 to 1.2 Pa.s with 10% concentration of light crude and reduced 0.375 Pa.s with 20% addition of crude oil. It was also found that crude oil exhibit the thixotropic area at normal temperature as 321.65 kPa/s which reduced to 118.62 kPa/s at 65°C. This happened due to that light crude oil approximate eliminates the thixotropic nature of crude oil. The mixture of 10% concentration of the light crude oil reduces the complex modulus of the heavy crude oil.

Homayuni et al. [2012] investigated the flow behaviour of two different Iranian heavy crude oils. They prepared the emulsion of crude oil with three different surfactants like Naphtha, light crude and kerosene to analyze the flowability. They used 10% of Nowrooz oil for blending and 15% of naphtha for diluting of crude oil with at 25°C. It was found that use of

light hydrocarbon as diluents is an expensive choice because approximately 20% concentration is required to reduce the viscosity of heavy crude to a desirable level. Results show that reduction of viscosity of the heavy crude by the formation of emulsions that contain between 25 and 30% water is a more likely approach due to cheaper cost than either light crude or kerosene.

Karami et al. [2012] studied the influences of various parameters on pressure drop in transportation pipeline. It was due to adding little amounts of drag reducing agent. In this experiment pressure drop of pipelines was measured with crude oil and combination of crude and DRA on same operating conditions. Experiments were performed for three types of drag reducing agent at 4, 15, 29 and 41°C. First pipe had relative roughness of 0.0059 and 0.0254 m diameter and galvanized iron material. Second pipe was of carbon steel having 0.0018 relative roughness having diameter 0.0254 m and third pipe had diameter 0.0127 m and 0.0118 roughness index. The length of pipeline was kept constant i.e. 8.8 meters. They show that drag reducing percentage increases with concentration of DRA.

Kaushik et al. [2012] performed a numerical study on crude oil core-annular flow by using water in sudden expansion and contraction pipeline. They used two different three dimensional model using CFD code FLUENT. The nature of interfacial waves is found three dimensional for contracted and expanded test rig. The fluid velocity nature was asymmetrical across the radial plane surface was observed for both cases. Either increasing the velocity or pipe diameter the fouling was minimum in pipeline network. Results show that oil volume fraction was constant above the 10 L/D contraction and increases up to downstream in case of expansion.

Taiwo et al. [2012] investigated the deposition and precipitation of waxes of crude oil at lower temperature to improve the flowability crude oil petroleum refining and operation in petroleum industry. They performed the rheological experiments on three undoped and doped Nigerian crude. The rate of shear straining was kept constant initially below 50 s^{-1} and gradually increases above 50 s^{-1} . This happens due to consumption energy for breaking off wax matrix bonds. Doping of crude oil results in better rheological characteristics of crude oil. Bingham plastic model best suited experimentally result with correlation coefficient

Benziane and Said [2013] studied the rheological properties of Algerian crude oil at different temperatures. The experimental results obtained by rheometer can be used to predict the crude oil flow characteristics in pipeline. Results of rheogram show the non-Newtonian behaviour of crude oil which follows the Ostwald law. The comparison of shear stresses computations obtained from an analytical model and the MPTT model had given the friction factor distribution across the pipe section.

Desamala et al. [2013] investigated two phase flow pattern transition in horizontal pipeline by using CFD code FLUENT. There applied VOF model for two different boundaries were used for prediction of flow such as wavy stratified, stratified mixed flow by using VOF technique. The simulation results were validated by comparison with experimental results. The experimental result has been well valid for transition boundary. On the other hand mixed stratified, wavy stratified transition boundaries in oil-water had not predicted well. Simulation and analysis had taken long time for giving accurate result.

Maghzi et al. [2013] investigated the rheological properties of polyacrylamide solution with addition of water by using power law at medium shear rate. They added 0.1 wt.% of nanoparticles is used. They found that increase in weight fraction of nanoparticle results in increase of viscosity of nano suspension. Also, the increase in weight percentage of polymer in solution leads to increase the viscosity and polymer flooding at economical level.

Yang et al. [2014] investigated the rheological characteristics and solubility of Kelamayi live oils by addition of different composition of alkane gases at pressure 0–2 MPa. They found that the gas-oil ratio of live oil increases with increase in saturation temperature on increasing the saturation pressure. They found that yield stress, the pour point, viscosity/equilibrium viscosity, abnormal point of the live oil decreases with increase in saturation pressure. Results show that gas dissolves in live oil improves the rheological properties.

Banerjee et al. [2015] performed an experimental study on rheological properties of crude oil with addition of natural surfactant. They investigated the different rheological properties such as thixotropic behavior, pour point, viscosity, yield stress and interfacial tension of crude oil. They added natural surfactant extracted from *Sapindus mukorossi* (soapnut) plant. Results show that the viscosity of crude oil decreased by 80%, thixotropic area to 94.64%,

yield stress by 98% and fluid interfacial tension by 97% with addition of natural surfactant. The FTIR results show that the mechanism inside the crude oil was responsible for its higher viscosity. FTIR results the reduction of C=O, C=C and groups to crude oil after mixing of natural surfactant. *Sapindus mukorossi* (soapnut) can be used in petroleum industry as natural surfactant for improving flowability in pipeline.

Banerjee et al. [2015] studied the rheological behaviour of light crude oil such as crystal size distribution, shape of wax crystal with addition of natural surfactant. They extracted natural surfactant from *sapindus mukorossi* and nonionic surfactant. They used Brij-30 crude oil sample which was collected from ONGC, Gujarat, India. Results show that the viscosity and pour point of light crude oil was reduced significantly after adding natural surfactant. Also, the wax shape of crude oil deforms drastically with the addition of natural surfactant. FTIR results show that flow exhibits functional groups like long chain alkanes and alcoholic groups which decreased with addition of *Sapindus mukorossi*. The addition of surfactants in crude oil transportation enhances the smooth flowability.

Kumar et al. [2015] performed a study to analyze the effect of addition of natural surfactants on rheological characteristics of heavy crude oil. They used the crude oil collected from Mehsana Asset, Gujarat, India to perform the experiments. They investigated the rheological properties including steady and unsteady flow, viscoelastic and thixotropic. They had added the *Madhuca longifolia* in heavy crude oil as an additive. The surfactant was mixed in heavy crude oil in quantity of 1000 and 2000 ppm. The heavy crude oil shows the non-Newtonian flow characteristics at low temperature and decreases with increase in temperature. Fourier transform infrared spectroscopy (FTIR) results reveals that a significant decrease in concentration was found in alcoholic, ketones and alkanes group which increases the viscosity of crude oil. The rheological results show that there is a reduction in viscosity with addition of *Madhuca longifolia* as additive in heavy crude oil suspension which is useful for design of pipeline of oil transportation system.

Rukthong et al. [2015] studied the thermal properties such as thermal conductivity, ambient temperature, wall thickness, surrounding heat transfer coefficient. They correlated the transport profile of crude oil inside the thick-wall pipeline. It was obtained that flow pattern was quite similar to CFD simulation system. The profile obtained from without thick wall

and with thick well is confirmed the necessary of thick-wall in transportation pipeline. The effect of thermal parameters on transport profile of pipeline was obtained by using experimental design data. Heat transfer coefficient, ambient temperature and their interaction had importance on near the pipe wall. Heat transfer coefficient and temperature was affected on pipe center of transportation network.

Cruz et al. [2016] performed experimentation on different properties of Mexican crude oil sample from two different wells and SARA analysis by help of Dynamic Light Scattering (DLS). They also investigated the effects on aggregation state, crude composition, amount of resins and particle size. They used High-Resolution Transmission Electron Microscopy (HTEM) to analyze the presence of asphaltene particle aggregation and ultrafine oriented structures. Results show that increase in C1-RC of crude oil causes decrease in aggregate size of particle by asphaltene disaggregation.

Chapter 3

Experimentations & Results

3.1 Material

In present study, high sulphur crude oil (HSCO) and low sulphur crude oil (LSCO) were supplied from Indian Oil Corporation limited (I.O.C.L.), Panipat, India. Naturally available surfactant *Madhuca longifolia* was used as an additive. *Madhuca longifolia* was collected from Sultanpur, Uttar Pradesh (U.P.), India.

3.2 Preparation of Emulsion

Firstly, the surfactant was extracted from *Madhuca longifolia* fruit. The procedure adapted for surfactant extraction from *Madhuca longifolia* is represented in Fig 3.2. *Madhuca longifolia* fruit was washed with clean tap water for removal of sand from it. Afterwards, moisture of *Madhuca longifolia* was removed by vacuum drying process. Now, the refluxing of *Madhuca longifolia* was performed with ethyl alcohol for 48 hrs. The refluxing of *Madhuca longifolia* with ethyl alcohol was helpful in providing distillate products (ethyl alcohol). At last process, the surfactant was extracted by using ethyl acetate. After preparation of surfactant, two different emulsions of crude oil were prepared by mixing the low sulphur crude oil and *Madhuca longifolia* surfactant with the help of magnetic stirrer. Magnetic stirrer was run at 1500 rpm for each emulsion with time duration of 1 hrs. The concentration *Madhuca longifolia* of surfactant and LSCO in HSCO was taken as 10 and 15% (by volume) which is shown in Fig 3.1.

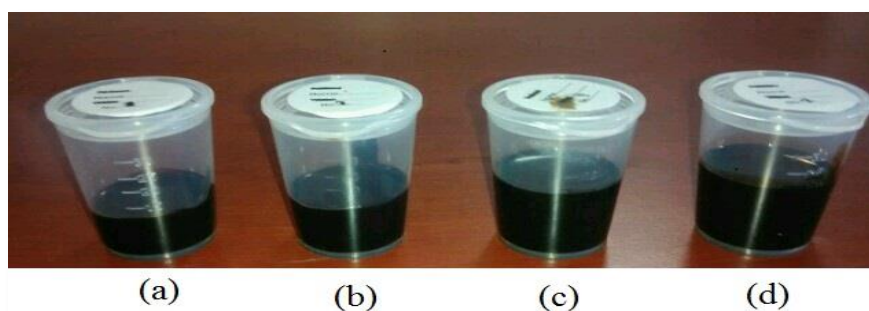


Figure 3.1: (a) 90% HSCO-10% LSCO (b) 85% HSCO-15% LSCO (c) 90% HSCO -10% *Madhuca longifolia* (d) 85% HSCO-15% *Madhuca longifolia*

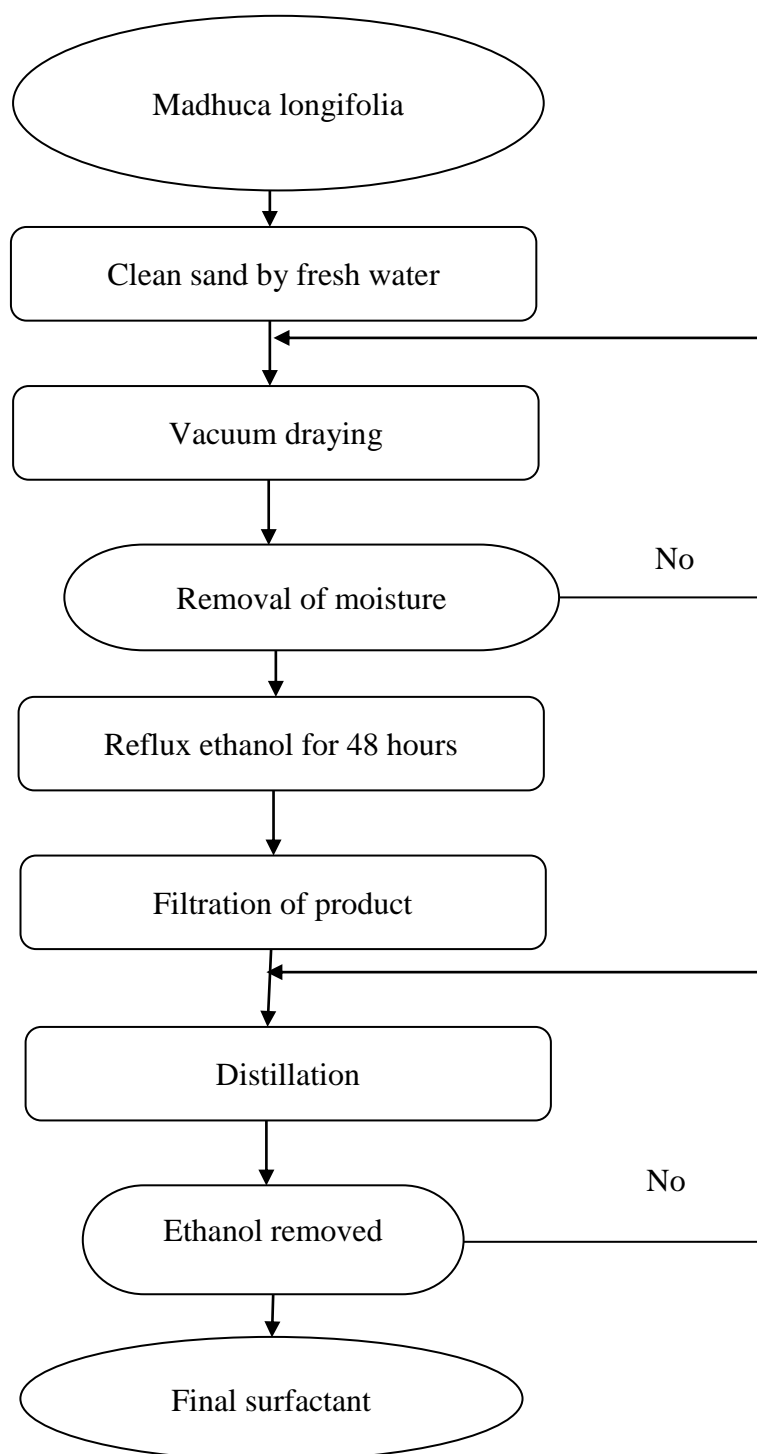


Figure 3.2: Flow diagram of surfactant extraction from *Madhuca longifolia*

The physical parameters namely density, viscosity, pour point, basic sediment & water percentage were tested by using American Society of Testing Materials (ASTM) methods i.e. shown in Table 3.1. The rheological characteristic of crude oil and its emulsions (with low

sulphur crude oil and surfactant) was evaluated using ISO certified Rheometer (Rheolab Q-C, APC Ltd. Germany).

Table 3.1: Physical properties and test method

S. No.	Parameter	Units	Method	HSCO	LSCO
1	Density	kg/m ³	ASTM D1250	874.6	837.6
2	Basic sediment & water	wt. %	ASTM D4007	0.125	0.10
3	Water	wt. %	ASTM D4928	0.06	0.04
4	Sulphur	wt. %	ASTM D4294	2.58	0.18
5	Viscosity	Pa.s	Rheometer	.006	.0054
6	Pour point	^o C	ASTM D97	55	53
7	Color	-	-	Black	Black

3.3 Experiment setup

In present study, rheology, Fourier transforms Infrared Spectroscopy (FTIR) Dynamic Light Scattering (DLS) and Optical Microscopy (OM) of crude oil and its emulsions were performed. The rheological characteristic of crude oil and its emulsions (with low sulphur crude oil and surfactant) was evaluated using ISO certified Rheometer (Rheolab Q-C, APC Ltd. Germany).the rheometer is shown in Fig 3.3. Rheological experiments were conducted for temperature range 25 to 45°C at various operating modes like oscillation test (OSC), universal controlled rate (CR) and controlled stress (CS) mode. During experiments, the drive shaft of rheometer was centralized with help of bearing to ensure adequate transmission of applied stress on given fluid. A digital encoder that possesses 10⁶impulses/revolution was used to obtain the resulting deformation in emulsion. Each resolution produces small strain or shear rate and yield stress value. Cone plate sensor was used for sensing the measuring only feeding value. At initial state, various measurements were taken to evaluate reproducibility of rheometer. Reproducibility of experiment measurements was found satisfactory and relative error was found about 4%.



Figure 3.3: Rheometer (Anton Paar, Germany)

3.4 Results and Discussion

3.4.1 Rheological properties measurement

Present study is carried out to investigate the possibility of transporting heavy crude oil with natural surfactant and light crude oil. Steady flow behavior, yield stress behaviour thixotropic behavior and inner molecular structure of crude oil and emulsions are investigated.

3.4.2 Steady Flow Behavior

In present study, CR mode of rheometer is used to determine the viscosity (ν) and shear rate of HSCO and its emulsions which represent their flow behavior. The comparisons were made to investigate the behavior of LSCO and natural surfactant (*Madhuca longifolia*). It was observed that viscosity (ν) of *Madhuca longifolia* was less than that of HSCO with LSCO. The presence of 10% LSCO caused strong reduction in viscosity from 5.8 to 5.4mPa.s. For *Madhuca longifolia*, the viscosity reduction in HSCO and with LSCO was found from 5.8 to 5.1mPa.s at 25°C as shown in Fig 3.4 and 3.6. While HSCO with 15% LSCO was used the viscosity drops from 5.8 to 4.5mPa.s whereas 5.8 to 5.3mPa.s for *Madhuca longifolia*, as shown in Fig 3.5 and 3.7. Addition of 10 and 15% by volume of LSCO decreases the viscosity of HSCO by 31.0% and 44.8%, respectively at 35°C whereas decreased 10.3% and 27.5% of *Madhuca longifolia* at same temperature.

Table 3.2: Properties of crude oil at shear rate of 500 s^{-1}

Sample	25°C		35°C		45°C	
	N	DVR	v	DVR	N	DVR
S1	5.8	-	5.6	3.4%	4.3	25.8%
S2	5.4	6.9%	5.2	10.3%	4.1	29.3%
S3	5.3	13.8%	4.2	27.5%	4.0	31.0%
S4	5.1	12.1%	4.0	31.0%	3.5	39.6%
S5	4.5	22.4%	3.2	44.8%	2.5	56.9%

It can be observed that viscosity reduction remains significant at low temperatures also. Dynamic viscosity reduction (DVR %) of HSCO was reduced more economically by using *Madhuca longifolia* which can be confirmed from Table 3.2. Figure 3.8 represents the flow behavior of HSCO. It was observed that HSCO shows non-Newtonian shear thinning behavior while increasing the temperature from 25 to 45°C. This happens due to fact that the component of high molecular weight like waxes, resins and asphaltenes etc. does not form complex bond at high temperature which results in viscosity reduction [Zahrani and Fariss, 1998].

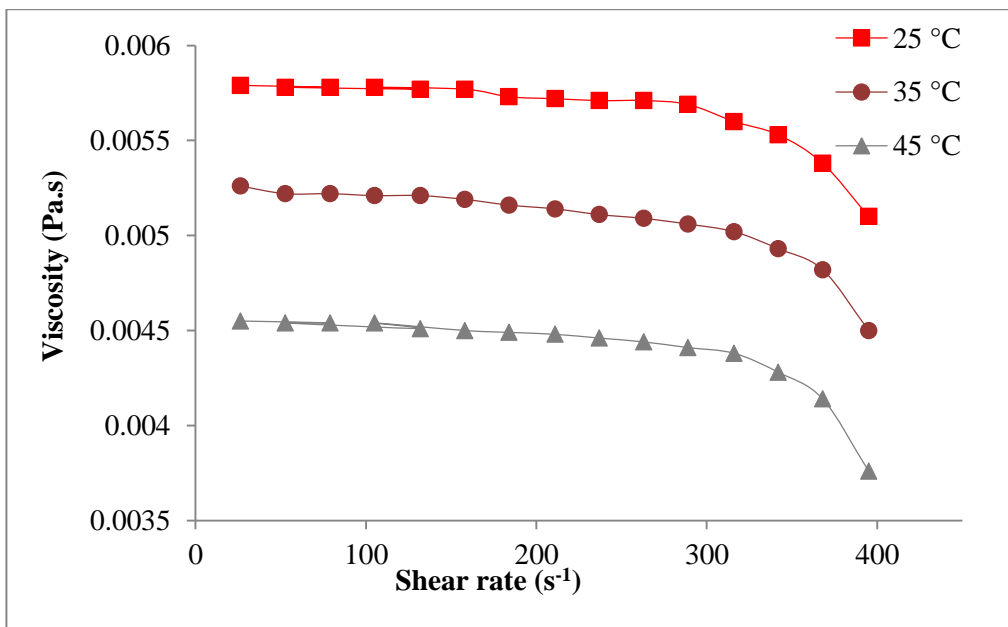


Figure 3.4: Viscosity behavior of 90% high sulphur crude oil -10% *Madhuca longifolia*

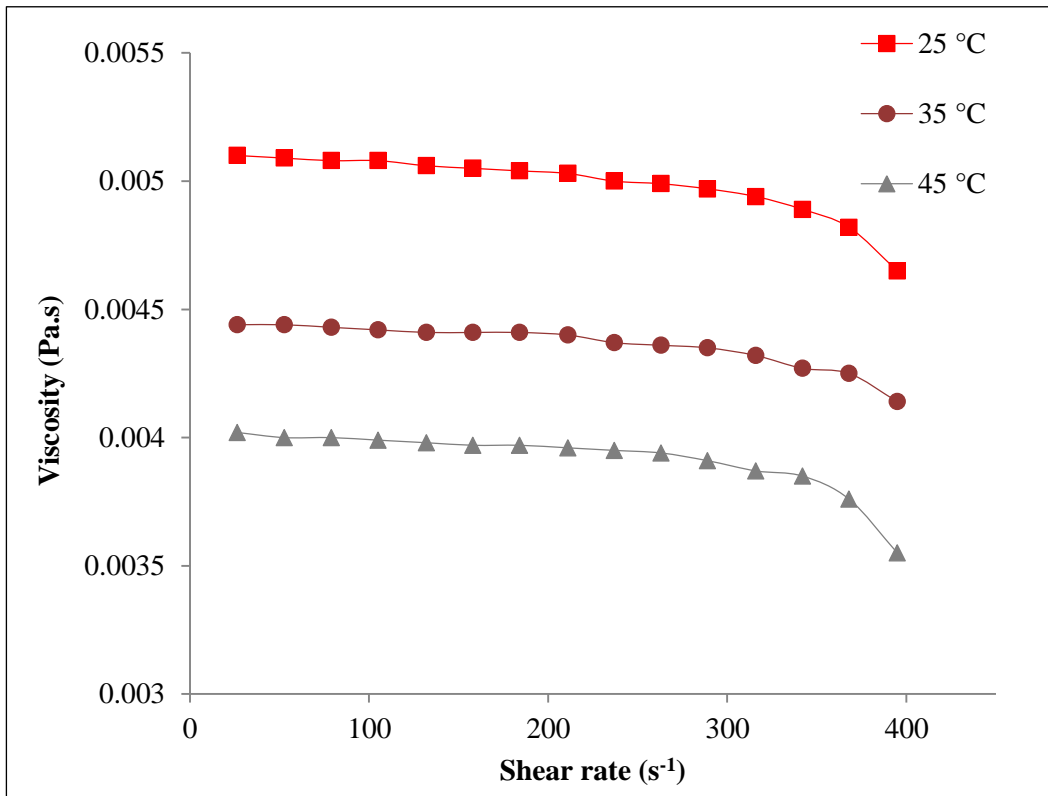


Figure 3.5: Viscosity behavior of 85% high sulphur crude oil -15% Madhuca longifolia

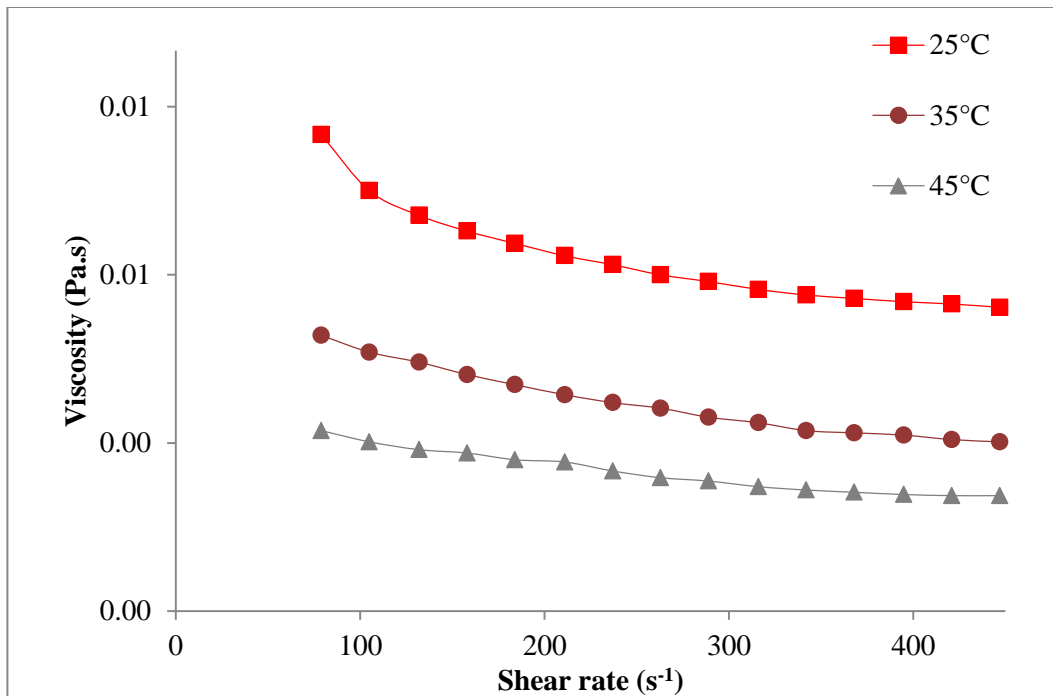


Figure 3.6: Viscosity behavior of 90% high sulphur crude oil -10% light sulphur crude oil

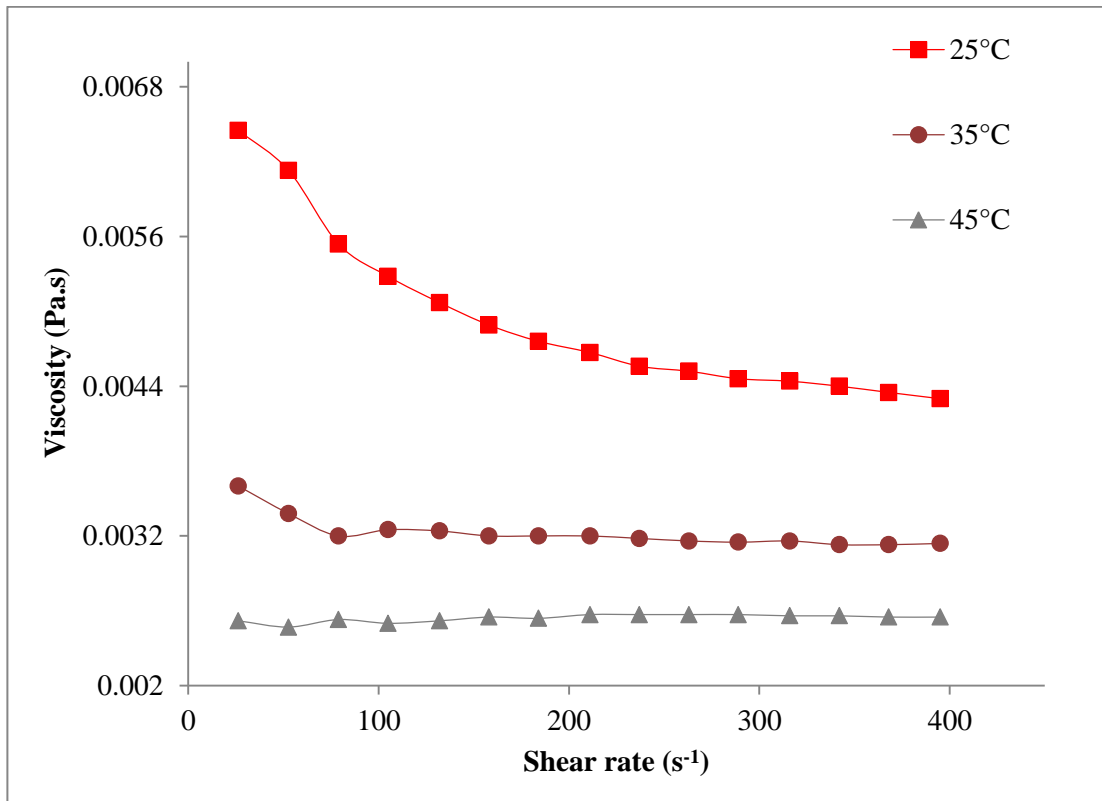


Figure 3.7: Viscosity behavior of 85% high sulphur crude oil -15% light sulphur crude oil

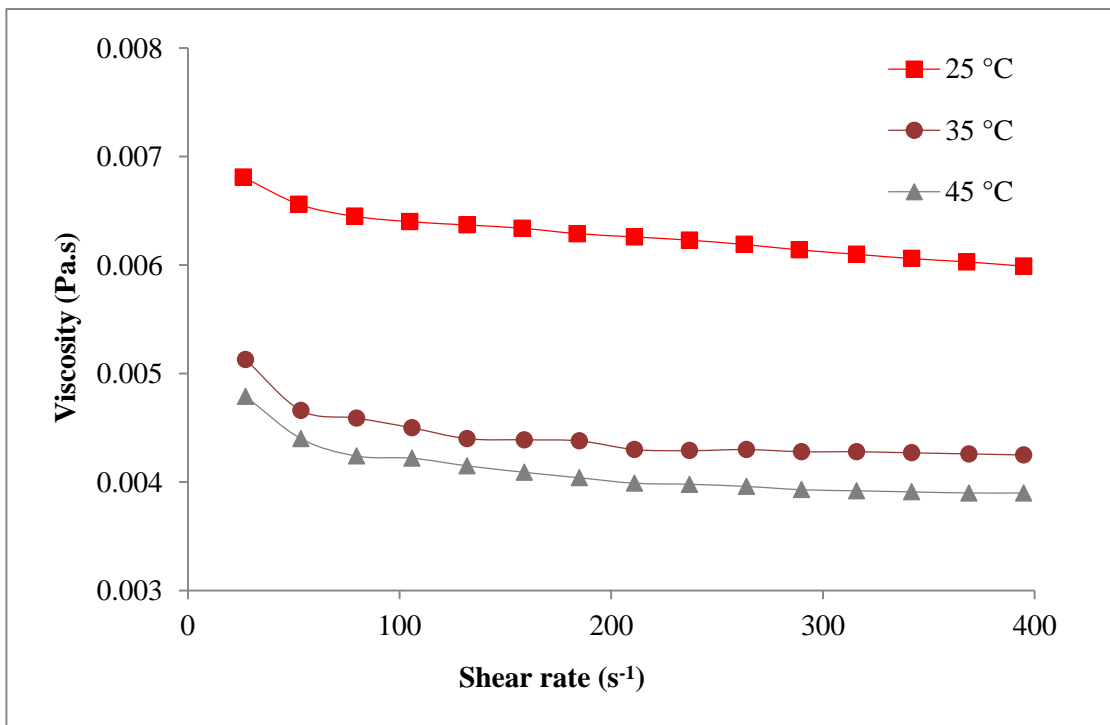


Figure 3.8: Viscosity behavior of 100% high sulphur crude oil at different temperature

3.4.3 Yield stress Flow behavior

In present study, yield stress was determined from shear stress to shear rate curve obtained from rheometer. The controlled stress (CS) mode of rheometer is used to measure the yield stress which produce high precision results as compare to controlled rate (CR) mode, as recommended by Schramm et al. [Rashed et al., 2016]. Yield stress of each sample was recognized with help of Bingham model. As per the observation, yield point decreases with increase in temperature. Figure 3.9 and 3.11 indicates that apparent yield stress diminishes with the addition of 10% of Madhuca longifolia and LSCO respectively in HSCO. This happens due to elimination of stresses from crude oil with addition of surfactant which tends toward decrease in viscosity of crude oil while 15% of Madhuca longifolia and LSCO was added more the stresses in HSCO were eliminated due to change in inner mechanism of crude oil, as shown in Fig 3.10 and 3.12. The small variation in stress level causes a significant change in mechanical properties of structured fluid. However, the material tends to deforms elastically below the specified stress level. This happens due to reason that beyond this stress level the applied stress produce continuous deformation in the fluid which results in smooth flow of crude oil emulsion. The shear stress to shear rate response at different temperatures of is represented by Fig 3.13. The yield point of HSCO shifts from 1.6 to 1 Pa with increase in temperature from 25 to 45°C.

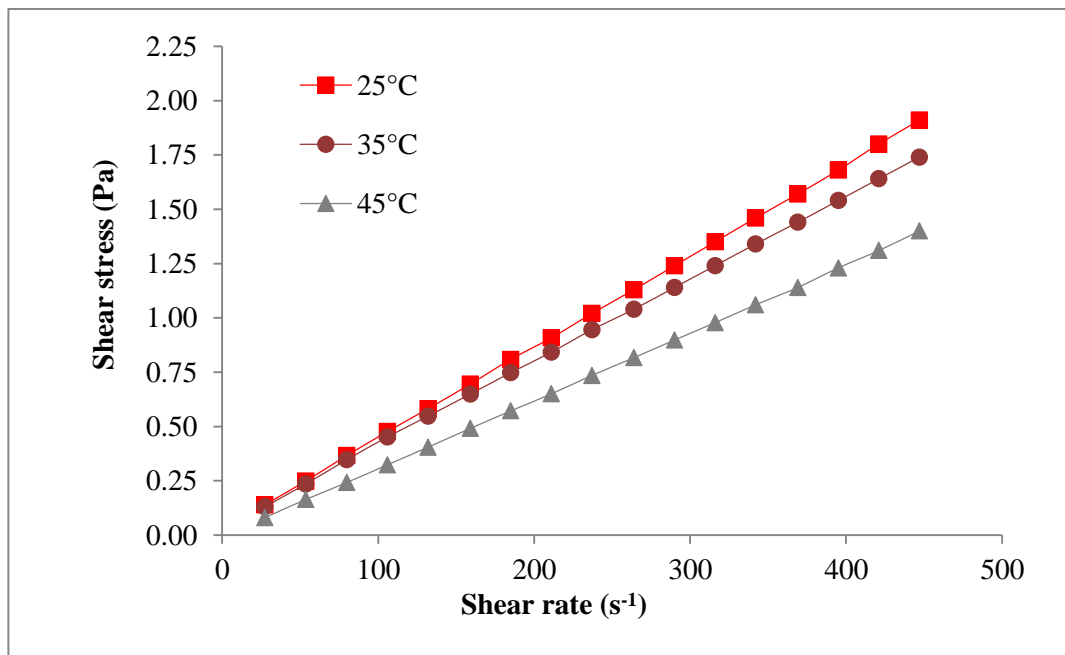


Figure 3.9: Yield stress behavior of 90% high sulphur crude oil -10% Madhuca longifolia

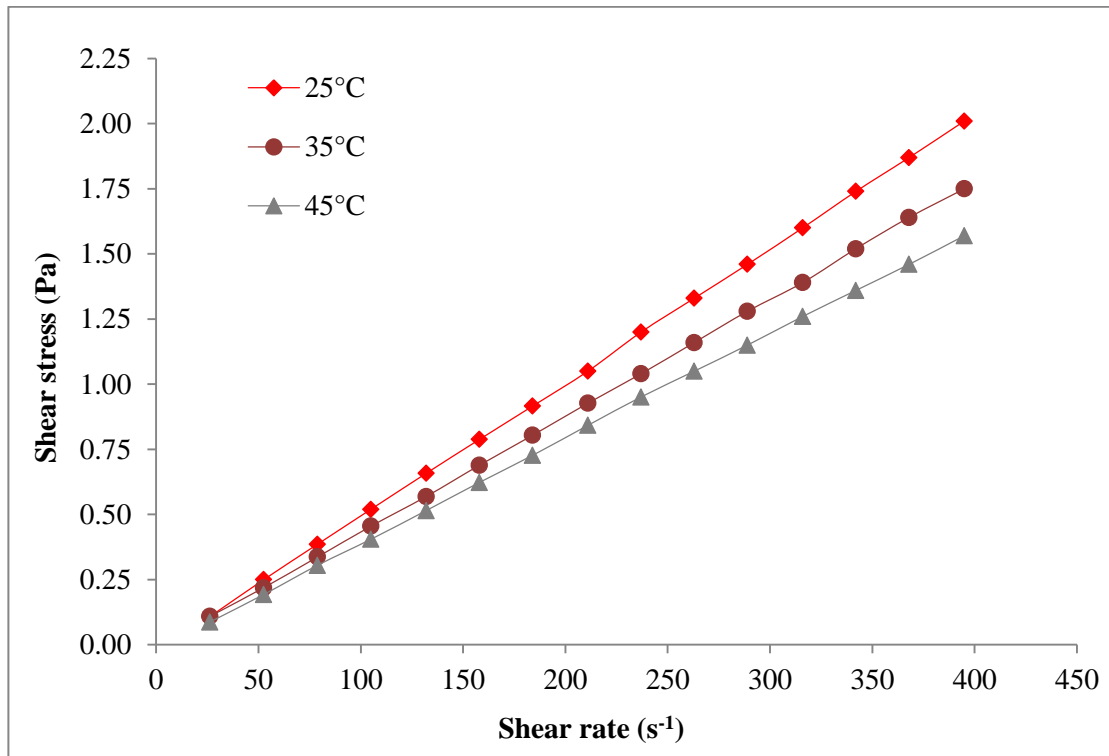


Figure 3.10: Yield stress behavior of 85% high sulphur crude oil -15% Madhuca longifolia

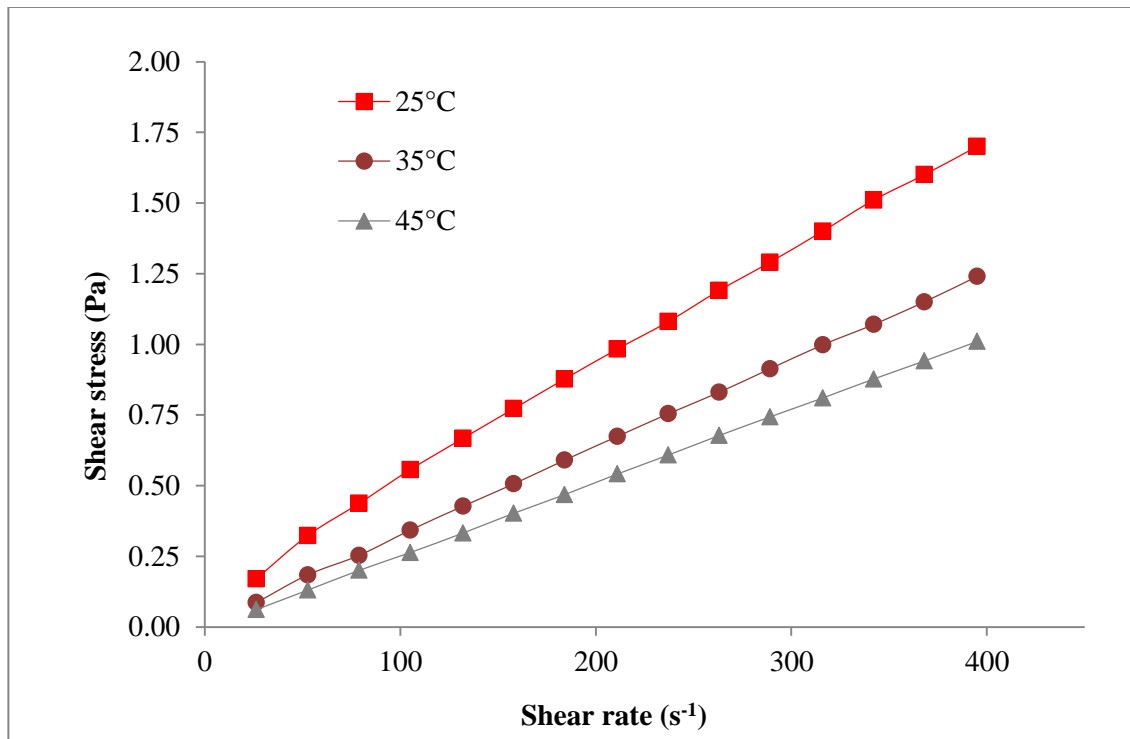


Figure 3.11: Yield stress behavior of 90% high sulphur crude oil -10% light sulphur crude oil

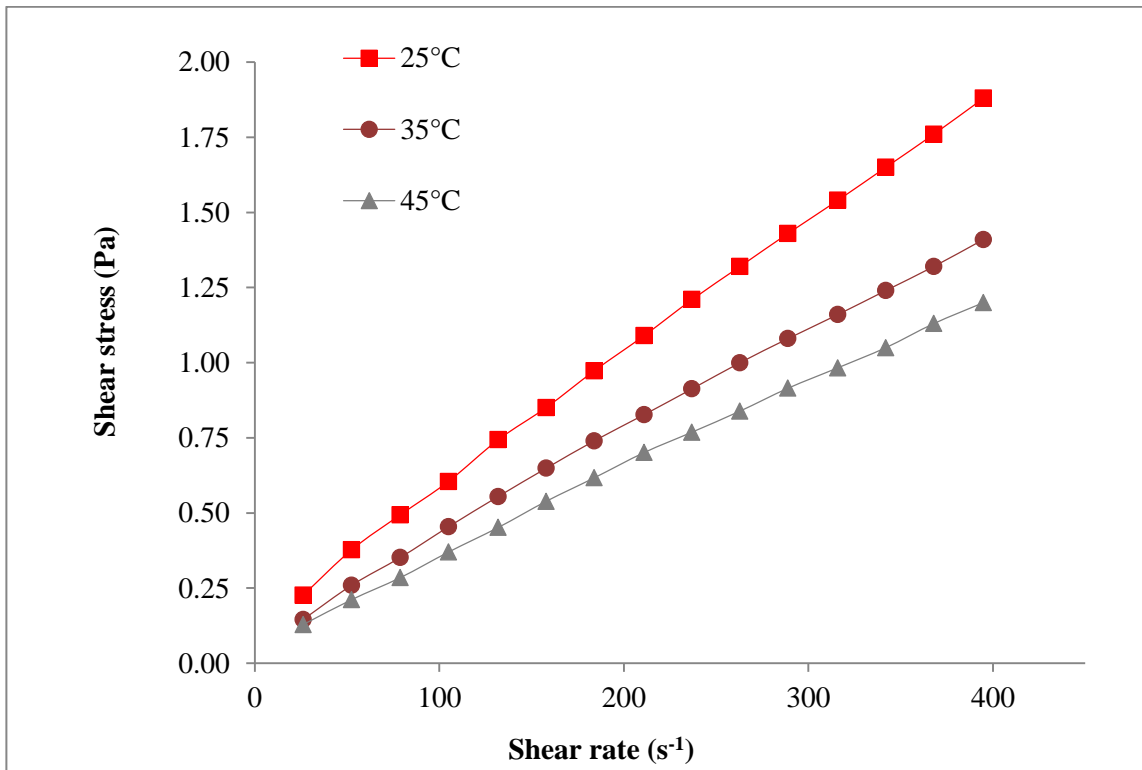


Figure 3.12: Yield stress behavior of 85% high sulphur crude oil -15% light sulphur crude oil.

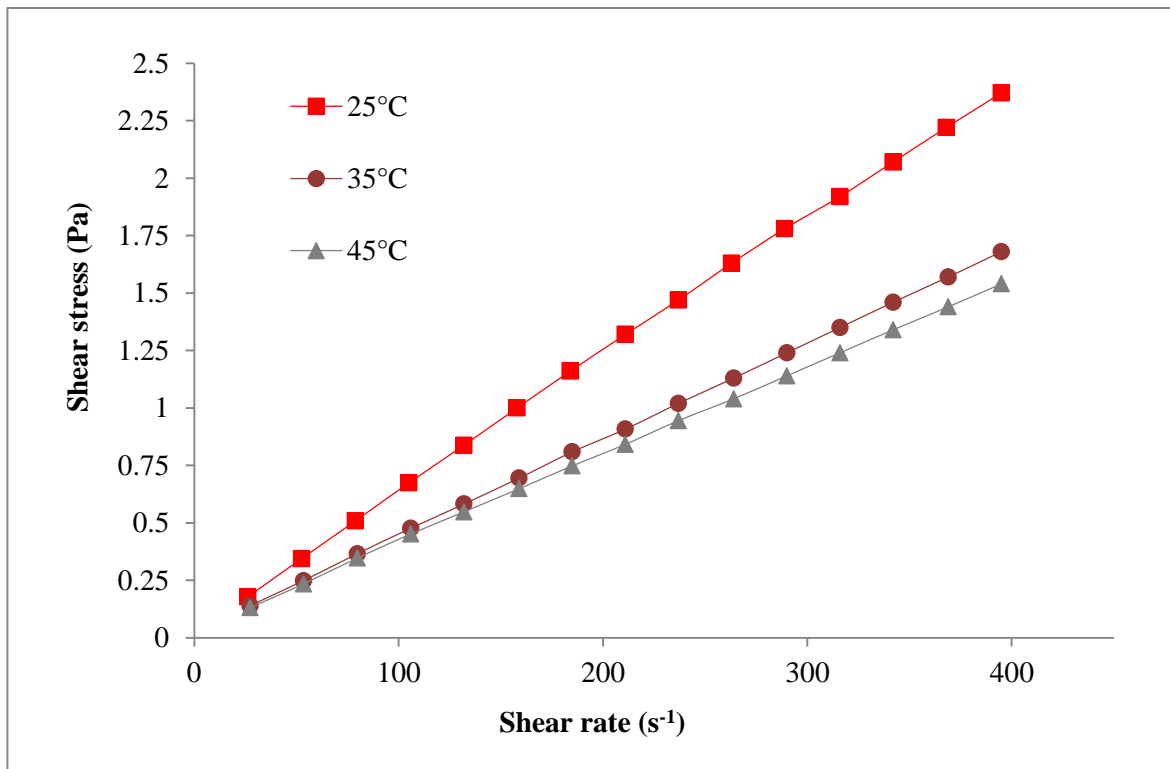


Figure 3.13: Yield stress behavior of 100% high sulphur crude oil at different temperature.

3.4.4 Thixotropic Flow behavior

Thixotropic behavior of HSCO, HSCO-LSCO mixture and HSCO-Madhuca longifolia mixture was investigated in present study to determine the magnitude of change in microstructure from one state to other and vice versa. Thixotropic experiments were carried out on HSCO for up and down cycle of 100 seconds which is required to break the thixotropic structure of HSCO. The shear rate ramped up 0.8 to 700 s^{-1} within 100 seconds and the quickly ramped down from 700 to 0.8 s^{-1} in equal time. The value of thixotropy in terms of energy per unit volume was calculated from the hysteresis loop area which enclosed between the up-curve and down-curve rheograms [Wang et al., 2016]. Hysteresis loop area of HSCO and its emulsions is summarized in Table 3.3. It was found that the mixing of Madhuca longifolia and LSCO in HSCO depletes the thixotropic behavior and results in the reversal of processes which makes the up and down curve to coincide for concentration of 10% and 15% respectively which is show in Fig 3.14-3.17. An identical up and down curve was noticed at temperature of 25°C and 35°C which indicates the unnoticeable thixotropic behavior of HSCO. Thixotropic behavior of HSCO at different temperatures is shown in Fig 3.18.

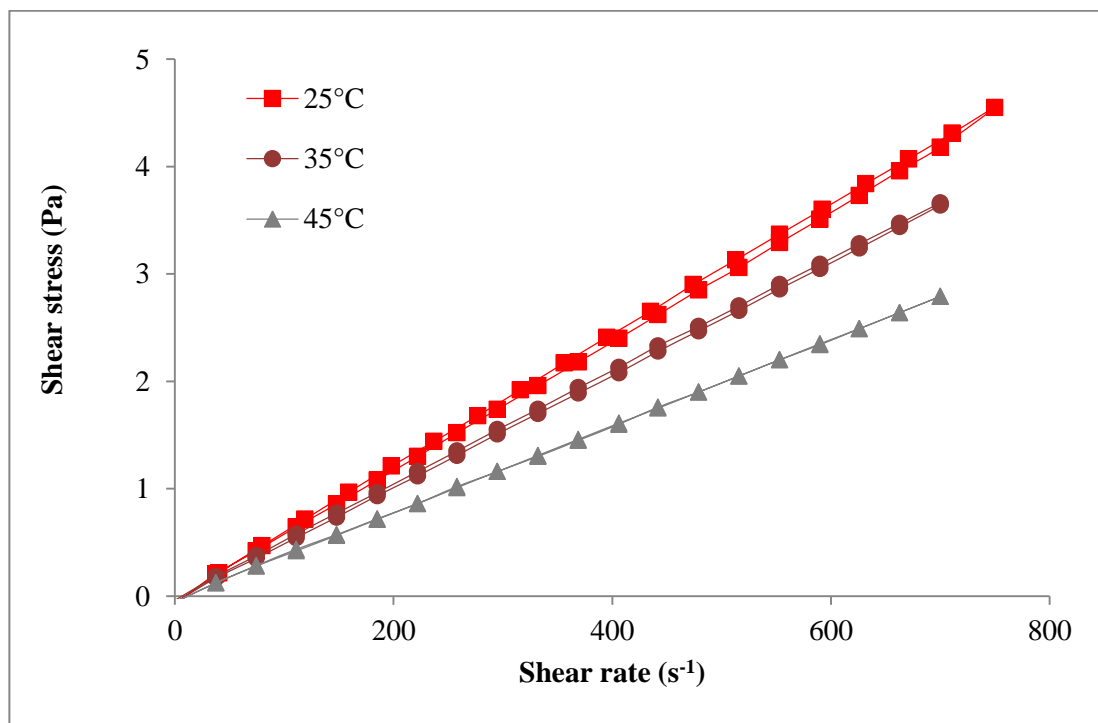


Figure 3.14: Thixotropic behavior of 90% high sulphur crude oil -10% Madhuca longifolia

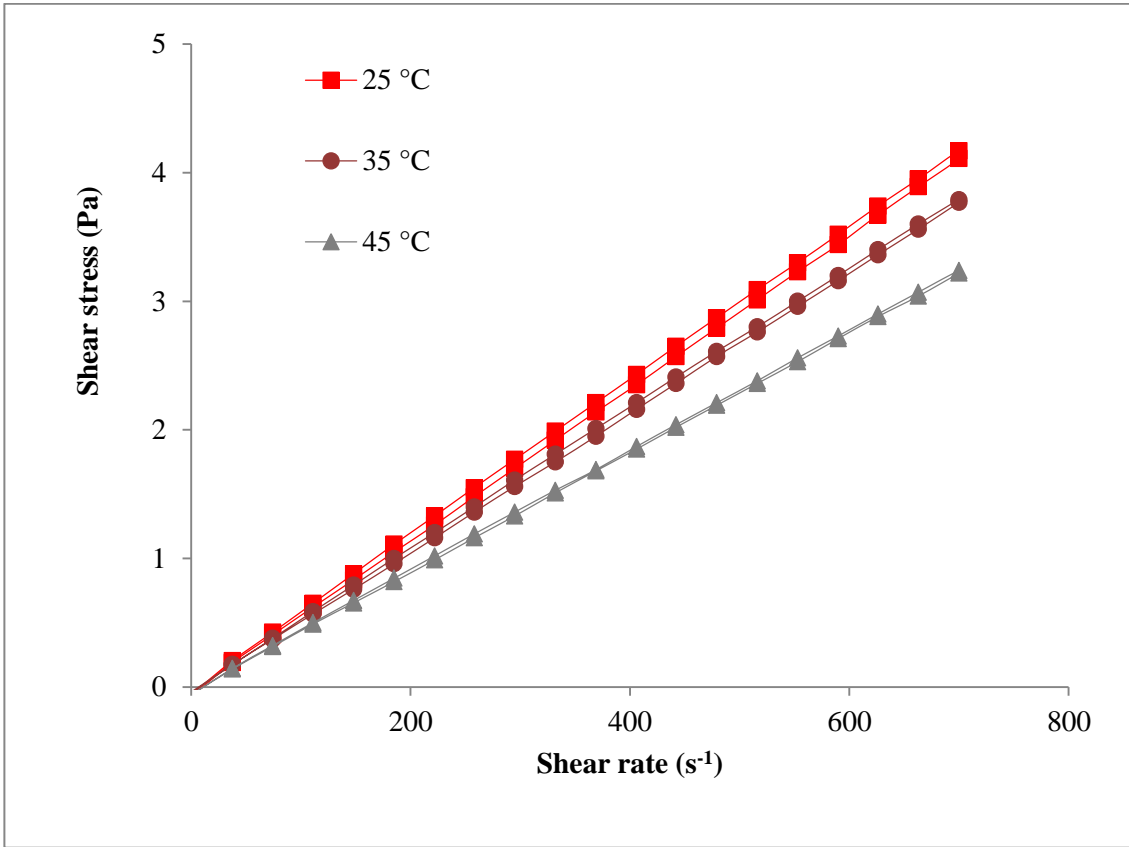


Figure 3.15: Thixotropic behavior of 85% high sulphur crude oil -15% Madhuca longifolia

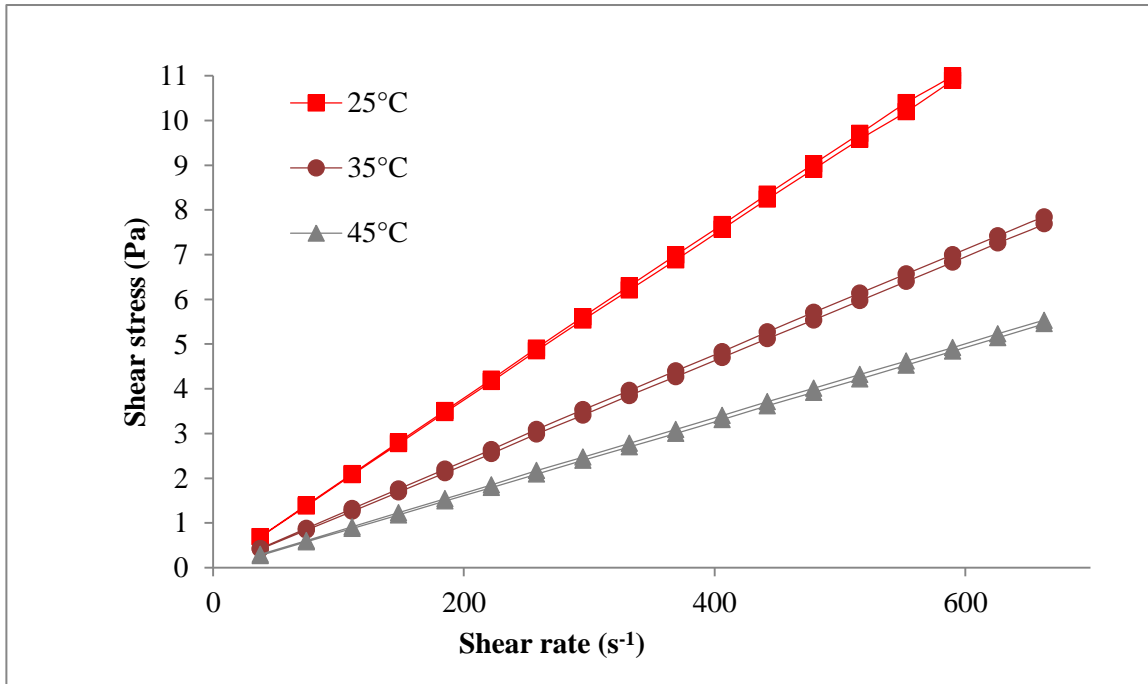


Figure 3.16: Thixotropic behavior of 90% high sulphur crude oil -10% light sulphur crude oil

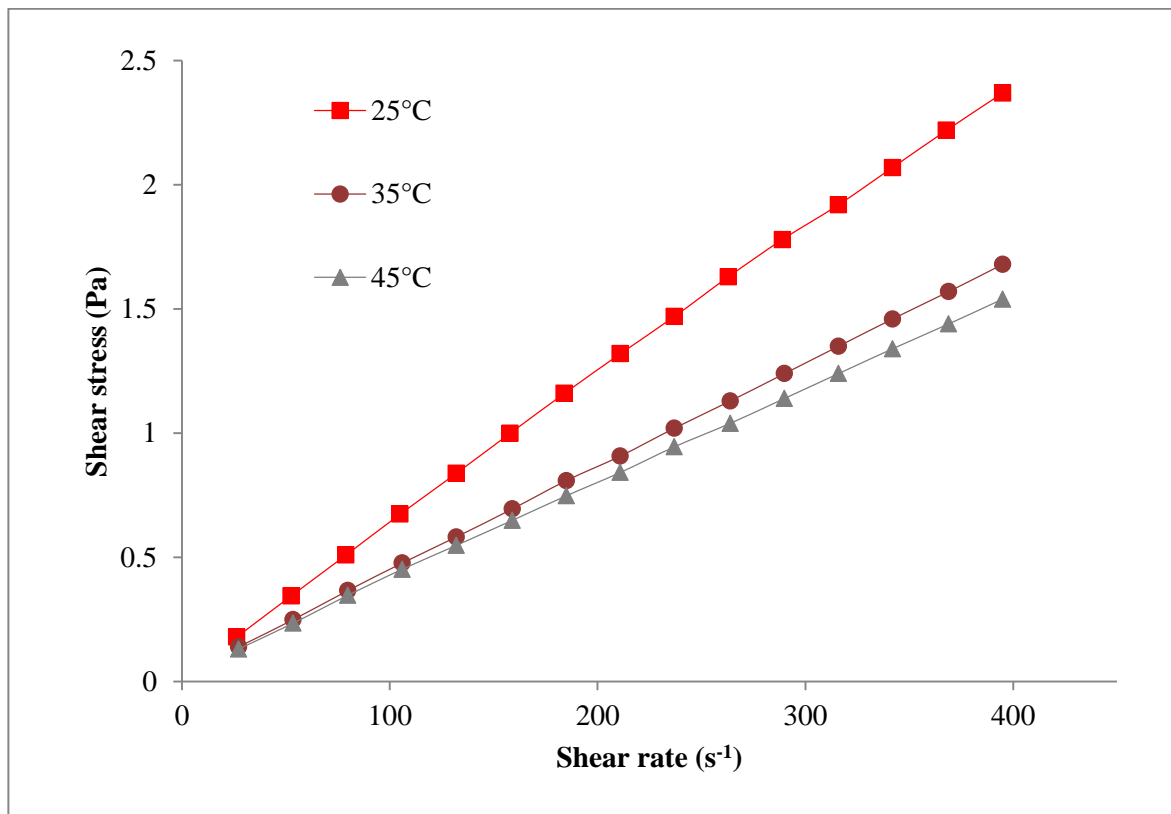


Figure 3.17: Thixotropic behavior of 85% high sulphur crude oil -15% light sulphur crude oil

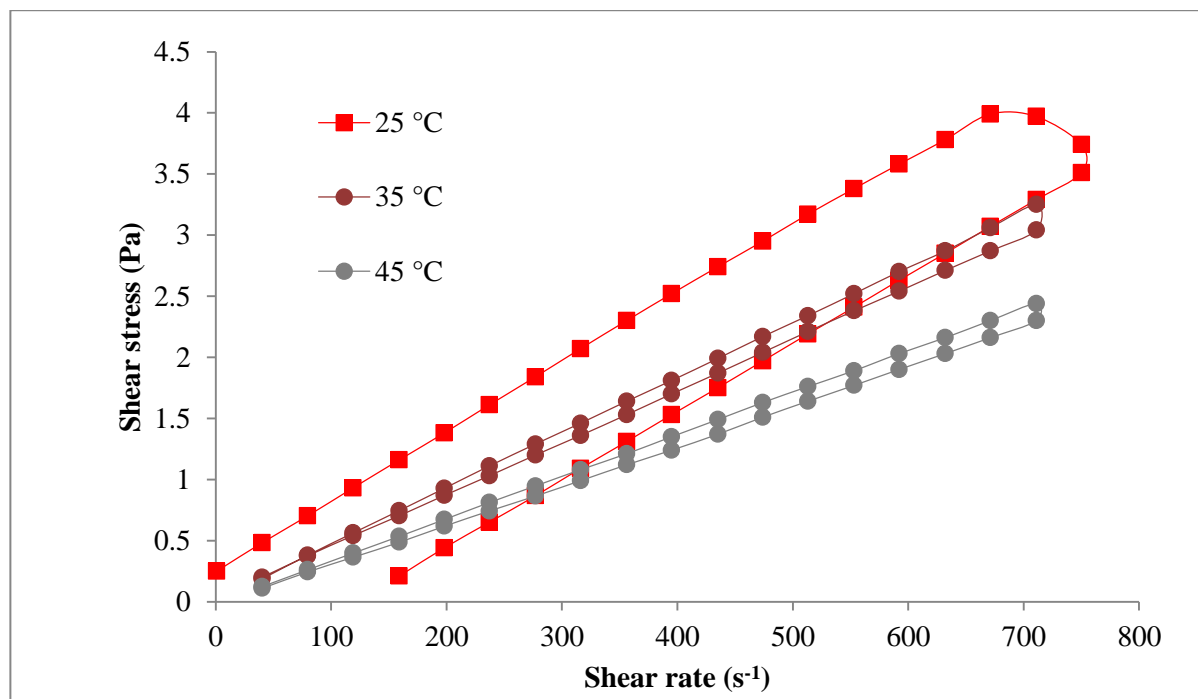


Figure 3.18: Thixotropic behavior of 100% HSCO at different temperature

Table 3.3: Hysteresis area at different temperatures

S.No.	Temperature (°C)	Hysteresis area (Pa.s ⁻¹)				
		S1	S2	S3	S4	S5
1	25	226	195	130	120	60
2	35	196	192	126	70	10
3	45	89	0	0	64	0

3.5 Optical Microscopy (OM)

Optical Microscopy (OM) was used to analyze the change of wax crystal sizes before and after addition of LSCO and Madhuca longifolia. A simple polarized light based inverted microscope (Model MA100, ECLIPSE, Nikon Metrology, Europe) was used to perform the optical microscopy at 25 °C .the optical microscope is shown in Fig 3.19.



Figure 3.19: Optical Microscope (Source: Microscope science)

Microscopic images of HSCO are shown in Figure 3.20. From Figure 3.20, the larger sized spherical globules appeared in HSCO. Larger sized globulite structure adhere the smooth flowability. The effect of addition of LSCO and Madhuca longifolia is shown in Figure 3.21 and 3.22 respectively. From Figure 3.21, the addition of LSCO in HSCO decreases the size of wax particles. From Figure 3.22, it can be observed how the morphology of the wax crystals changes with type of surfactant. The addition of Madhuca longifolia in HSCO dispersed the globulite structure of wax particles. Also, the natural surfactant changes the globulite structure rod-like structure. Therefore, the flowability of HSCO increases with addition of natural surfactant. Natural surfactant acts as a better wax inhibitor than LSCO.

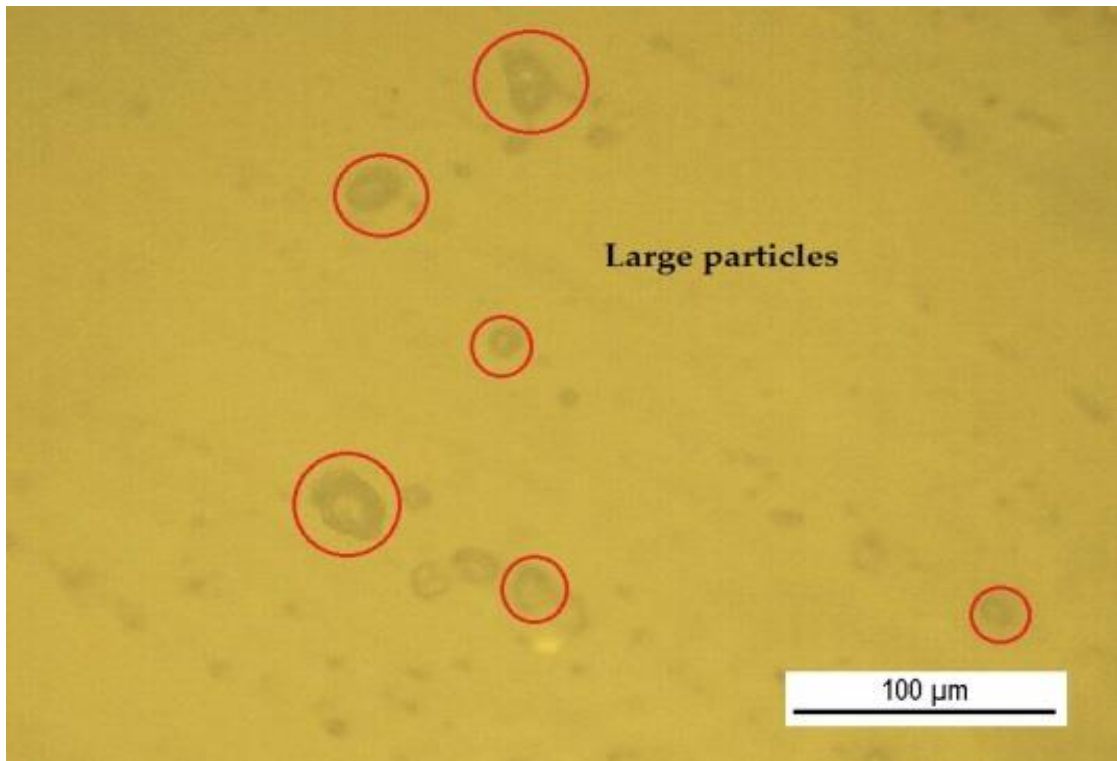


Figure 3.20: Optical microscopic images of 100% high sulphur crude oil

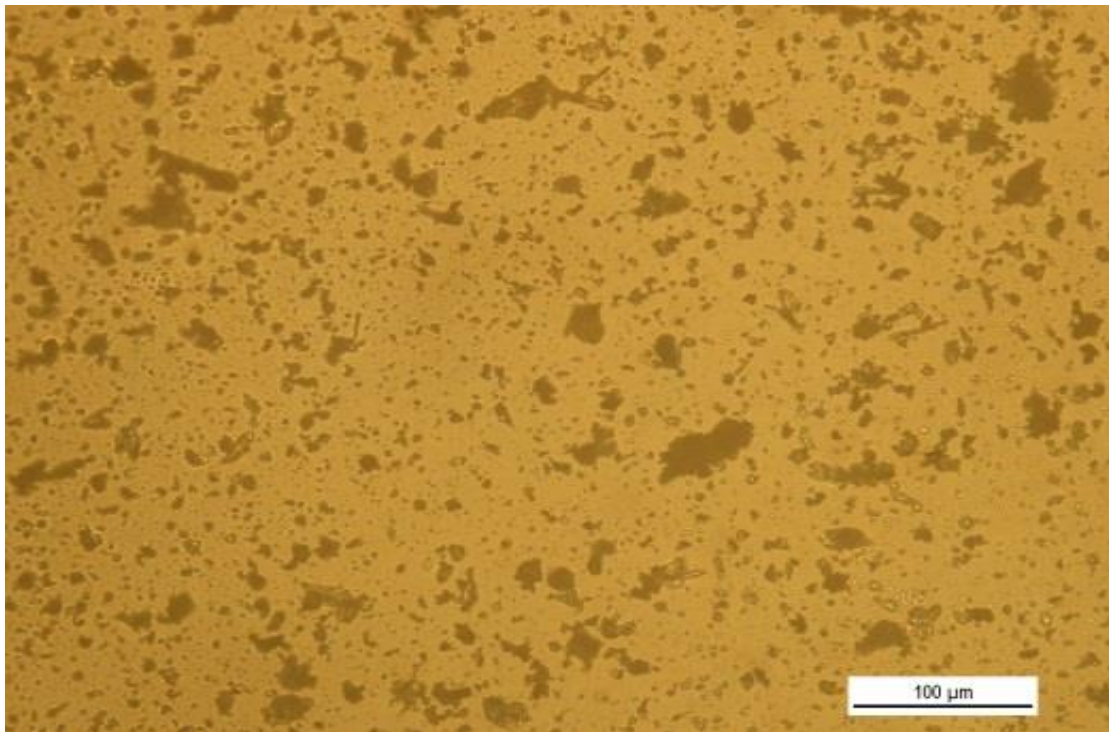


Figure 3.21: Optical microscopic images of 85% high sulphur crude oil -15% light crude oil

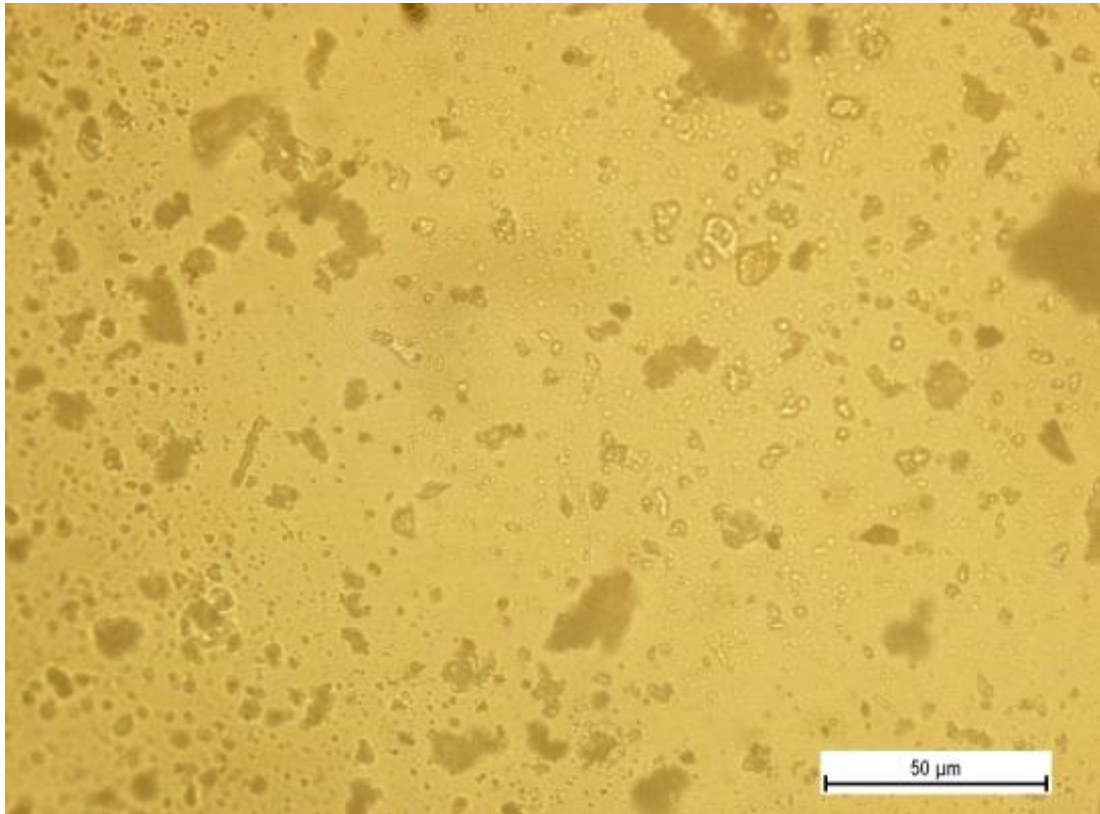


Figure 3.22: Optical microscopic images of 85% high sulphur crude oil -15% Madhuca longifolia at 25 °C.



Figure 3.23: Photograph of Fourier Transform Infrared Spectrometer

3.6 Fourier Transform Infrared Spectroscopy (FTIR)

In present study, FTIR study was conducted to determine the functional group which changes the inner structure of crude oil emulsion and reduces its viscosity. A FTIR spectrometer (Model Cary 600 series, Agilent Technologies, Victoria, Australia) was used to conduct the FTIR study which is shown in Fig 3.23. Wave numbers of crude oil and emulsions obtained from FTIR study is listed in Table 3.4 which represents the dominant peaks. The comparative occurrence of functional groups in HSCO-LSCO and HSCO-Madhuca longifolia mixture determine their dependability for viscosity reduction. The wave number 1710 cm^{-1} for aldehydic group (CH=O) group were found responsible in spectra of HSCO. It was found that spectra of HSCO and HSCO-Madhuca longifolia mixture are identical. However, amines and hydrogen bonded alcohol creates major difference between HSCO and HSCO-Madhuca longifolia mixture FTIR spectra. It was also found that concentration of ketones, aldehyde reduces with addition of surfactant in crude oil. FTIR peak of high sulphur crude oil is shown in Fig 3.25-3.26. HSCO-Madhuca longifolia mixture has a lesser degree of aliphaticity as compared to pure HSCO. It indicates that carbon-carbon (C=C), carbon-hydrogen (C-H) and carbon-oxygen (C=O) bonds dissipate in presence of surfactant functional group. Inner component of high sulphur crude oil agglomerates with addition of surfactant which results in viscosity reduction and flow behavior improvement. Similar phenomenon was found by [Coto et al., 2014].

Table 3.4: Wave numbers (cm^{-1}) of HSCO and its emulsions

S. No.	Functional Group	HSCO	85% HSCO + 15% LSCO	85% HSCO+ 15% Madhuca longifolia
1	Alkanes	1470.30	1458.12	1459.029
2	Alkenes	1625.00	1603.700	1638.029
4	Amino compound	1375	1370.32	-
5	Aldehydes and ketones	1710.00	1690.31	1705.48
6	Carboxylic acids	2012.16	2023.50	-
7	Alcohol and phenols	-	-	3354.548
8	Nitro compounds	1510.00	1375.539	1374.607

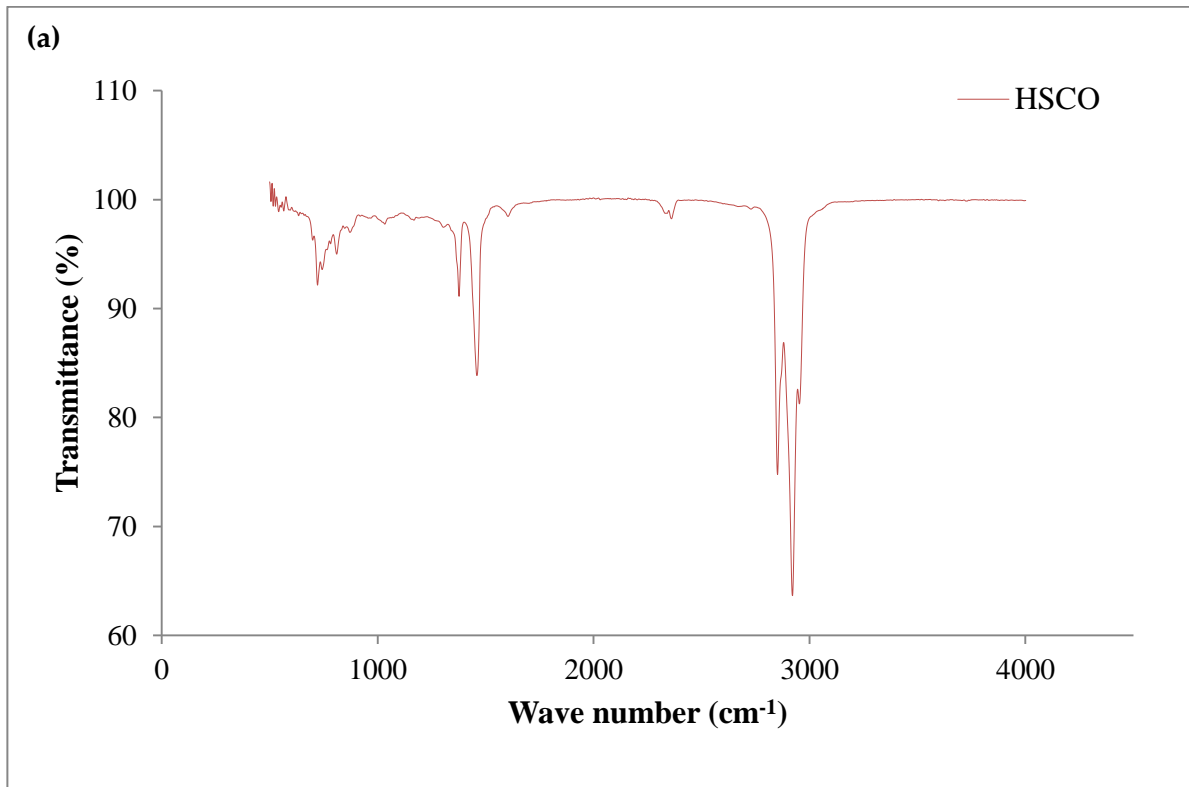


Figure 3.24: FTIR spectra of HSCO without additives

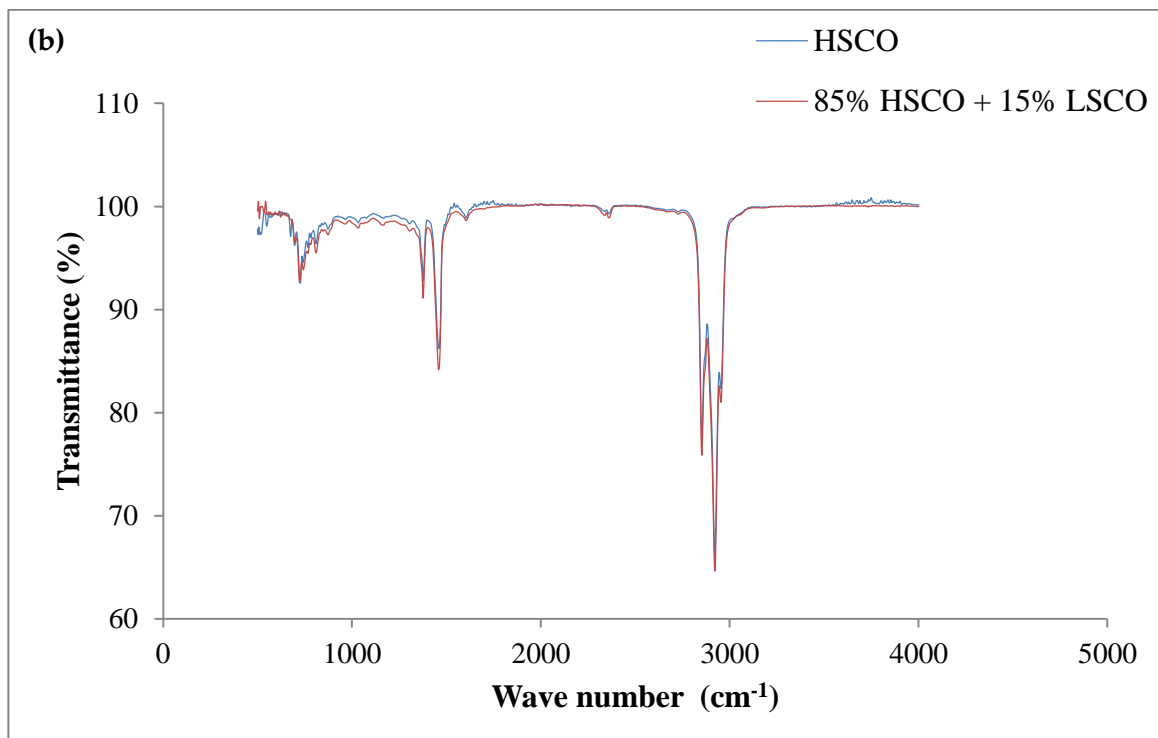


Figure 3.25: FTIR spectra of HSCO with 85% HSCO + 15% LSCO

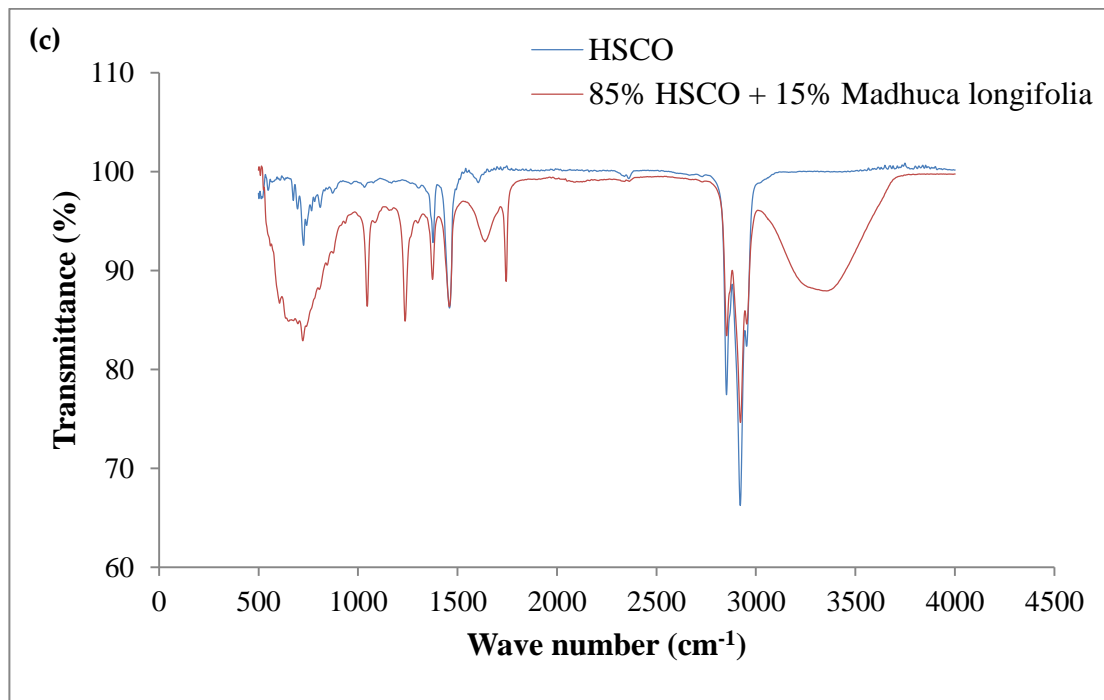


Figure 3.26: FTIR spectra of HSCO with 85% HSCO + 15% Madhuca longifolia at 25 °C.



Figure 3.27: Photograph of Dynamic Light Scattering instrument

3.7 Dynamic Light Scattering (DLS)

Dynamic Light Scattering instrument (Model ZEN3600, Malvern Instruments Ltd., Malvern, U.K.) is used to measure the particle size by diffusing scattered light through the crude oil.

Zetasizer system of DLS instrument had analyzed the diameter of particle crystals by calculating Brownian motion then interprets their diameter using recognized theories. The Dynamic Light Scattering instrument is shown in Fig 3.27. Zetasizer module determines the size distribution of wax particles with the help of relation between diffusion speed and size. The size of particles can be found by analyzing their movements. While the position of wax particles from each other appears same and their movements were minimum then it denotes the existence of larger sized wax particles. While a movement of particles becomes arbitrary from each other than it denotes towards their small size. In present study, DLS instrument was used to perform the quantitative analysis of the micrographs of pure crude oil and its emulsions with LSCO and natural surfactant. Figure 5 represents the DLS graphs of pure crude oil and its emulsions. From Figure 3.28, It is found that the radius of HSCO wax crystals lie in the range of 2000–3100 nm. The average size of wax crystals seems to be larger i.e. approximately 2550 nm which will abstract the smooth flow in pipeline. From Figure 3.29, the size distribution of wax particles decreases with addition of 15% addition of *Madhuca longifolia*. The wax crystal particle size was ranging from 210–350 nm. Figure 3.30 represents the DLS graph of 85% HSCO and 15% LSCO mixture. From DLS, the radius of wax crystal was found in range 600–1100 nm. The average wax crystal particle size was found approximately 850 nm which is comparatively higher than 85% HSCO and 15% natural surfactant mixture.

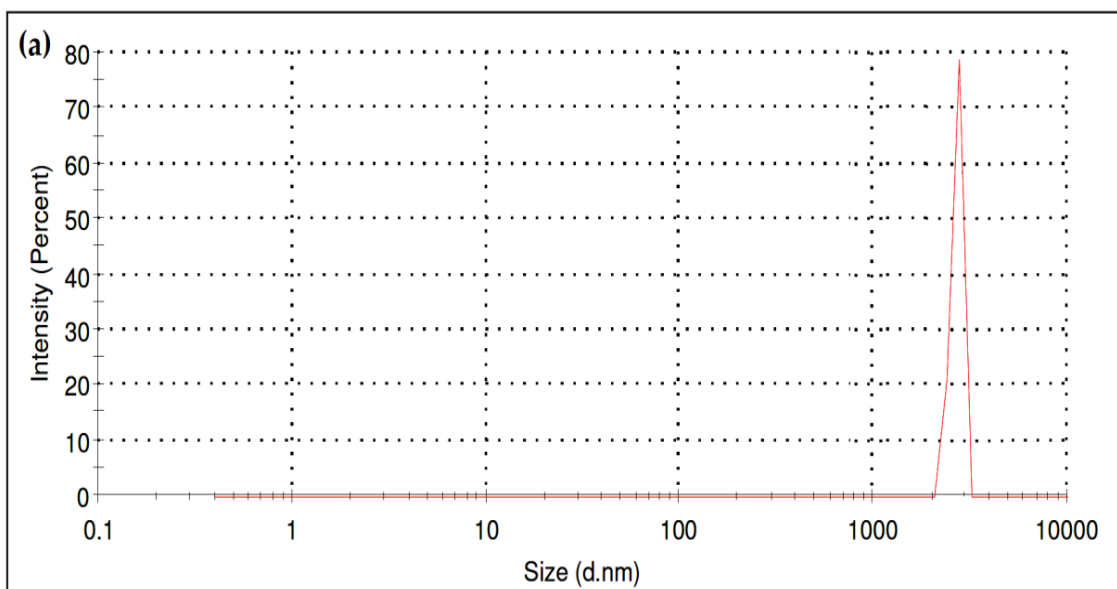


Figure 3.28: Average particle size of Average particle size of 100% HSCO paraffin crystals ranges from 700–1200 nm

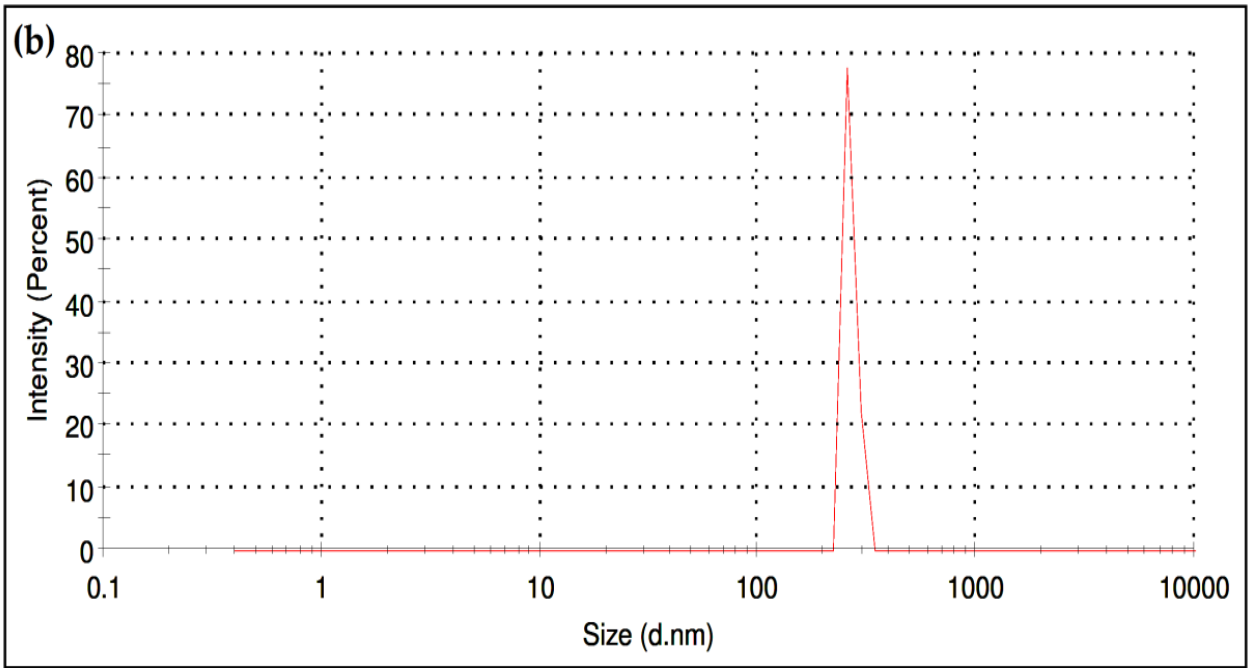


Figure 3.29: Average particle size of 85% HCSO-15% Madhuca longifolia wax crystal ranging from 210–350 nm

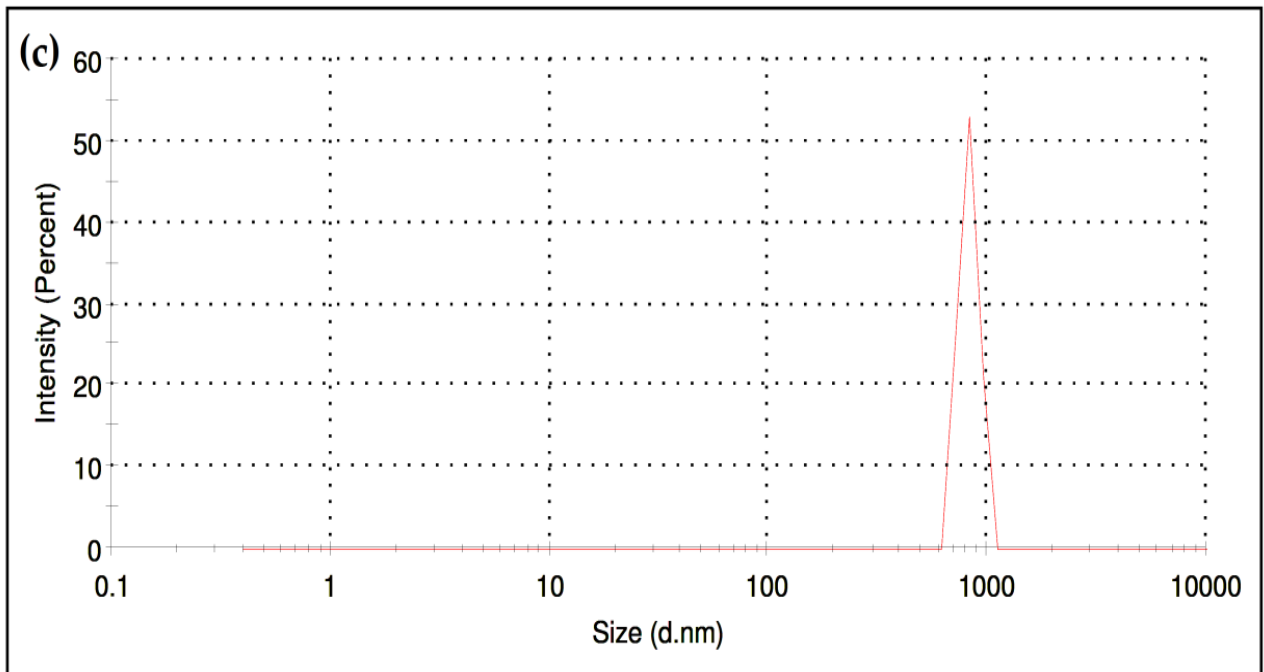


Figure 3.30: Average particle size of 85% HCSO-15% LSCO wax crystal ranging from 600–1100 nm.

Chapter 4

Pressure drop characteristics of crude oil

In pipeline bend

4.1 Introduction

In this investigation, a detailed analysis of the flow behavior of crude oil through pipeline is simulated by using ANSYS 15.0. Computational fluid dynamics, or CFD, computer programs have been suggested as an alternative to physical experimentation which can eliminate the costs associated with obtaining materials to build an experimental model and requiring hours of man labor to conduct an experiment. Given the proper CFD single phase code, and bearing in mind the limitations of the CFD program's solving capabilities, it may be possible to reproduce physical experimental results within a small range of error (~5%). CFD can also be useful to test conditions that are not practical to experiment with in the laboratory.

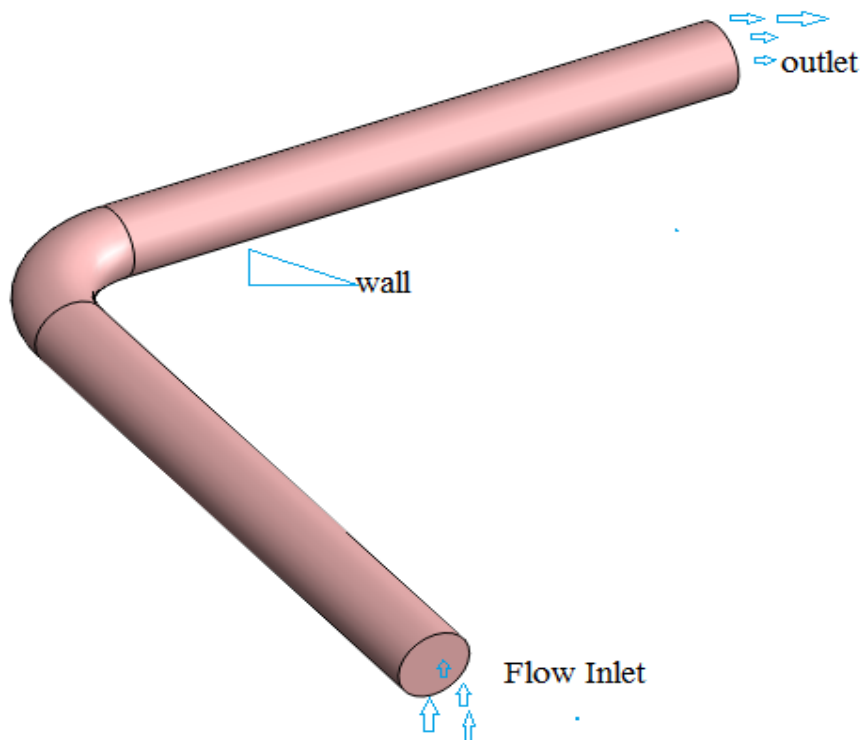


Figure 4.1: Geometry of pipe bend

Table 4.1 Description of Pipeline Geometry

S.No.	Description		
	Curvature-Diameter ratio (R_C/D)	Diameter (mm)	Length of pipe (mm)
1	1.5	100	2000
2	2.0	150	2000
3	2.5	200	2000
4	3.0	250	2000

4.2 Piping materials and attributes

A mild steel pipe bend is considered for analysis of flow characteristics. In this study the length of pipe 500 m and is sufficient enough to maintain fully developed flow .the geometry of pipe was modeled in solid work software. Figure 4.1 show the detailed view of the flow domain. Figure 4.1 shows a model of transportation pipeline which was generated by solid work in 2012. The model consists crude oil inlet and fluid outlet and wall of the pipe. A detailed geometry of the pipeline was shown in Table 4.1.

4.3 Flow Domain

Pipeline geometry was modeled by using ANSYS R15.0 software package. The length of the pipe bend was taken as 2000 m which was sufficient enough to maintain fully developed flow. Figure 4.2, Figure 4.3 shows schematic diagram of pipe bend geometry. The diameter of pipe was varied from 100 to 250 mm. The radius-to-diameters ratio (r/D) was taken as 1.5, 2.0, 2.5 and 3.0. Three different bend angle pipes were used to analyze the effect of bend angle on erosion wear. Material of pipelines was considered as mild steel. Two phase fluid containing water was taken as liquid phase and natural additive was injected at inlet face of pipeline. The solid concentration of natural additive was kept 20 to 25% (by volume). The velocity of flowing fluid was varied from 1 to 2 m/s. The properties of crude oil and natural additive are discussed in Table 4.1. Simulations were carried out at Windows based Intel Xenon E51407v2 3.0 machine having 2.59 GHz processing unit and 14 GB RAM and converged when residuals of governing equations drops below 10^{-5} .

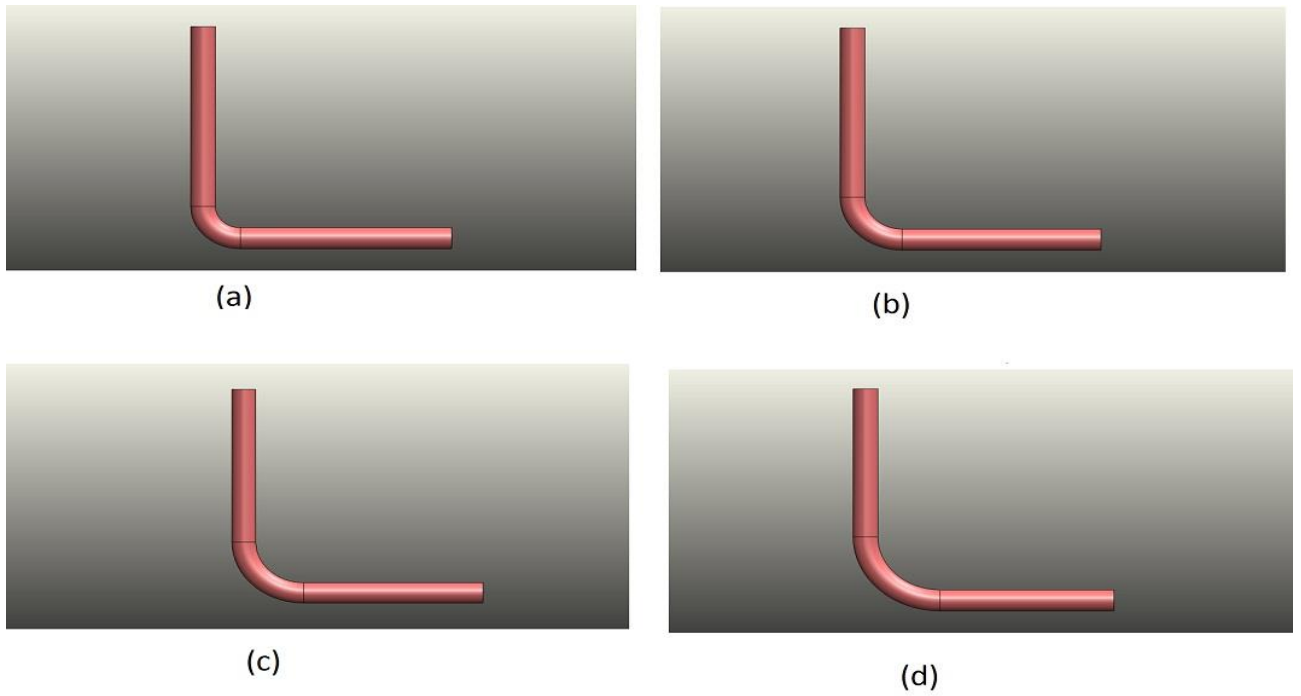


Figure 4.2: Geometry of Pipe bend at different curvature-ratio diameter (a) $Rc/D = 1.5$, (b) $Rc/D = 2.0$ (c) $Rc/D = 2.5$ (d) $Rc/D = 3.0$

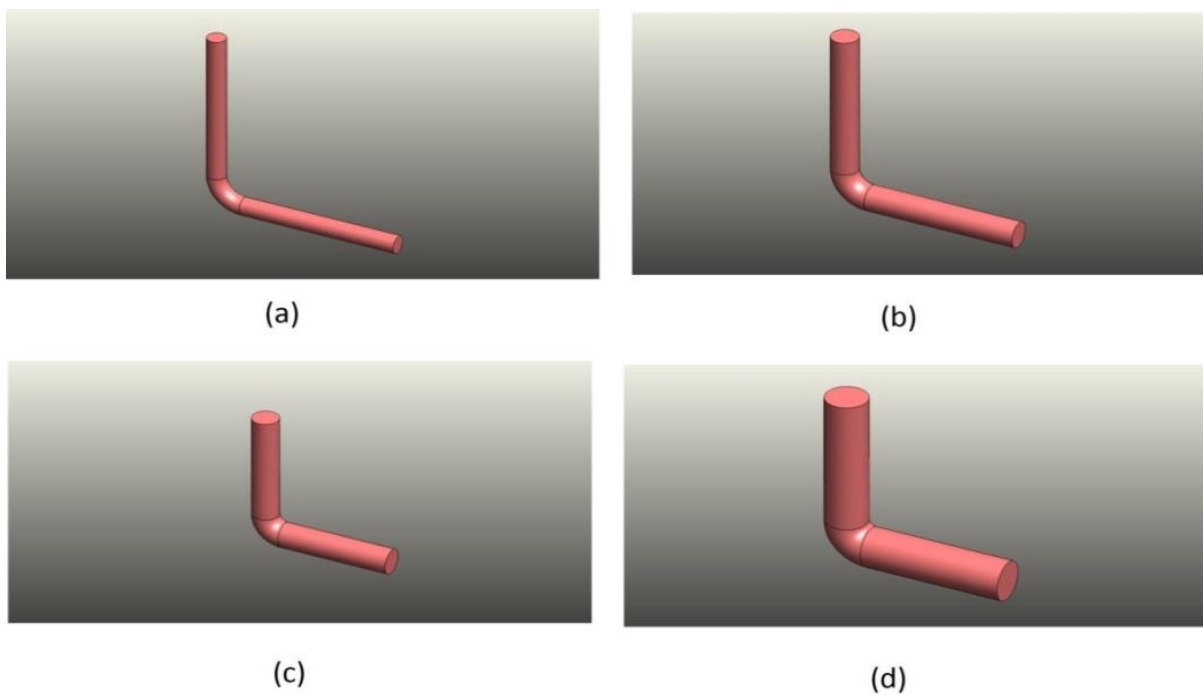


Figure 4.3: Geometry of Pipe bends at different diameter (a) $D = 100$ mm, (b) $D = 150$ mm, (c) $D = 200$ mm, (d) $D = 250$ mm

Table 4.2: properties of crude oil and additive

Flowing fluid	Density(Kg/ m ³)	Viscosity (Kg/m-s)
Crude oil	874.4	0.004
Additives (Madhuca longifolia)	855	0.0051

4.4 Discretization of the Domain

In order to evaluate the flow behaviour accurately at every section of pipe, the pipe was discretized into smaller number of elements. The systematic meshed domain of 90° pipe bend is shown in Fig.4.4. In present work, the domain was divided into 192130, 182974, 153385 and 127144 tetrahedral elements for r/D ratios of 1.5, 2.0, 2.5 and 3.0.

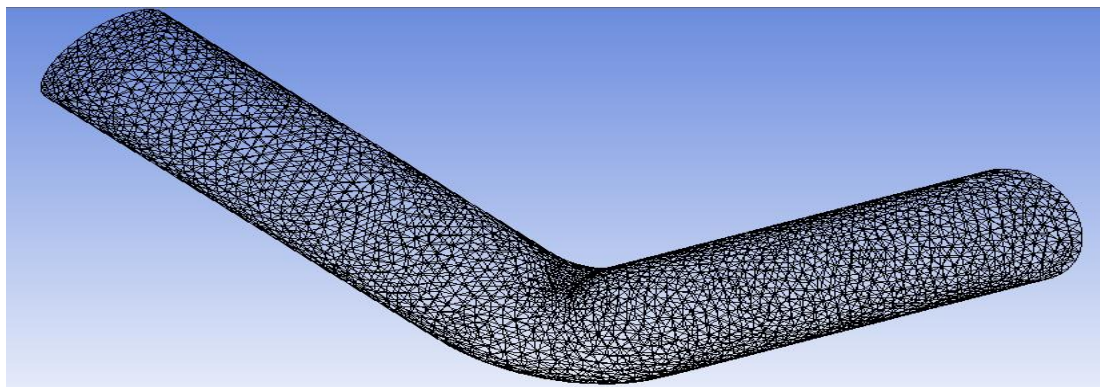
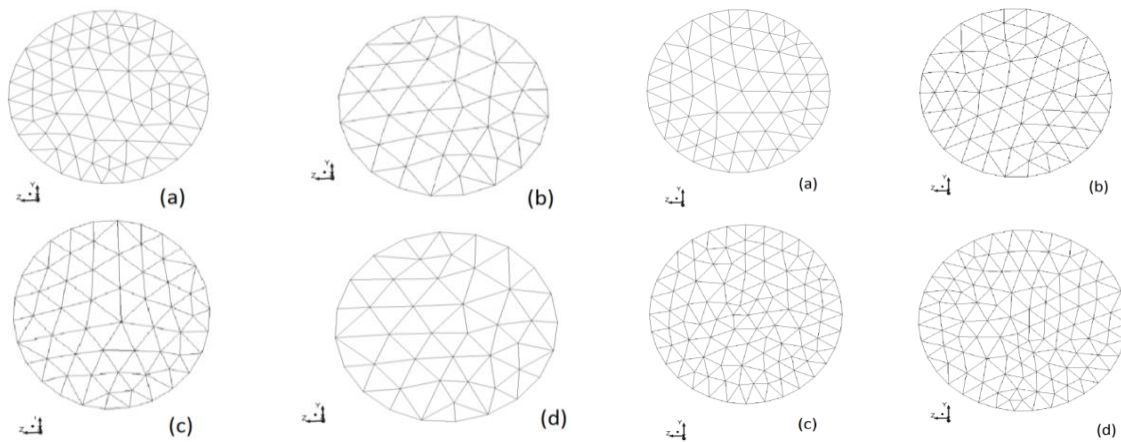


Figure 4.4: Discretization of the domain

4.5 Boundary Conditions

Three boundary conditions were applied for calculating the domain; the velocity inlet, pressure outflow and no slip conditions.

Type	Description	Input
Model	Turbulence Scheme	<ul style="list-style-type: none"> • Standard K-ϵ • RNG
	Two-Phase modeling	<ul style="list-style-type: none"> • Model: Volume of fluid • Phase : 1 • Scheme: Implicit • Near wall treatment :Standard wall function
Material	Description	<ul style="list-style-type: none"> • Flowing fluid:Crude oil • Additive fluid: Natural Surfactant
Injection Type	Release from surface : inlet	<ul style="list-style-type: none"> • Velocity • Concentration • Total flow rate
Operating Conditions	Gravitational acceleration pressure	<ul style="list-style-type: none"> • -9.81 on vertical downward • 101325 Pa
Boundary Conditions	Inlet	<ul style="list-style-type: none"> • Velocity Inlet = 1m/s
	Outlet	<ul style="list-style-type: none"> • Pressure outflow
	Wall	<ul style="list-style-type: none"> • Stationary • No slip • Turbulence Intensity : 5% • Turbulence viscosity ratio : 10% • Volume fraction : 0.2
Solution Method	Scheme :SIMPLEC	<ul style="list-style-type: none"> • Momentum: second order upwind • Turbulence kinetic energy: Second order upwind
Solution initialization	Hybrid Initialization	<ul style="list-style-type: none"> • Relative to cell zone • No. of iterations =10

Run calculation	Calculation	<ul style="list-style-type: none"> • No. of iterations = 1000 • Profile interval =1 • Reporting Interval =1
-----------------	-------------	--

4.6 Results and discussion

4.6.1 Pressure field analysis

Pressure drop characteristics of crude oil in pipeline are investigated for the influence of velocities, diameter of pipe and radius-to-diameter ratio. Figure 4.5 represents pressure drop characteristics of crude oil in 100 mm pipeline of different radius-to-diameter at different velocities. The velocity of crude oil was varied as 0.5 to 2.0 m/s. The r/D ratio of elbow was ranging from 1.5 to 3.0. It is found that the pressure drop was increased with increase in velocity. Maximum pressure drop was found as 2.1814×10^4 , 2.1839×10^4 , 2.1876×10^4 and 2.12×10^4 Pa/m at velocity of 0.5, 1.0, 1.5 and 2.0 m/s respectively at r/D ratio 3.0 . Minimum pressure drop was observed at 2.1611×10^4 , 2.1639×10^4 , 2.1667×10^4 and 2.1704×10^4 Pa/m at velocity of 0.5, 1.0, 1.5 and 2.0 m/s respectively at r/D ratio 2.0. The pressure drop was marginally increased at 2.5. The optimum r/D ratio was found as 2.0. Similar type of phenomenon was observed by [Bozzini et al. 2003].

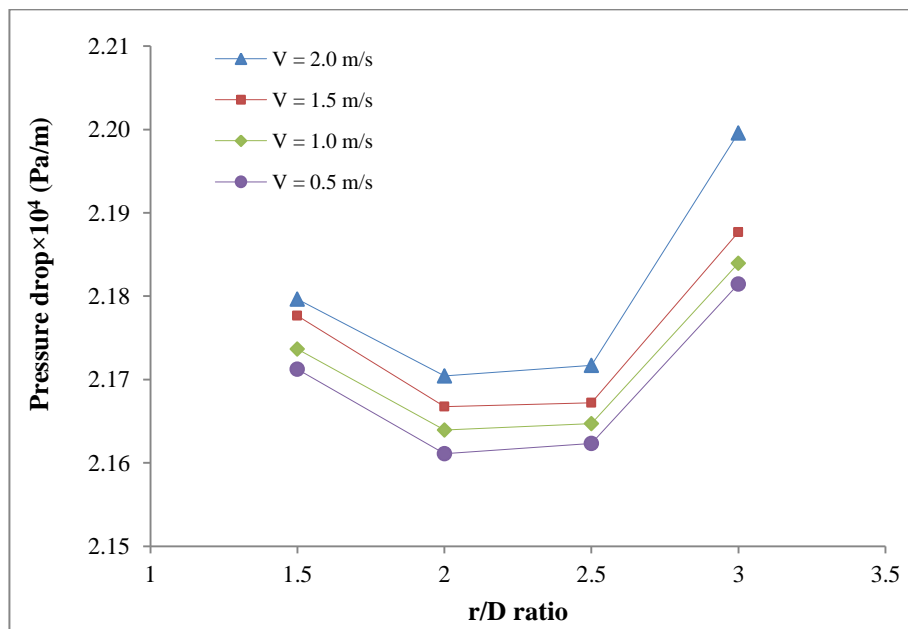


Figure 4.5: Pressure drop characteristics of crude oil in 100 mm pipeline of different radius-to-diameter at different velocities

Figure 4.6 represents pressure drop characteristics of crude oil in pipeline having r/D ratio of 2.0 at different diameter at different velocities. The velocity of crude oil was varied as 0.5 to 2.0 m/s. The diameter of pipe elbow was ranging from 100, 150, 200 and 250 mm. It is found that the pressure drop was decreased with increase in diameter. Maximum pressure drop was found as 1.0432×10^4 , 1.5009×10^4 , 2.0505×10^4 and 2.7893×10^4 Pa/m at 0.5, 1.0, 1.5 and 2.0 m/s respectively for 100 mm pipe bend. Minimum pressure drop was observed at 2.598×10^4 , 3.343×10^4 , 5.643×10^4 and 8.981×10^4 respectively for 250 mm pipe bend. Similar type of phenomenon was observed by [Mazumder,2012].

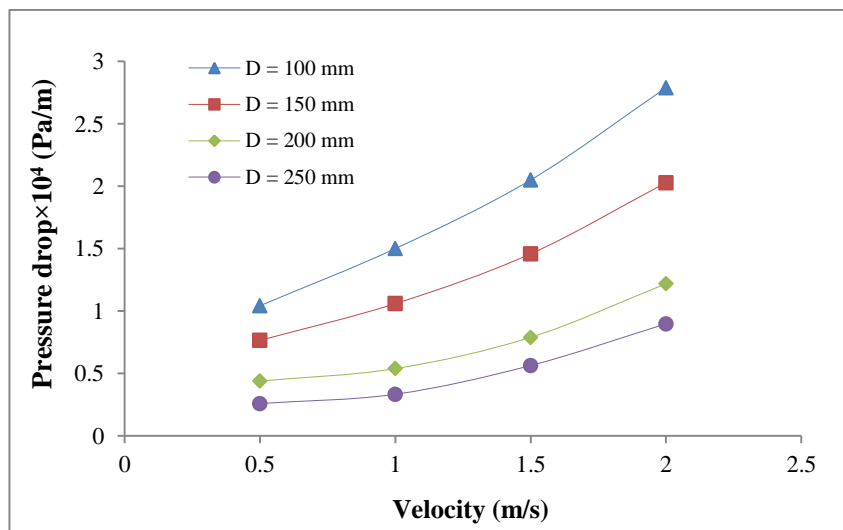


Figure 4.6: Pressure drop characteristics of crude oil in pipeline ($r/D = 1.5$) of different diameter at different velocities

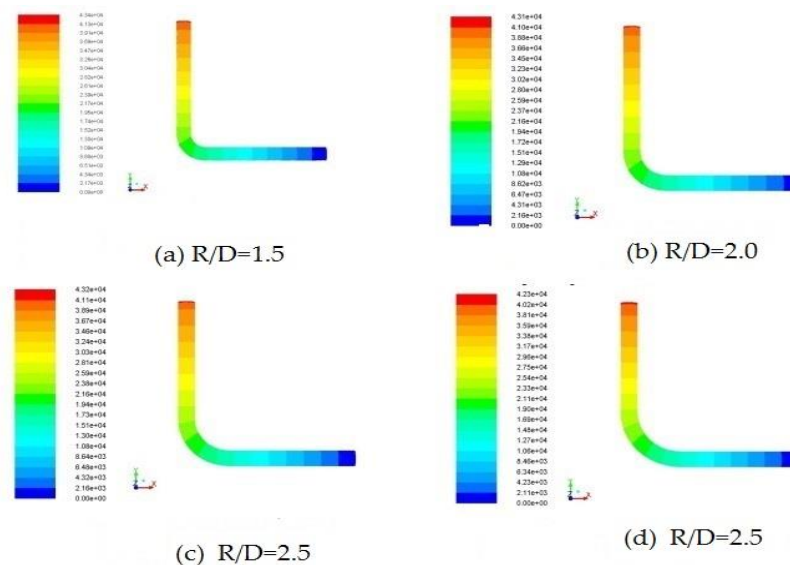


Figure 4.7: Pressure drop contours at different R/D ratio

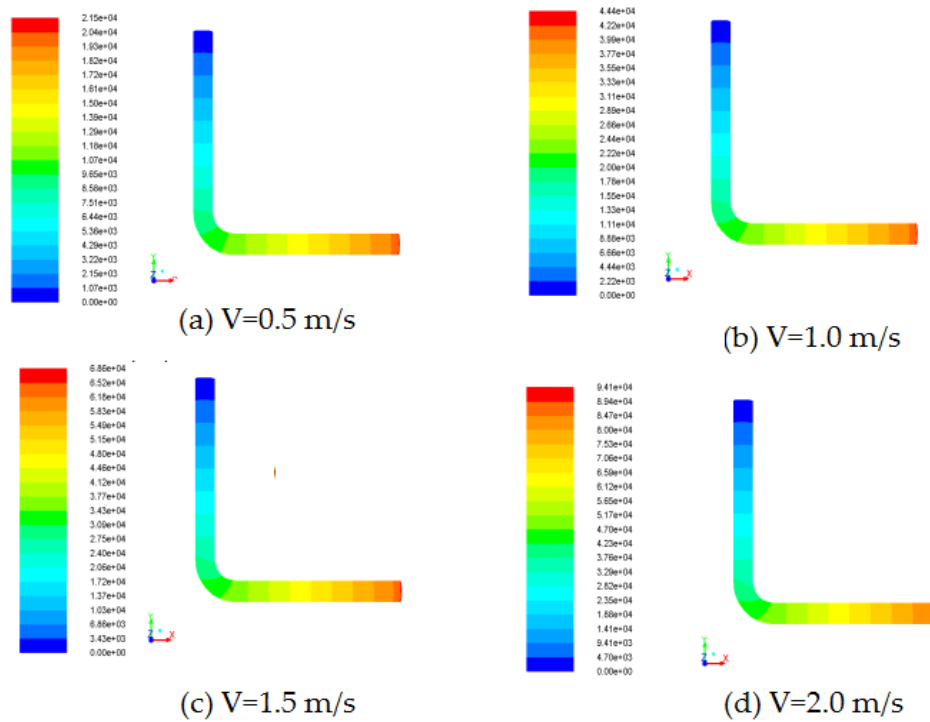


Figure 4.8: Pressure drop contours at different velocity

In the case of elbow with different curvature-diameter ratio, the initial velocity was set as 2 m/s is shown in Fig 4.7. The highest pressure was produced at the entrance, compare with the pressure of inlet, the outlet pressure reduced. The reason is that fluid change its velocity direction rapidly when passing through the bending section, cause fluid impact force, form the whirlpool and the secondary motion phenomenon, reduce the energy and pressure of the fluid. Secondly, the pressure at the outer wall of the bending section is greater than the pressure at the inner wall. The analysis shows that it is because the pressure difference which caused by the secondary motion phenomenon. Then, with the increase of R/D , the corresponding pressure gradient decreases. On account of the R/D is greater, the bend section is more gentle, then the flow of the fluid is relatively flat, the smaller the impact of the fluid is, the smaller the pressure gradient is. As shown in Figure 4.8, when $R/D=1.5$, the initial velocity is 1m/s, 5m/s, 10m/s, respectively, consistent with the actual situation, the pressure drop increased in turn. The greater the velocity is, the greater the impact. Then produce a greater pressure drop across the elbow.

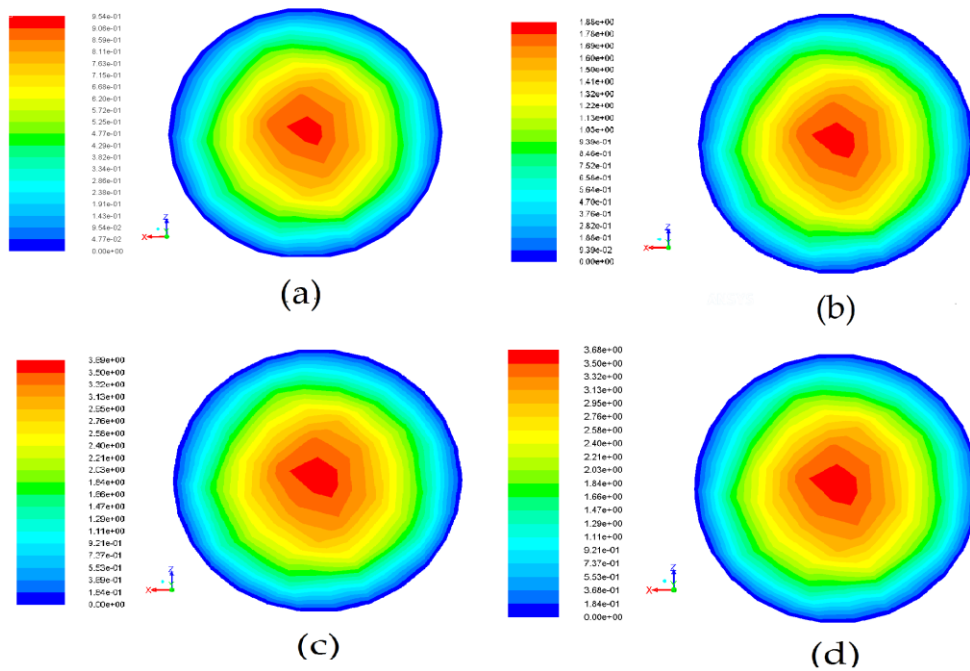


Figure 4.9: Velocity contours at outlet of pipe bend with concentration 20% NS,80% HCO with velocity 1m/s at different curvature-ratio diameter (a) $Rc/D = 1.5$, (b) $Rc/D = 2.0$ (c) $Rc/D = 2.5$ (d) $Rc/D = 3.0$

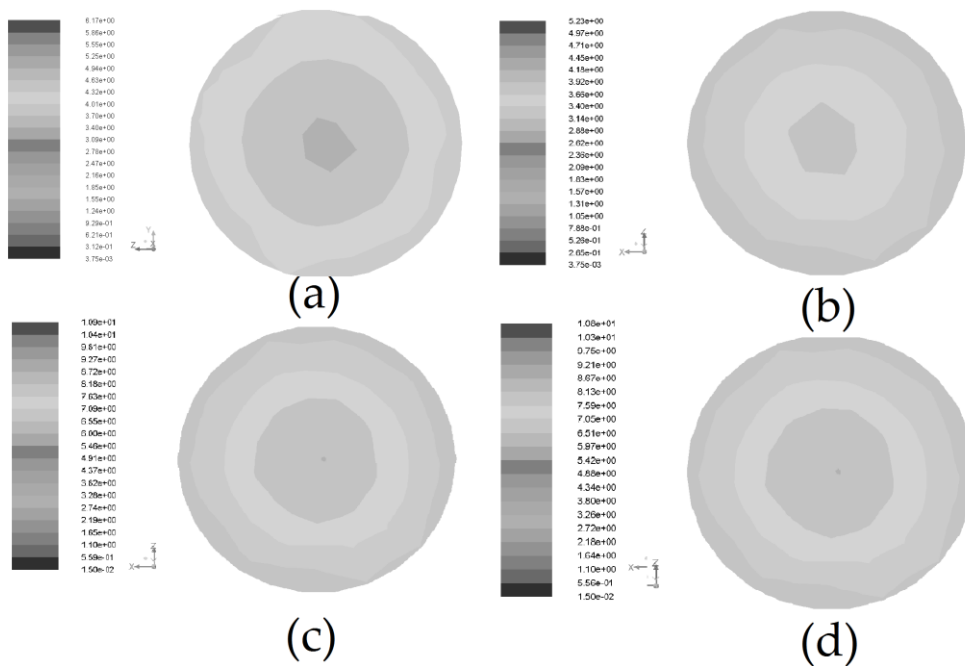


Figure 4.10: Turbulence intensity contours at outlet of pipe bend with concentration 20% NS,80% HCO with velocity 1m/s at different curvature-ratio diameter (a) $Rc/D = 1.5$, (b) $Rc/D = 2.0$ (c) $Rc/D = 2.5$ (d) $Rc/D = 3.0$

4.6.2 Influence of radius-to-diameter (R/D) ratio

The velocity, turbulence intensity and phase changes was investigated on pipe bends of four different radius-to diameter (r/D) ratios namely 1.5, 2.0, 2.5 and 3.0 respectively for bend angle of 90° . The Natural surfactant concentration was taken as 20% (by volume) at velocity of 2 m/s. Fig. 4.9 represents velocity distribution contours for different r/D ratios bends at pipe outlet. From Figure 4.9, the maximum velocity region was found near the bend wall for pipe bends of different r/D ratios. At $r/D = 1.5$, the high velocity region seems like contracted whereas it gets wider for other pipe bends. It was found the turbulence increases with increase in R/D ratio above and below 1.5 shown in figure 4.10. On increasing R/D the mechanism inner structure of natural structure from globule-like to circular structure which is shown in Fig 4.11.

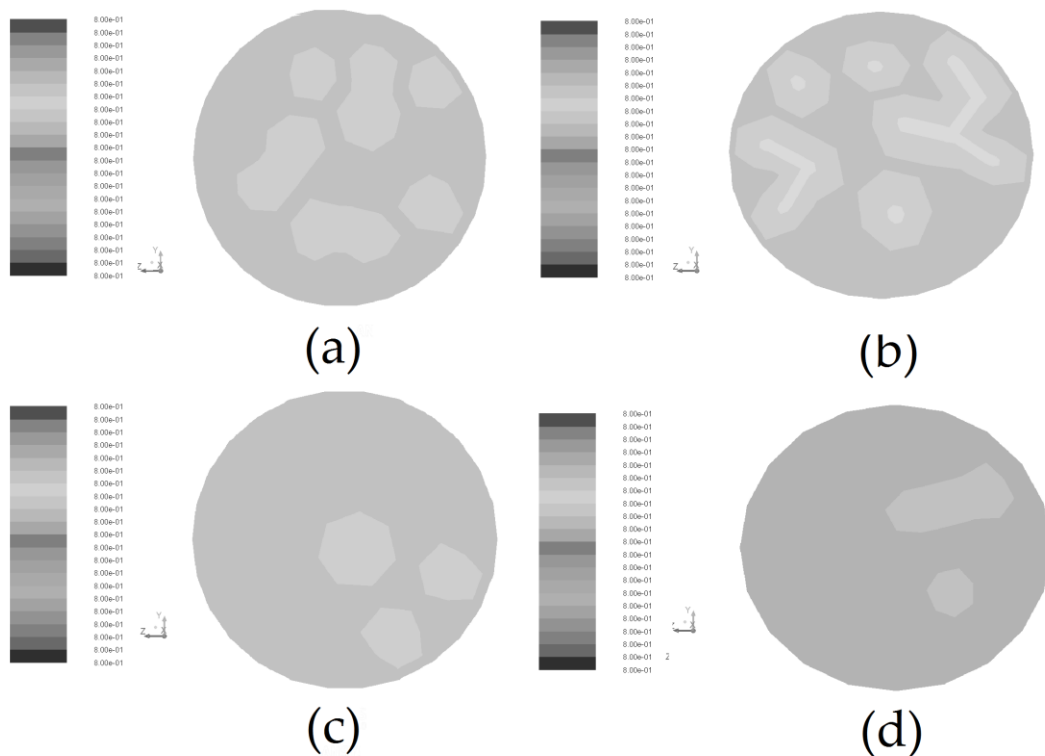


Figure 4.11: Contours of HCO and NS phase with concentration 20% NS,80% HCO with velocity 1m/s different curvature-ratio diameter (a) $Rc/D = 1.5$, (b) $Rc/D = 2.0$ (c) $Rc/D = 2.5$ (d) $Rc/D = 3$

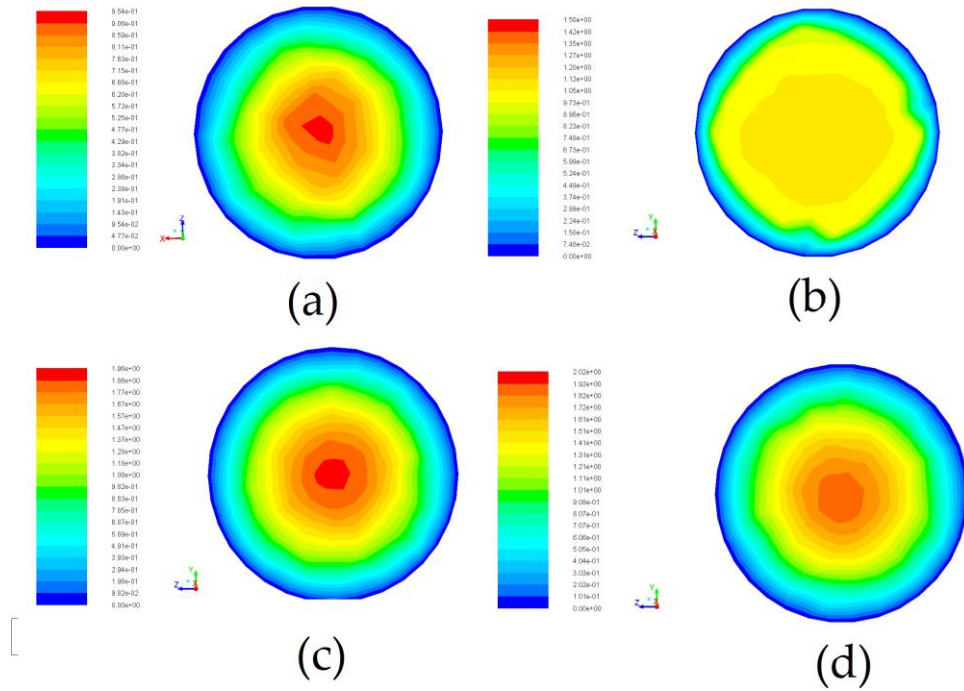


Figure 4.12: Velocity contours at outlet of pipe bend with concentration 20% NS,80% HCO with velocity 1m/s at different diameter (a) D =100 mm, (b) D = 150 mm (c) D = 200 mm (d) D = 250 mm

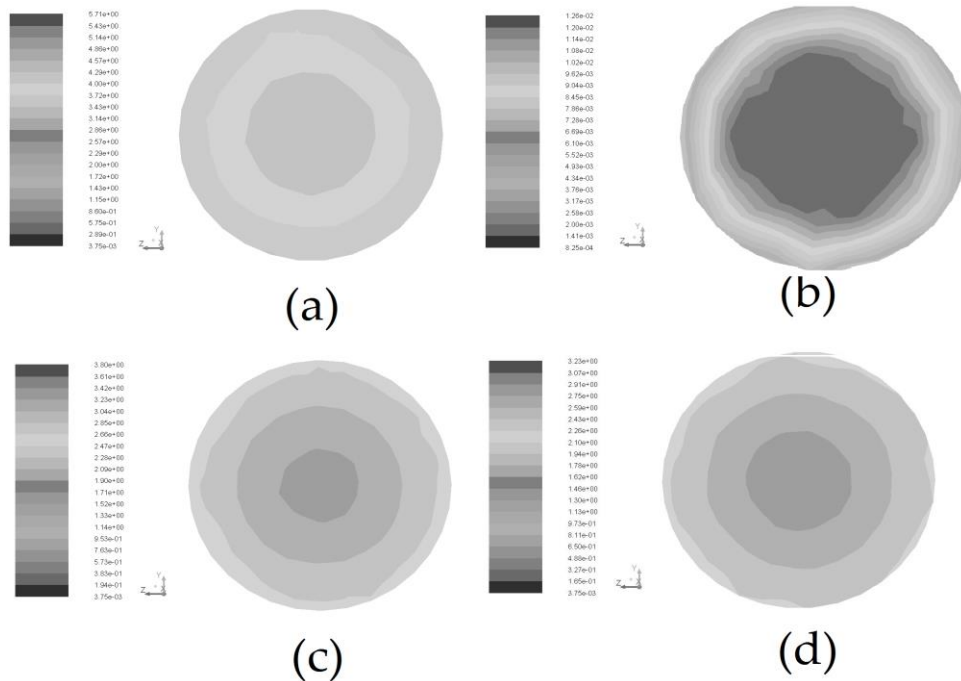


Figure 4.13: Turbulence intensity contours at outlet of pipe bend with concentration 20% NS,80% HCO with velocity 1m/s at different (a) D =100 mm, (b) D = 150 mm (c) D = 200 mm (d) D = 250 mm

4.6.3 Influence of pipe diameter (D)

The diameter of pipe was varied as 100, 150, 200 and 250 mm having bend angle of 90°. The natural additive concentration was taken as 20% (by volume). The velocity of flow was kept as 2 m/s. The velocity contour at outlet is shown in Fig 4.12. The influence of pipe diameter flow behavior is represented by Fig 4.12. Figure 4.13 shows turbulence distribution at pipe outlet for pipes of different diameters. From Figure 4.13, it was found that as the pipe diameter increases the magnitude of turbulence intensity also decreases. For $D = 100$ mm, the intense turbulence was observed which helps in particle-extrados wall collision with extra momentum. For $D = 250$ mm, the area of fluid flow increases. It was found that fluid flow was stable near the central line of pipe. Very low turbulence intensity was observed at extrados wall. This happens due to low particle-wall interactions however, the particle-particle interactions increase with increase in pipe diameter at same time. On increasing the diameter of pipe, the phases of natural surfactant combine which is shown in Fig 4.14. This is due to viscosity of fluid reduce and easy to transport in pipe line.

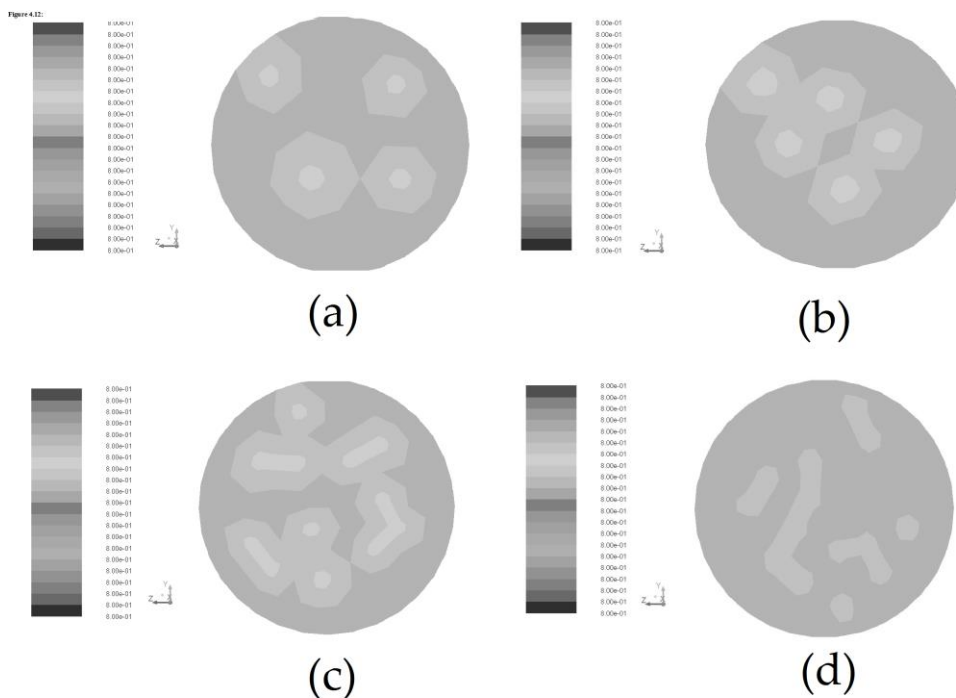


Figure 4.14: Contours of HCO and NS phase with concentration 20% NS,80% HCO with velocity 1m/s different at different (a) $D = 100$ mm, (b) $D = 150$ mm (c) $D = 200$ mm (d) $D = 250$ mm

4.6.4 Influence of velocity (V 0.5 to 2.0)

A velocity profile represents the magnitude and intensity of velocity varying from zero to maximum value. Figure 4.15 shows the velocity distributions for 100 mm diameter pipe bend at different efflux velocities range from 0.5 to 2.0m/s. The natural additive concentration was taken as 20% (by volume). Figure illustrates that velocity distributed asymmetrically around horizontal axis and its magnitude becomes high at middle plane. Asymmetric velocity distribution is observed at lower velocity. As the velocity increases the asymmetric nature of velocity distribution reduced and shifts towards symmetric as observed in Figure 4.15. The velocity at bend outlet changes in transverse direction from intrados to extrados wall which is shown in Fig 4.15.

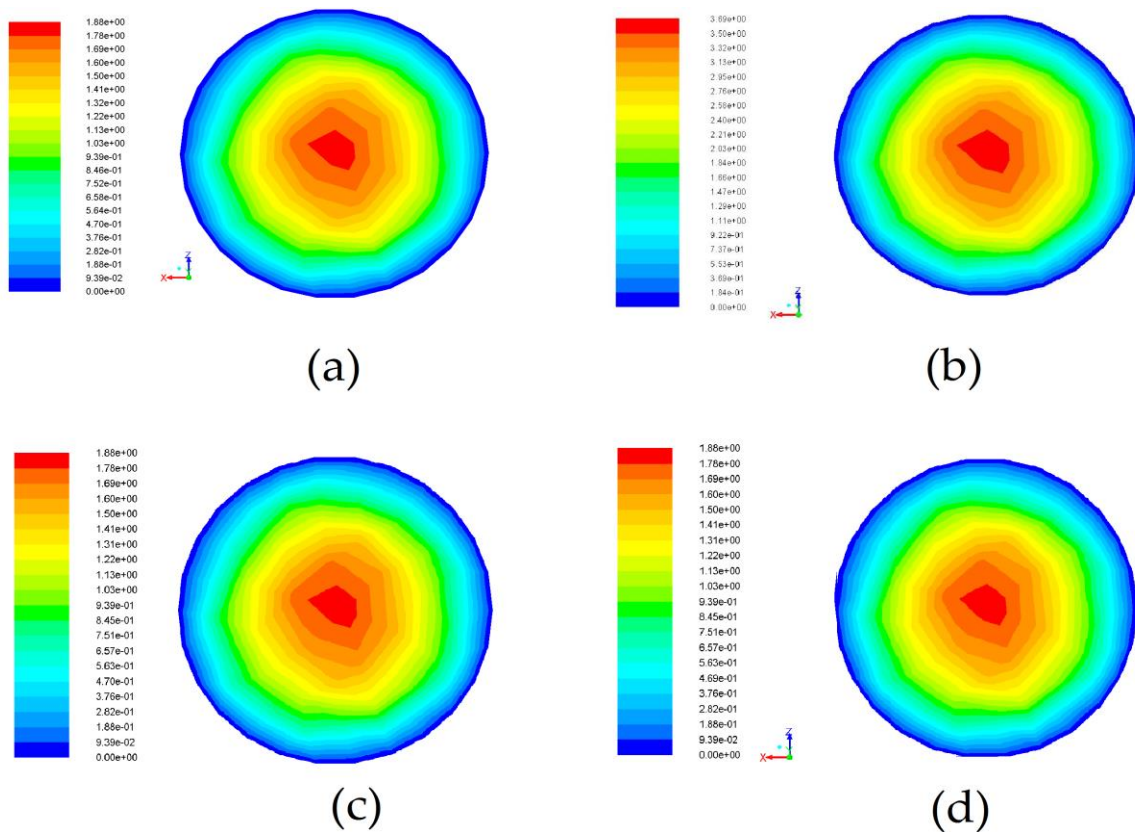


Figure 4.15: Velocity contours at outlet of pipe bend with concentration 20% NS, 80% HCO and diameter 100 mm with different velocity (a) $v = 0.5$ m/s (b) $v = 1.0$ m/s (c) $v = 1.5$ m/s (d) $v = 2$ m/s

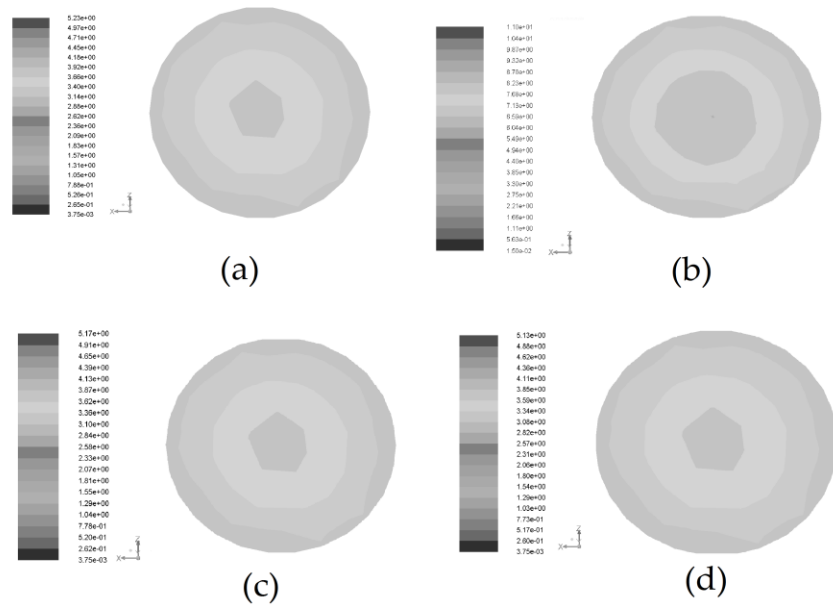


Figure 4.16: Turbulence intensity contours at outlet of pipe bend with concentration 20% NS, 80% HCO and diameter 100 mm with different velocity (a) $v = 0.5 \text{ m/s}$ (b) $v = 1.0 \text{ m/s}$ (c) $v = 1.5 \text{ m/s}$ (d) $v = 2 \text{ m/s}$

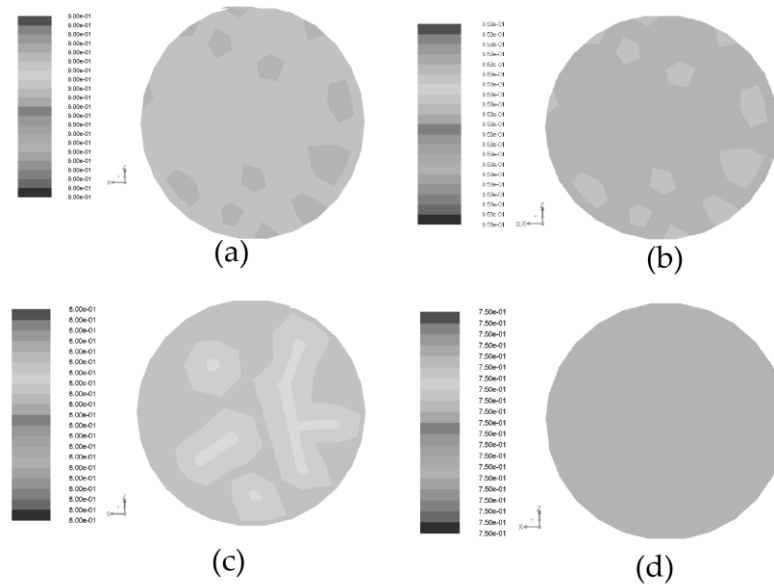


Figure 4.17: Contours of HCO and NS phase with concentration 20% NS, 80% HCO with diameter 100 mm different velocity (a) $v = 0.5 \text{ m/s}$ (b) $v = 1.0 \text{ m/s}$ (c) $v = 1.5 \text{ m/s}$ (d) $v = 2 \text{ m/s}$

It was observed from the velocity vectors that fluid flow push the bottom ash particles to the extrados wall. As the fluid reaches to 90° in pipe bend, maximum transverse recirculation of flow takes place due to the centrifugal effect along the curvature of the bend. Maximum

magnitude of velocity was found at intrados wall of bend which can be visualized the impact energy of the flow becomes high due to which the fluid particles collides with extrados wall with more force resulting turbulence enhance. Figure 4.15 also indicates that high velocity zone exists at low velocities ($V = 1$ and 2 m/s) was quite concentric which represents the steady behaviour of fluid. As the velocity increase the high velocity zone shifts towards the extrados wall, as represented in Fig.4.15. The turbulence intensity increases with increase in velocity. Very low turbulence region exist nearby extrados wall at low velocities however; it becomes concentric with increase in velocity, as represented in Fig 4.16. The no phase change inside the pipeline which is shown in Fig 4.17.

4.6.5 Influence of natural additive concentration

Figure 4.18 shows the effect crude-natural surfactant emulsion 100 mm diameter pipe bend. The surfactant concentration was taken as 10% to 25% (by volume) with velocity of 5 m/s. velocity contour remain constant throughout is shown in Fig 4.16. The turbulence intensity changes when concentration increases in pipeline. The turbulence intensity is maximum at 15 % (by volume) concentration represent in Fig 4.19. On increasing the concentration the inner mechanism of fluid changes in Figure 4.20 natural surfactant appears and when concentration increasing the phase changes completely.

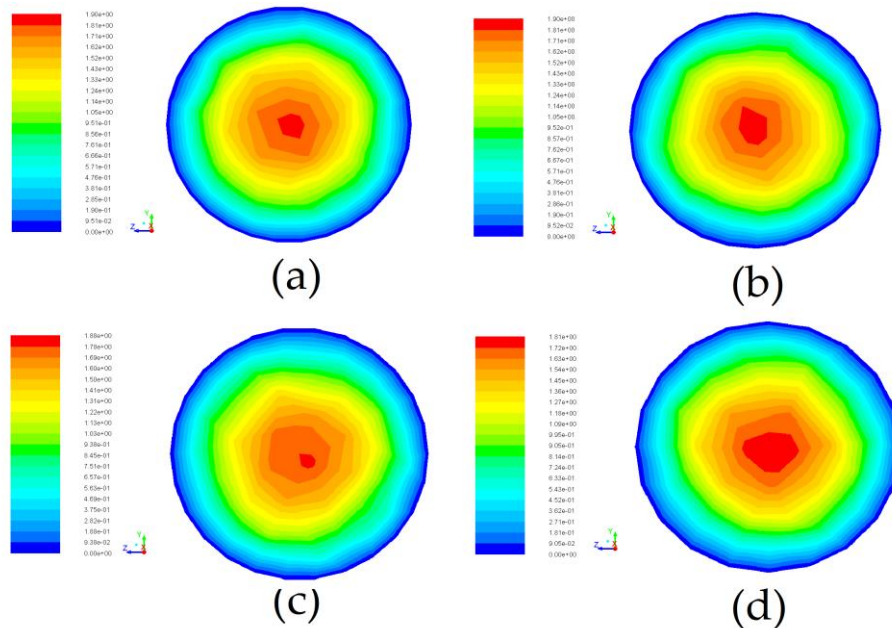


Figure 4.18: Velocity contours at outlet of of HCO and NS phase with concentration by volume (a) 10% (b) 15% (c) 20% (d) 25% for diameter 100 mm and velocity 1 m/s

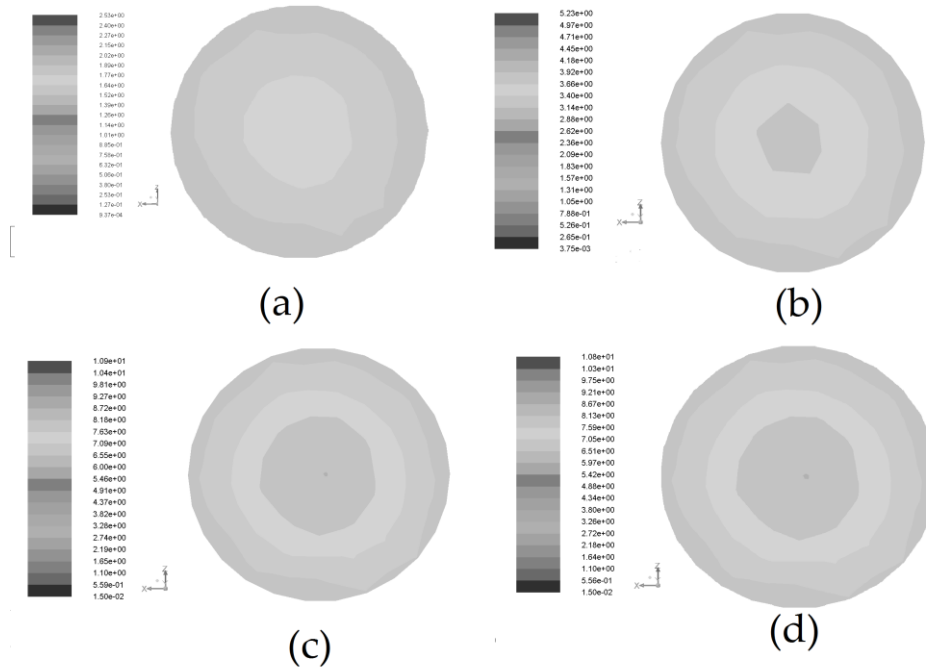


Figure 4.19: Turbulence intensity contours at outlet of HCO and NS phase with concentration by volume (a) 10% (b) 15% (c) 20% (d) 25% for diameter 100 mm and velocity 1 m/s

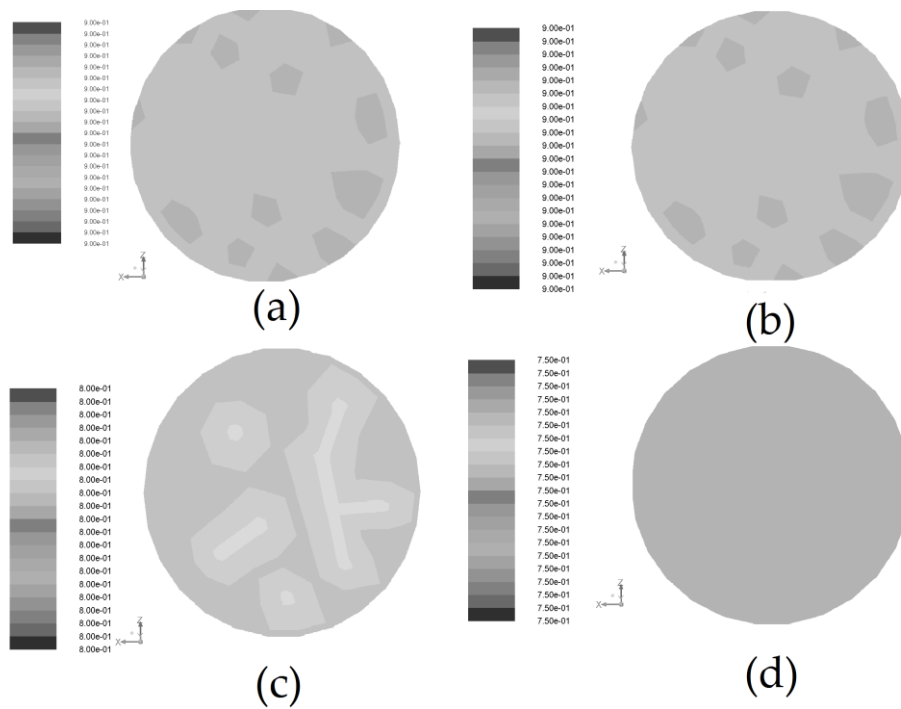


Figure 4.20: Contours of HCO and NS phase with concentration by volume (a) 10% (b) 15% (c) 20% (d) 25% for diameter 100 mm and velocity 1 m/s

Chapter 5

Conclusion

The following conclusions can be drawn based on present investigation:

- a) The presences of natural surfactant in crude oil approximately eliminate the thixotropic behaviour of high sulphur crude oil.
- b) The high sulphur crude oil shows the non-Newtonian shear thinning characteristics. As the temperature increases viscosity of crude oil decreases and shows the Newtonian flow behaviour at 55°C.
- c) The concentration of ketones, aldehyde present in crude oil reduces significantly with addition of *Madhuca longifolia* surfactant.
- d) The addition of *Madhuca longifolia* as additive in heavy crude oil suspension can be useful for design of pipeline of oil transportation system.

5.1 Future Scope of the Work

The various works that can augment the present study are:

- a) Investigation of rheological behaviour of crude oil with natural additives.
- b) Investigation of rheological behaviour of crude oil with refine product.
- c) investigating behaviour of crude oil with different metals for enhance the petroleum
- d) Transportation.
- e) To develop a new empirical model in order to predict the viscosity of the heavy crude oil –light crude oil mixture as a function of oil content, shear rate and temperature.
- f) To perform an efficient pipeline design and evaluate the pumping power required and the cost needed to pump the heavy crude oil with low viscosity.

There is still a large scope for further research work in the field of petroleum industry for its efficient utilization and transportation.

References

- Adeyanju, O. and Oyekunle, L., 2012. An experimental study of rheological properties of nigerian waxy crude oil. *Petroleum Science and Technology*, 30(11), pp.1102-1111.
- Ahmed, N.S., Nassar, A.M., Zaki, N.N. and Gharieb, H.K., 1999. Stability and rheology of heavy crude oil-in-water emulsion stabilized by an anionic-nonionic surfactant mixture. *Petroleum science and technology*, 17(5-6), pp.553-576.
- Al-Zahrani, S.M., 1997. A generalized rheological model for shear thinning fluids. *Journal of Petroleum Science and Engineering*, 17(3-4), pp.211-215.
- Al-Zahrani, S.M. and Al-Fariss, T.F., 1998. A general model for the viscosity of waxy oils. *Chemical Engineering and Processing: Process Intensification*, 37(5), pp.433-437.
- Aske, N., Kallevik, H. and Sjöblom, J., 2001. Determination of saturate, aromatic, resin, and asphaltenic (SARA) components in crude oils by means of infrared and near-infrared spectroscopy. *Energy & Fuels*, 15(5), pp.1304-1312.
- Bacon, M.M., Electricwala, M. and Romero-Zeron, L.B., 2011. The Effect of Weathering on the Rheology of an Atypical Waxy Crude Oil. *Petroleum Science and Technology*, 29(4), pp.349-357.
- Banda Cruz, E.E., Rivas Gallardo, N.V., Páramo García, U., Estrada Moreno, I.A., Pozas Zepeda, D. and Reyes Gómez, J., 2016. Crude oil aggregation by microscopy and dynamic light scattering. *Petroleum Science and Technology*, 34(22), pp.1812-1817.
- Banerjee, S., Kumar, R., Mandal, A. and Naiya, T.K., 2015. Use of a novel natural surfactant for improving flowability of indian heavy crude oil. *Petroleum Science and Technology*, 33(7), pp.819-826.
- Banerjee, S., Kumar, R., Mandal, A. and Naiya, T.K., 2015. Effect of Natural and Synthetic Surfactant on the Rheology of Light Crude Oil. *Petroleum Science and Technology*, 33(15-16), pp.1516-1525.
- Bozzini, B., Ricotti, M.E., Boniardi, M. and Mele, C., 2003. Evaluation of erosion–corrosion in multiphase flow via CFD and experimental analysis. *Wear*, 255(1), pp.237-245.
- Cabrera, C.A. and Silverman, M.A., 2012. Upgrade heavy oil more cost-efficiently. *Hydrocarbon Processing*, 91(9), pp.55-60.

- Chang, C., Nguyen, Q.D. and Rønningsen, H.P., 1999. Isothermal start-up of pipeline transporting waxy crude oil. *Journal of Non-Newtonian Fluid Mechanics*, 87(2), pp.127-154.
- Chen, W., Zhao, Z. and Yin, C., 2010. The interaction of waxes with pour point depressants. *Fuel*, 89(5), pp.1127-1132.
- Coto, B., Martos, C., Espada, J.J., Robustillo, M.D. and Peña, J.L., 2014. Experimental study of the effect of inhibitors in wax precipitation by different techniques. *Energy Science & Engineering*, 2(4), pp.196-203.
- Desamala, A.B., Dasari, A., Vijayan, V., Goshika, B.K., Dasmahapatra, A.K. and Mandal, T.K., 2013, January. CFD simulation and validation of flow pattern transition boundaries during moderately viscous oil-water two-phase flow through horizontal pipeline. In *Proceedings of World Academy of Science, Engineering and Technology* (No. 73, p. 1150). World Academy of Science, Engineering and Technology (WASET).
- Farah, M.A., Oliveira, R.C., Caldas, J.N. and Rajagopal, K., 2005. Viscosity of water-in-oil emulsions: Variation with temperature and water volume fraction. *Journal of Petroleum Science and Engineering*, 48(3), pp.169-184.
- Ghannam, M.T. and Esmail, N., 2006. Flow enhancement of medium-viscosity crude oil. *Petroleum science and technology*, 24(8), pp.985-999.
- Ghannam, M.T., Hasan, S.W., Abu-Jdayil, B. and Esmail, N., 2012. Rheological properties of heavy & light crude oil mixtures for improving flowability. *Journal of Petroleum Science and Engineering*, 81, pp.122-128.
- Goodwin, J.W. and Hughes, R.W., 2008. *Rheology for chemists: an introduction*. Royal Society of Chemistry.
- Guevara, E., Ninez, G. and Gonzalez, J., 1997, January. [8] 4 Highly Viscous Oil Transportation Methods in the Venezuelan Oil Industry. In *15th World Petroleum Congress*. World Petroleum Congress.
- Maghzi, A., Mohebbi, A., Kharrat, R. and Ghazanfari, M.H., 2013. An experimental investigation of silica nanoparticles effect on the rheological behavior of polyacrylamide solution to enhance heavy oil recovery. *Petroleum Science and Technology*, 31(5), pp.500-508.
- Hasan, S.W., Ghannam, M.T. and Esmail, N., 2010. Heavy crude oil viscosity reduction and rheology for pipeline transportation. *Fuel*, 89(5), pp.1095-1100.

- Hashim, E.T. and Hassaballah, A.A., 2003. An improved viscosity-temperature correlation for crude oils. *Petroleum science and technology*, 21(11-12), pp.1625-1630.
- Hassanean, M.H., Awad, M.E., Marwan, H., Bhran, A.A. and Kaoud, M., 2016. Studying the rheological properties and the influence of drag reduction on a waxy crude oil in pipeline flow. *Egyptian Journal of Petroleum*, 25(1), pp.39-44.
- Holmberg, K., Jönsson, B., Kronberg, B. and Lindman, B., 2004. Surfactants and polymers in aqueous solution. *Journal of Synthetic Lubrication*, 20(4), pp.367-370.
- Homayuni, F., Hamidi, A.A. and Vatani, A., 2012. An experimental investigation of viscosity reduction for pipeline transportation of heavy and extra-heavy crude oils. *Petroleum Science and Technology*, 30(18), pp.1946-1952.
- Kane, M., Djabourov, M. and Volle, J.L., 2004. Rheology and structure of waxy crude oils in quiescent and under shearing conditions. *Fuel*, 83(11), pp.1591-1605.
- Karami, H.R. and Mowla, D., 2012. Investigation of the effects of various parameters on pressure drop reduction in crude oil pipelines by drag reducing agents. *Journal of Non-Newtonian Fluid Mechanics*, 177, pp.37-45.
- Kaushik, V.V.R., Ghosh, S., Das, G. and Das, P.K., 2012. CFD simulation of core annular flow through sudden contraction and expansion. *Journal of Petroleum Science and Engineering*, 86, pp.153-164.
- Khan, M.R., 1996. Rheological properties of heavy oils and heavy oil emulsions. *Energy Sources*, 18(4), pp. 385-391.
- Krieger, I.M. and Dougherty, T.J., 1959. A mechanism for non-Newtonian flow in suspensions of rigid spheres. *Transactions of the Society of Rheology*, 3(1), pp.137-152.
- Kumar, R., Banerjee, S., Kumar, N., Mandal, A. and Kumar Naiya, T., 2015. Comparative Studies on Synthetic and Naturally Extracted Surfactant for Improving Rheology of Heavy Crude Oil. *Petroleum Science and Technology*, 33(10), pp.1101-1109.
- Li, H. and Gong, J., 2011. The pressure effect on rheological behavior of water content of waxy crude oil. *Petroleum Science and Technology*, 29(13), pp.1344-1352
- Mazumder, Q.H., 2012. CFD analysis of the effect of elbow radius on pressure drop in multiphase flow. *Modelling and Simulation in Engineering*, 2012, p.37.
- Meriem-Benziane, M., Abdul-Wahab, S.A., Benaicha, M. and Belhadri, M., 2012. Investigating the rheological properties of light crude oil and the characteristics of its emulsions in order to improve pipeline flow. *Fuel*, 95, pp.97-107.

- Meriem-Benziane, M. and Bou-Saïd, B., 2013. Determination of friction factor of Algerian crude oil during flow in pipe-lines. *Flow Measurement and Instrumentation*, 33, pp.28-35.
- Ranodolph, A., 2012. *Theory of particulate processes: analysis and techniques of continuous crystallization*. Elsevier.
- Rashed, M.K.; Salleh M.A.M; Abdulbari, H.A.; Ismail M.H.S. Enhancing the drag reduction phenomenon within a rotating disk apparatus using polymer-surfactant additives. *Appl. Sci.* 2016, Volume 6(355) , pp. 1-11.
- Reinhardt, U., 1997. Rotational Rheometry-a Look into the Future. *Applied Rheology*, 7(1), pp.25-30
- Roberto, C.D., Enrique, G.A. and Chavez, A.E., 2006. Viscoelastic models for Mexican heavy crude oil and comparison with a mixture of heptadecane and eicosane. *Fuel*, 85(4), pp.559-568.
- Rukthong, W., Weerapakkaron, W., Wongsiriwan, U., Piumsomboon, P. and Chalermssinsuwan, B., 2015. Integration of computational fluid dynamics simulation and statistical factorial experimental design of thick-wall crude oil pipeline with heat loss. *Advances in Engineering Software*, 86, pp.49-54.
- Taiwo, E., Otolurin, J. and Afolabi, T., 2012. Crude oil transportation: Nigerian Niger delta waxy crude. INTECH Open Access Publisher
- Tao, R. and Xu, X., 2006. Reducing the viscosity of crude oil by pulsed electric or magnetic field. *Energy & fuels*, 20(5), pp.2046-2051.
- Tao, R. and Tang, H., 2014. Reducing viscosity of paraffin base crude oil with electric field for oil production and transportation. *Fuel*, 118, pp. 69-72.
- Urquhart, R.D.,(1986), "Heavy Oil Transportation - Present and Future", *The Journal Canadian Petroleum Technology*, pp 68-71.
- Wang, Z.; Yu, X.; Li, J.; Wang, J.; Zhang, L. The use of biobased surfactant obtained by enzymatic syntheses for wax deposition inhibition and drag reduction in crude oil pipelines. *Catalysts* 2016, Volume 6(61), pp. 1-16.
- Yang, F., Li, C., Li, B. and Lu, Y., 2014. The Solubility and Rheology of Live Oils Saturated by Different Alkane Gases. *Petroleum Science and Technology*, 32(11), pp.1340-1348.

Web References:

Know more about piping <http://pipinglearning.blogspot.in>, (accessed on – 24/07/2016).

Transmission lines, <https://www.watershedcouncil.org/pipelines-101.html>, (accessed on – 13/10/2016).

Microscopescience, <http://www.microscopescience.com>, (accessed on – 18/02/2017).

Publications

- **Rheological and Computational Analysis of Crude Oil Transportation** *World Academy of Science, Engineering and Technology, International Journal of Mechanical, Aerospace, Industrial, Mechatronic and Manufacturing Engineering Vol:11, No:2, 2017. (SCOPUS Indexed).*
- **Effect of natural surfactant on the rheological characteristics of heavy crude oil.** *Materials today proceedings (SCOPUS Indexed).*